URBAN FLUX AND CONCENTRATION MEASUREMENTS OF VOLATILE ORGANIC COMPOUNDS AND CO_2 IN MEXICO CITY

By

HECTOR ERIK VELASCO SALDAÑA

A dissertation submitted in partial fulfillment of
the requirements for the degree of

DOCTOR OF PHILOSOPHY

WASHINGTON STATE UNIVERSITY
Department of Civil and Environmental Engineering

DECEMBER 2005

To the Faculty of Washington State University:

The members of the Committee appointed to examine the dissertation of HECTOR ERIK VELASCO SALDAÑA find it satisfactory and recommend that it be accepted.

_____
Chair

_____

_____

_____

ACKNOWLEDGMENTS

First and foremost I would like to acknowledge my two primary advisors, Dr. Hal Westberg and Dr. Brian Lamb for their guidance, encouragement and support throughout the entire process of this dissertation. This dissertation represented to me a unique and magnificent opportunity to develop my skills as engineer and researcher, meeting my professional objective to help to solve the air pollution problem of Mexico City. The teaching and direction of my other advisors, Dr. George Mount and Dr. Tom Jobson were fundamental for this research and my academic formation, as well as all the lab and field support provided by Gene Allwine. Also, I would like to express my appreciation to the rest of the Laboratory of Atmospheric Research (LAR), fellow graduate students and friends, in particular to Shelley Pressley, Obie Cambaliza, Tara Strand and Jack Chen, who made of my student life a wonderful experience.

A special acknowledgement to Dr. Luisa Molina and Dr. Mario Molina, leaders of the MCMA-2003 field campaign and of the Integrated Program on Urban, Regional and Global Air Pollution Program of the Massachusetts Institute of Technology (MIT), who have given me the opportunity to collaborate in their project of cleaning the Mexican sky. Also, other special acknowledgement is for the colleagues of the National Center for Environmental Research and Training (CENICA) of the National Institute of Ecology of Mexico (INE) and for the colleagues of the Atmospheric Monitoring Network of Mexico City (RAMA) for all their assistance in this research.

In particular, I would like to thank the following colleagues that through their assistance, discussion, data and expertise made possible this research: Miguel Zavala and Benjamin de Foy (MIT), Berk Knigthon (Montana State University), Scott Herndon and Charles Kolb (Aerodyne), Michael Alexander and Peter Prazeller (Pacific Northwest National Laboratory), Gustavo Sosa (National Institute of Petroleum), Michael Grutter (National Autonomous University of Mexico), William Brune (Pennsylvania State University), Victor Gutierrez-Avedoy, Adrian Fernandez,

Felipe Angeles, Salvador Blanco and Rosa Maria Bernabe (CENICA & INE) and Victor Hugo Paramo, Rafael Ramos and Armando Retama (RAMA).

An additional acknowledgement is for the National Commission of Science and Technology of Mexico (CONACyT), which has followed and supported all my graduate formation. My gratitude with CONACyT, which represents the scientific interests of the Mexican people, is a responsibility that I will be happy to carry with me throughout my entire life.

Last but not least, I thank my family to make of me the person who I am. And specially, I thank Elvagris Segovia for all her emotional support, demonstrating that the Pacific Ocean was not a barrier for our love.

ATTRIBUTIONS

The research presented in this dissertation is the result of the participation of Washington State University (WSU) in the MCMA-2002 & 2003 field campaigns in Mexico City. Both campaigns were funded by the Integrated Program on Urban, Regional and Global Air Pollution Program of the Massachusetts Institute of Technology (MIT) and the Metropolitan Commission of Environment of Mexico City (CAM). Erik Velasco was partially funded by the National Commission of Science and Technology of Mexico (CONACyT) with assistance for housing and living.

The research contained in this dissertation is a compilation of many ideas and data collection efforts from many people. Dr. Brian Lamb and Dr. Hal Westberg were invited to participate in the MCMA-2002 and 2003 field campaigns and both prepared the initial proposal to measure concentrations and fluxes of volatile organic compounds (VOCs) in the urban core of Mexico City. In the course of the research, new goals and activities were added, including collaborations with other groups involved in the MCMA field campaigns. Although multiple authors contributed to the three manuscripts presented in this dissertation, Erik Velasco was the primary author of all of them. Erik Velasco was responsible for essentially all of the data analysis and had a primary role in many of the measurements performed during 2003.

Chapter 2 presents an integrating manuscript of several VOC measurements performed in the 2002 and 2003 field campaigns by different research groups at different locations. Data contributions were made by Erik Velasco, Brian Lamb, Hal Westberg and Gene Allwine of WSU, Tom Jobson, Michael Alexander and Peter Prazeller of the Pacific Northwest National Laboratory (PNNL), Berk Knigthon of Montana State University (MSU), Scott Herndon and Charles Kolb of Aerodyne, Jose Luis Arriaga and Gustavo Sosa of the National Institute of Petroleum (IMP), Michael Grutter of the National Autonomous University of Mexico (UNAM) and Miguel Zavala, Benjamin de Foy, Luisa Molina and Mario Molina of the Massachusetts Institute of Technology (MIT). Chapter 3 is a paper that has been published and which presents

results of the VOC flux measurements performed in 2003. This manuscript contains contributions of Erik Velasco, Shelley Pressley, Brian Lamb, Hal Westberg and Gene Allwine of WSU, Tom Jobson, Michael Alexander and Peter Prazeller of PNNL and Luisa Molina and Mario Molina of the MIT. Chapter 4 is a paper that has been published and presents CO_2 flux measurements conducted by WSU in 2003. The authors of this paper include Erik Velasco, Shelley Pressley, Gene Allwine Hal Westberg and Brian Lamb.

URBAN FLUX AND CONCENTRATION MEASUREMENTS OF VOLATILE ORGANIC COMPOUNDS AND CO_2 IN MEXICO CITY

Abstract

by Hector Erik Velasco Saldaña, Ph.D.
Washington State University
December 2005

Chair: Hal Westberg

Measurements of ambient concentrations and fluxes of volatile organic compounds (VOCs) and CO_2 in the atmosphere of Mexico City are reported here. These measurements were part of the MCMA-2002 and 2003 field campaigns. In both campaigns, a wide array of VOC measurements were conducted using a variety of methods with different spatial and temporal scales at locations in the urban core, in a heavily industrial area and at boundary sites. The VOC data were analyzed to document their distribution, diurnal pattern, origin and reactivity in Mexico City. In the 2003 field campaign, an eddy covariance flux system was deployed at the CENICA site to perform direct measurements of emissions of CO_2 and selected VOCs (olefins, acetone, methanol, toluene and C_2-benzenes) from sources in an urban neighborhood. This work demonstrates the use of micrometeorological techniques coupled with fast-response sensors to measure fluxes of trace gases from urban landscapes, where the spatial variability of emission sources, surface cover and roughness is very complex. The capability to evaluate emission inventories using these techniques as described in this work is a valuable and new tool for improving air quality management.

Overall, it was found that the VOC burden is dominated by alkanes (60%), followed by aromatics (15%) and olefins (5%). However, in terms of ozone production olefins are the most important hydrocarbons in Mexico City. Ambient concentrations and fluxes of VOCs and CO_2 exhibited clear diurnal patterns with distinct correlation with vehicular traffic. The flux

measurements showed that the urban landscape is nearly always a net source of VOCs and CO_2. The exception was acetone, which showed negative fluxes before sunrise. Fluxes of olefins, acetone, toluene and C_2-benzene were compared to the emissions reported in the local emissions inventory. For the grid where the CENICA site was located, the emissions inventory generally agreed with the measured fluxes. Furthermore, a comparison of the ambient VOC concentrations in terms of lumped modeling VOC classes to the emissions inventory suggests that some, but not all classes are underestimated in the inventory by factors of 3, as suggested in previous studies.

TABLE OF CONTENTS

LIST OF TABLES

CHAPTER 2

CHAPTER 3

LIST OF FIGURES

LIST OF ABBREVIATIONS

ATDD	Atmospheric Turbulence and Diffusion Division of NOAA
BTEX	sum of benzene, toluene, ethylbenzene and xylenes
BTX	sum of benzene, toluene and xylenes
BVOC	biogenic VOC
CAM	Metropolitan Environmental Commission of Mexico City
CENICA	National Center for Environmental Research and Training
CIT	California Institute of Technology airshed model
c_χ'	instantaneous deviation of the trace gas
d	zero displacement plane
DEA	disjunct eddy accumulation
DEC	disjunct eddy covariance
DOAS	UV Differential Optical Absorption Spectrometer
EC	eddy covariance
EPA	Environmental Protection Agency
ETBE	Ethyl tertiary-butyl ether
FFT	Fast Fourier Transform
FID	flame ionization detector
FOS	Fast Olefin Sensor
FTIR	Fourier Transform Infrared Spectrometer
F_χ	flux of a trace gas
GC	gas chromatography
GC-FID	gas chromatography/flame ionization detection
GC-MS	gas chromatography/mass spectroscopy detection
$I_{1\text{-}2}$	intersections between avenues 1 and 2 in Figure 3.3
$I_{2\text{-}3}$	intersections between avenues 2 and 3 in Figure 3.3
IMP	Mexican Petroleum Institute
INE	Mexican National Institute of Ecology
IRGA	open-path InfraRed Gas Analyzer
k	Von Karman constant
L	Monin-Obuhkov length
LPG	Liquefied petroleum gas
MCMA	Metropolitan Area of Mexico City
MCMA-2002	Metropolitan Area of Mexico City 2002 field campaign
MCMA-2003	Metropolitan Area of Mexico City 2003 field campaign
MILAGRO	Megacity Initiative: Local and Global Research Observations
MIT	Massachusetts Institute of Technology
MS	mass spectroscopy
MSU	Montana State University
MTBE	Methyl tertiary-butyl ether
NOAA	National Oceanic and Atmospheric Administration
PM	particulate matter
PM_{10}	particulate matter with an aerodynamic diameter equal or smaller to 10 μm
$PM_{2.5}$	particulate matter with an aerodynamic diameter equal or smaller to 2.5 μm

PNNL	Pacific Northwest National Laboratory
ppbv	part per billion volume
ppmv	part per million volume
p_r	percentage due to random error
p_s	percentage due to systematic error
PTR-MS	Proton Transfer Reaction-Mass Spectrometer
RAMA	Automated Atmospheric Monitoring Network of Mexico City
REA	relaxed eddy accumulation
S_0	source strength
T	ambient temperature measured by the sonic anemometer
TDLAS	Tunable Diode Laser Spectroscopy
TOC	total organic compounds
u	mean wind velocity
UNAM	National Autonomous University of Mexico
VOCs	volatile organic compounds
w	vertical wind speed
WSU	Washington State University
w'	instantaneous deviation of the vertical wind velocity
x	upwind distance or effective source footprint
z_0	surface roughness parameter
z_{city}	height of the urban canopy
z_m	measurement height
z_{tower}	height of the flux tower
ξ	atmospheric stability index

CHAPTER 1

INTRODUCTION

1.1. Overview

Poor air quality in an increasingly urbanized world directly threatens the health of a large fraction of the world's population. Increases in pollutant concentrations impact the viability of important natural and agricultural ecosystems in regions surrounding highly urbanized areas, and increasing emissions of radiatively important trace gases, such as carbon dioxide (CO_2), contribute significantly to global climate change. These issues are particularly acute in the developing world where the rapid growth of megacities is producing atmospheric pollution of unprecedented severity and extent. It has been recognized that in developing megacities the main sources of pollutants are vehicles and industries. However, there are a number of other significant sources that cannot be identified or quantified accurately. These include unregulated factories and domestic activities, such as residential cooking and heating. Uncertainties in emissions are particularly large in third world megacities for volatile organic compounds (VOCs) and CO_2. The VOCs are reactive species that contribute to the creation of photochemical smog and tropospheric ozone (O_3), while CO_2 is the most significant anthropogenic greenhouse gas. With the aim of improving our understanding of the emissions of VOCs and CO_2 in megacities, we participated in the Mexico City Metropolitan Area (MCMA) field campaigns in 2002 and 2003. Our participation involved two main activities. First we investigated the distribution and diurnal pattern of VOCs at several different sites within and near Mexico City. VOC signatures for airshed boundary sites, central urban core and downwind urban receptor sites were obtained from ambient samples collected using canisters and analyzed by gas chromatography/flame ionization detection (GC-FID) methods. Continuous olefin mixing ratios were measured from a tower erected on a laboratory building in southeastern Mexico City (CENICA super site) using a fast chemiluminsecent olefin sensor (FOS). Additional diurnal VOC concentration measurements made by other participants included use of a Proton Transfer Reaction-Mass

Spectrometer (PTR-MS) onboard a mobile laboratory, a second PTR-MS located at the CENICA super site, and long path measurements of selected VOCs using UV Differential Optical Absorption Spectrometers (DOAS) and Fourier Transform Infrared Spectrometers (FTIR) located near of the center of the city and at the CENICA super site.

Our second activity involved the deployment of micrometeorological flux instruments on the tower at the CENICA supersite to directly measure fluxes of VOCs and CO_2 from the urban landscape. Fluxes of olefinic VOCs were measured using the FOS and processed by the eddy covariance technique (EC). Fluxes of acetone, methanol, C_2-benzenes and toluene were measured using the PTR-MS and computed by the disjunct eddy covariance technique (DEC). Fluxes of CO_2 and water vapor were measured by an open path infrared sensor and processed by EC. The stationarity and frequency distribution of turbulence for the flux measurements were examined to demonstrate the applicability of micrometeorological techniques to the heterogenous urban landscape where the spatial variability of emission sources, surface cover, and roughness is high. The measured fluxes were analyzed as functions of the upwind direction and extent of the source footprint to identify the strongest sources. Traffic counts were used to examine the relationship between fluxes of VOCs and CO_2 with vehicular activity. Finally, the measured fluxes were compared to emissions inventory data for the grid where the flux tower was located, and the VOC data from the canisters samples were examined in terms of the relative composition of lumped modeling VOC classes and compared to the composition from the most recent emissions inventory used for modeling. At the end of this research, we expect to have improved our ability to evaluate emission inventories of trace gases through direct and indirect methods and to have demonstrated the feasibility of EC and DEC techniques to perform VOC flux measurements in an urban area using state of the art VOC sensors. It is important to recognize that this experiment was the first time that micrometeorological techniques were applied to measure fluxes of VOCs in an urban landscape as a new tool for improving air quality management.

The dissertation is divided into five chapters. The Introduction chapter provides a brief overview of the work plan, lists the objectives and a short review of the importance of using ambient concentrations to evaluate emissions inventories of VOCs and CO_2 in urban environments. The second chapter entitled "Distribution, magnitudes, reactivity, ratios and diurnal patterns of volatile organic compounds in the Valley of Mexico during the MCMA 2002 & 2003 field campaigns" presents a summary of all ambient VOC measurements performed in both MCMA field campaigns, analysis of the VOC data in terms of reactivity to form ozone, VOC distributions and diurnal patterns, an examination and comparison of the ambient VOC data with vehicle exhaust profiles, and a comparison in terms of lumped modeling VOC to the actual emissions inventory. This chapter will be reformed and submitted to the Journal of Atmospheric Chemistry and Physics for publication. The third and fourth chapters are manuscripts that were published in specialized journals. The versions included here correspond to the final drafts. The manuscript corresponding to the third chapter is entitled "Flux measurements of volatile organic compounds from an urban landscape". This manuscript presents the flux measurements performed at the CENICA supersite as part of the MCMA-2003 field campaign. This manuscript was published in Geophysical Research Letters (Velasco et al., 2005a). The fourth chapter is a manuscript entitled "Measurements of CO_2 fluxes from the Mexico City urban landscape". The CO_2 fluxes discussed in this manuscript were measured in parallel with the VOC fluxes presented in chapter three. This manuscript was published in Atmospheric Environment (Velasco et al., 2005b). Finally, the fifth chapter contains a brief summary and presents the final remarks for this dissertation.

1.2. Objectives

The overall goal of this research was to improve our understanding of atmospheric emissions in megacities and, thus, to improve our ability to evaluate emission inventories for a better design of strategies to reduce air pollution. This study focused on VOC and CO_2 emissions in Mexico City. In particular, VOCs are important species in the evolution of ozone and other toxic pollutants, while CO_2 is known to be the most important greenhouse gas of anthropogenic origin. In pursuing this goal, we addressed the objectives listed below.

1) To explore the use of micrometeorological techniques to evaluate emissions of all anthropogenic and biogenic sources in urban landscapes.
2) To demonstrate the feasibility of using micrometeorological techniques to measure urban fluxes of trace gases in urban environments where the spatial variability of surface cover, emission sources and roughness is high.
3) To evaluate the use of state of the art fast-response sensors to measure VOC fluxes from urban landscapes.
4) To determine the diurnal pattern of fluxes of CO_2 and VOCs from a typical neighborhood of Mexico City, and to determine their magnitudes as a function of the upwind direction and footprint to identify the strongest sources.
5) To provide direct measurements of emissions for a number of VOCs for comparison to existing gridded emission inventories.
6) To analyze the relationship between fluxes of both, VOCs and CO_2 with the vehicular activity.
7) To investigate the VOC signature and its diurnal pattern at selected urban sites in Mexico City to improve our understanding of atmospheric chemistry and anthropogenic emissions.
8) To evaluate the underestimation of VOC emissions in the gridded emission inventory as suggested in previous studies.

1.3. Megacities and air pollution

About half of the world's population now lives in urban areas because of the opportunity for a better quality of life. Many of these urban centers are expanding rapidly, leading to the growth of megacities, which are defined as metropolitan areas with populations exceeding 10 million inhabitants (Molina and Molina, 2004). At present, there are 20 megacities with a combined population of 292 million (UN, 2004), and more than 100 smaller cities worldwide that have similar characteristics. These agglomerations of people are leading to increased stress on the natural environment, with impacts at urban, regional and global scales (Decker et al., 2000).

In recent decades, air pollution has become one of the most important problems of megacities. In some cases, megacities emit plumes of pollutants at rates even greater in size than entire countries (Gurjar and Lelieveld, 2005). These plumes contain large amounts of toxic pollutants, including ozone precursors, aerosols and greenhouse gases, which produce serious impacts on public health, ecosystems and global change. In different megacities around the world, the adverse effects of pollution on human health have been demonstrated with similar conclusions: particulate matter (PM), O_3, and other air pollutants attack the cardiovascular and respiratory systems and are associated with premature mortality as well as sickness (Dockery et al., 1993; Evans et al., 2002). The export of air pollutants from a megacity to regional and global environments is a major concern because of wide-ranging potential consequences for natural ecosystems, visibility degradation, weather modification, changes in precipitation chemistry, changes in radiative forcing and tropospheric oxidation or self-cleaning capacity (Jacob et al., 1999; Chameides et al., 1994; Kiehl, 1999; Gauss et al., 2003; Prinn et al., 2001).

Clearly air pollution in megacities is an important issue. However, emission estimates for megacities are highly uncertain and not much is known about atmospheric chemistry in the tropics, where much of the urban world population growth occurs. This represents an enormous scientific challenge due to the complexity of social, physical and chemical processes that must be understood.

1.3.1. Mexico City, a suitable megacity for air quality studies

Although, no one megacity can fully represent all of world's megacities, Mexico City is a good location for investigations to improve our understanding of the atmospheric pollution in megacities. Mexico City has the following properties:

- Mexico City is the world's second largest megacity after Tokyo, and will continue to be one of the most populous cities, with a current population near 19 million.
- Mexico City is situated in the tropics as are most of the world's fastest growing megacities.
- Its emission characteristics are roughly intermediate between those of a city in emerging economies and those of a city from a developed country.
- Extensive air quality measurements have been made for many years. Criteria pollutants have been routinely monitored for more than 15 years. A number of intensive studies have been performed during the last decade to provide insight into the local air quality problem.
- Emissions inventories have been developed and are being refined.
- Compared with other tropical cities, Mexico offers good infrastructure and logistics to support the investigation of air quality in a megacity.

For the purposes of evaluating urban emissions of VOCs and CO_2 through direct measurements, Mexico City represents the ideal site for the reasons described above and because its VOC and CO_2 concentrations are among the highest in the world (Arriaga et al., 2004). Emissions of these species from combustion sources are accentuated by the high elevation of the city (2240 m.s.l.), which makes combustion processes less efficient. VOC evaporative emissions from a variety of sources such as cleaning, painting, and industrial processes are large due to the subtropical weather with temperatures above 20ºC and intense solar radiation year round. Lastly, the main contributor to high VOC and CO_2 concentrations in Mexico City is the extensive presence of aged industrial operations and a relatively old vehicle fleet. Figure 1.1 shows a map of the Valley of Mexico, where the metropolitan area and topography are shown.

Position: 19º25' N latitude' and 99º10' W longitude
Population: ~ 19 million (2003)[(a)]. 17.9% of the total Mexican population Growth projection to 20.6 million (2015). Second largest city in the world.
Density population: 12000 inhabitants per km^2 [(b)]
Urbanized area: 1500 km^2 (1999)[(b)]
GDP per capita: $7750 USA dollars (2000)[(b)]

[(a)] (UN, 2004), [(b)] (Molina et al., 2002).

Figure 1.1. Map of the Valley of Mexico showing the Mexico City Metropolitan Area and associated information.

1.3.2. Mexico City background

Mexico City lies in an elevated basin at an elevation of 2240 m. The nearly flat basin covers ~5000 km^2 of the Mexican Plateau and is confined on three sides (east, south, and west) by mountain ridges, with a broad opening to the north and a narrower gap to the south-southwest. The surrounding ridges vary in elevation, with several peaks reaching nearly 4000 m. Two major volcanoes, Popocateptl (5452 m) and Ixtacihuatl (5284 m), are on the mountain ridge southeast of the basin. The metropolitan area is on the southwest side of the basin and covers ~1500 km^2.

Mexico City is also named the Mexico City Metropolitan Area (MCMA), since it combines a conurbation proper with peripheral zones. The MCMA consists of 16 delegations of the Federal District and 37 contiguous municipalities from the State of Mexico and one municipality from

the State of Hidalgo, some with populations over 1 million that make up the total population of ~ 19 million.

The large population, 53,000 industries, 3.5 million vehicles, complex topography, and meteorology cause high pollution levels. The mountains, together with frequent thermal inversions, trap pollutants within the basin. The high elevation and intense sunlight also contribute to photochemical processes that create O_3 and other secondary pollutants. More than 47 million L of fuel consumed per day produce thousands of tons of pollutants. Air pollution is generally worst in the winter, when rain is less common and inversions more frequent (Molina et al., 2002).

Owing to the high altitude, MCMA air contains ~23% less oxygen than at sea level. Consequently, internal combustion engines need to be carefully tuned to the proper O_2-to-fuel ratio to improve combustion efficiency and reduce emissions. People at higher altitudes are more susceptible to respiratory ailments than those at sea level. More air must be inhaled for an equivalent amount of O_2 at high altitudes, which causes a higher dose of air pollutants (Molina and Molina, 2004).

High O_3 concentrations are measured throughout the year because the subtropical latitude and high altitude are conducive to photochemistry. The national air quality standard for ozone (110 ppb/1 hour average) is exceeded 70% of the days (GDF, 2004). Anticyclone high pressure systems appear during winter, resulting in light winds above the basin and nearly cloudless skies. This leads to the formation of strong surface-based inversions at night that persist for several hours after sunrise. Strong solar heating of the ground generates turbulent mixing that erodes these inversions in the morning, producing deep boundary layers by the afternoon. Pollutants trapped below the inversion layer are then mixed within the convective boundary layer, which can reach altitudes of 4 km. There is sufficient time for O_3 formation in the morning before the development of the deep convective boundary layer because of high emission rates and intense solar radiation. During the wet summer months (June to September), clouds inhibit photochemistry and rainfall removes many trace gases and PM; high O_3 episodes are less

frequent. Near-surface northerly winds during the day may transport pollutants to the southwest, where O_3 concentrations are the highest (Bossert, 1997).

1.4. Emission inventories

The design of emission controls requires detailed information on the status of the air quality (provided by monitoring networks) and the principal sources of pollution and their location, as characterized by emission inventories. Combining the information from monitoring and emission estimates with knowledge of dispersion characteristics for the city and chemical transformations of pollutants enables air quality models to be developed. Such models are powerful tools for air quality managers, but their results depend on the quality of the emissions estimates and meteorological inputs. A comprehensive emissions inventory must provide an accurate tally of all important air pollutant species and should include the temporal and spatial distribution of emissions in a region.

Emission inventories are typically constructed through an aggregation process that accounts for emission rates, activity levels, and the distribution of sources. Emissions inventories for Mexico City have been under development since 1986 and are periodically updated by the Mexican government. The most recent inventory, for the year 2002 by the Secretaria del Medio Ambiente del Gobierno del Distrito Federal (SMA-GDF, 2005), was constructed bottom-up from point, area, mobile and natural sources. Totals in Gg yr^{-1} are as follows: PM with an aerodynamic diameter equal or smaller to 10 μm (PM_{10}) ~ 23, PM with an aerodynamic diameter equal or smaller to 2.5 μm ($PM_{2.5}$) ~ 7, sulfur dioxide (SO_2) ~ 9, carbon monoxide (CO) ~ 1941, nitrogen oxides (NO_x) ~ 186, total organic compounds (TOC) ~ 709, methane (CH_4) ~ 164, VOCs ~ 490, and ammonia (NH_3) ~ 17. Substantial uncertainties exist, particularly concerning the VOC emissions.

Emission rates are often derived from laboratory or specific field measurements (i.e. vehicle dynamometer studies), activity levels can be obtained from traffic counts, surveys of sources and other information, and source distributions may come from roadway maps, aerial photographs, or

be derived as a function of population density. The propagation of errors associated with this bottom up inventory compilation can result in large uncertainties in urban areas, where it is almost impossible to identify and quantify all sources. This is particularly true for VOC emissions (Arriaga et al., 2004; Molina et al., 2002; Fujita et al., 1992). It has been recently reported that the VOC emissions inventory in Mexico City may be underestimated by a factor of 3 based upon comparison of photochemical model results and observations (West et al., 2004).

Emissions inventories have been evaluated through ambient measurements. The most direct evaluation has been to compare measured concentrations of NO_x and VOC with model results (West et al., 2004; Sillman, 1999; Trainer et al., 2000). Using this approach, input emissions in models are modified to obtain the closest possible agreement with ambient measurements, with the assumption being that all errors come from the emissions inventory and not from model or measurements uncertainties. Other evaluation methods are based on measured ratios between species (Goldan et al., 1995). For example, the morning VOC/NO_x ratio has been demonstrated to be useful for this purpose because chemical losses are relatively small during the morning and ambient concentrations reflect the ratio of directly emitted species (Arriaga et al., 2004; Sillman, 1999). In addition, the chemical mass balance receptor modeling technique has been successfully applied to improve emissions inventories by identifying the relative contribution of different sources to measured VOC fingerprint (Watson et al., 2001). For the case of mobile sources, emissions estimates have been evaluated using open path sensors positioned across roads and from tunnel studies. In general, air quality measurements in tunnels have proven to be useful to measure emissions from vehicles operating under real-world conditions (Sawyer et al., 2000). VOCs and other species are not subject to photochemical degradation in the tunnel and speciation data can be used to estimate the composition of vehicular emissions. Emission rates derived from data collected during remote sensing and tunnel studies are based on the relationship with CO_2 from the same source. CO_2 is the primary carbon-containing product of fuel combustion and provides a measure of the amount of fuel burned. The concentrations of emitted pollutants relative to the CO_2 concentration provide measurements of these emissions per

quantity of fuel consumed (McGaughey et al., 2004). These fuel-based emission factors, expressed as mass emitted per unit volume of fuel burned, are expected to vary less over the full range of driving conditions than travel-based emission factors (Singer and Harley, 1996).

1.4.1. Application of micrometeorological techniques to evaluate atmospheric emissions

In the case of biogenic hydrocarbon emissions, micrometeorological techniques have been successfully used to measure surface fluxes from woodlands and agricultural fields. Biogenic VOC (BVOC) fluxes have been measured by techniques such as surface layer gradient, relaxed eddy accumulation (REA), EC and DEC (Guenther et al., 1996; Westberg et al., 2001; Karl et al., 2002). The first two are indirect measurements of flux that rely on empirical parameterizations. EC is a direct flux measurement technique that requires a sampling rate of approximately 5 Hz. Fast-response sensors have recently become available so that EC methods can be used to measure VOC fluxes above a forest canopy (Guenther and Hills, 1998; Pressley, 2005) and over crop lands (Shaw et al., 1998). The capabilities of the PTR-MS have been expanded to allow direct flux measurements of a number of BVOC through DEC (Spirig et al., 2005; Karl et al., 2002; Rinne et al., 2001). This method calculates fluxes using measurements at a lower frequency compared to EC; the sample interval can be as long as 30 s. This makes it possible to use relatively slow sensors for flux measurements.

In urban areas, micrometeorological approaches have been previously applied to measure fluxes of momentum, heat and CO_2 (Grimmond et al., 2004; Moriwaki and Kanda et al., 2004; Soegaard and Møller-Jensen, 2003; Nemitz et al., 2002; Grimmond et al., 2002), as well as aerosols (Dorsey et al., 2002). Measurements of momentum and heat fluxes provide basic data to run air quality models and valuable information for understanding the dispersion of pollutants in the urban atmosphere. In particular, measurement of heat flux is important for determining the intensity of an urban heat island. An urban heat island influences urban ecology in a variety of ways by altering such things as the physiological comfort of humans, cooling requirements, duration of snow cover, cloud cover, precipitation rates, etc. CO_2 flux measurements have

validated urban emissions inventories and have shown that emission patterns depend on the diurnal cycle and climatic season. In general, urban landscapes are net sources of CO_2, and their emission magnitude depends on climatic conditions (e.g. temperature and humidity), fraction of land covered by vegetation, vehicular traffic, population density, etc. The only study reporting aerosol fluxes is that by Dorsey et al. (2002) who related aerosol flux with vehicular traffic and boundary layer stability in the City of Edinburgh.

1.5. VOCs: photochemical precursors and toxic pollutants

By definition the term VOC is used to denote all organic compounds that have a vapor pressure higher than 13.3 Pa at 25°C, according to ASTN test method D3960–90. However, in terms of air quality, VOCs encompass all of the individual reactive organics in the troposphere that contribute to the creation of photochemical smog and tropospheric ozone.

VOCs are a key piece in understanding photochemical air quality in urban atmospheres. In the presence of sunlight and NO_x, VOCs are oxidized to carbon dioxide and water via various intermediates: radicals (e.g., hydroxyl, hydroperoxy, organic peroxy), organics (e.g., aldehydes, acids, alcohols, nitrates, peroxides), and inorganics (e.g., carbon monoxide, ozone, hydrogen peroxide, nitric acid) (Finlayson-Pitts and Pitts, 1997). It has been demonstrated that many of these secondary compounds may have direct health impacts (Evans et al., 2002), and that some individual VOC are extremely toxic pollutants (e.g., the carcinogens benzene and 1-3-butadiene). Therefore, accurate and precise measurements of VOCs are mandatory for improving the air quality in urban areas, and especially in megacities, where the highest concentrations of ozone and VOCs have been reported (Molina and Molina, 2004; Barletta et al., 2002).

The almost universal approach for atmospheric hydrocarbon measurements is based upon gas chromatographic (GC) separation of the individual hydrocarbons and the detection of each compound using either a flame ionization detector (FID) or a mass spectrometer (MS). GC-MS is used to establish the identity of a particular compound through the combination of retention times and mass spectra and, of course, can also be used for quantification. However, GC-FID is

commonly used for more extensive quantitative measurements after the individual peaks have been identified (Parrish and Fehsenfeld, 2000). Collection of air samples in stainless steel canisters is the most common collection technique for VOCs (Westberg and Zimmerman, 1993).

New techniques are emerging that offer relatively fast response and continuous measurements of certain hydrocarbons. One method, designated here as the fast olefin sensor, is based on the chemiluminescent reaction between olefins and ozone (Guenther and Hills, 1998). Originally it was designed to measure isoprene for EC studies in natural landscapes. Recently, it has been applied in urban areas to measure the olefinic mix, since it has a significant response to alkenes including propylene, ethylene, and 1,3-butadiene, among others. Another novel technique is the Proton Transfer Reaction Mass Spectrometry, which is capable of accurate, selective and fast-response measurements of a number of oxygenated and aromatic hydrocarbons. This technique is based upon the property that proton transfer from H_3O^+ ions can ionize many hydrocarbons, usually without fragmenting the parent ion (Lindinger et al., 1998).

Optical techniques are a third method to measure ambient VOC. The three most common optical methods are: DOAS, FTIR, Tunable Diode Laser Spectroscopy (TDLAS). The DOAS technique is based on the UV-visible molecular absorption of atmospheric gases. It offers the possibility of measuring several VOCs simultaneously. It provides the average concentration over a long optical path (from 100 m to 10 km), thus avoiding local perturbations that can compromise point measurements. DOAS has been developed to the point that BTEX (benzene, toluene, ethylbenzene, xylenes) and other monocyclic aromatic hydrocarbons can be monitored with sensitivities of ppbv on minute time scales.

Air samples can contain hundreds of different hydrocarbons of natural and anthropogenic origin; for example, over 850 different hydrocarbons have been detected in the vapor over gasoline, and over 300 different hydrocarbons from a vehicle exhaust-polluted air sample have been identified (Parrish and Fehsenfeld, 2000). Not all VOCs have the same reactivity, or rather the same impact on the formation of ozone and other secondary pollutants. The relative reactivity of individual VOCs can differ by more than one order of magnitude (Rusell et al.,

1995). Ignoring the reactivity of emissions when regulations are developed may lead to ineffective, inefficient control strategies and possibly even lead to measures that worsen air quality.

1.6. CO_2, a greenhouse gas

Carbon dioxide is a greenhouse gas that absorbs infrared photons and reemits radiation in all directions, including back towards the Earth's surface. This additional back-radiation, from all greenhouse gases combined, makes the surface-air temperature about 33ºC warmer than it would be in the absence of such radiation. Water vapor is the most dominant greenhouse gas; CO_2 is second (Finlayson-Pitts and Pitts, 2000).

Fossil-fuel combustion adds CO_2 to the atmosphere, and it has been recognized that this additional source is contributing CO_2 faster than the oceans and terrestrial biosphere can remove it. Therefore, CO_2 is accumulating in the atmosphere and enhancing the greenhouse effect. Since the industrial revolution, the CO_2 concentration in the atmosphere has increased from approximately 280 ppmv to greater than 360 ppmv today. It is expected that atmospheric CO_2 levels will continue to rise, and during the century could well exceed 500 ppmv (IPCC, 2001). This rise would lead to a number of severe environmental and economic consequences: changes in frequency, intensity, and duration of extreme events, such as more hot days, heat waves, heavy precipitation events, and fewer cold days; an increase in threats to human health, predominantly within tropical and subtropical countries; crop yields could be adversely affected; and water shortages in many water-scarce areas of the world will be exacerbated (IPCC, 2001).

All urban areas, large and small, in developing and developed areas of the world have been identified as major sources of anthropogenic CO_2 (Decker et al., 2000). Many methodologies have been developed to estimate urban CO_2 emissions. Usually they are based on fuel inventories or by other indirect means that involve a number of uncertainties or require information that may not be available or reliable for cities in less developed countries. Direct measurements using micrometeorological techniques have only recently been applied in a few

cities (Soegaard and Møller-Jensen, 2003; Moriwaki and Kanda, 2004; Grimmond et al., 2004). Despite the fact that three-quarters of the world's 3 billion urban residents live in developing countries, few, if any, flux measurements have been made in these urban areas. For these cities, emission inventories will have to be built by combining micrometeorological techniques, remote sensing, and conventional methodologies.

1.7. References

Arriaga-Colina, J.L., West, J.J., Sosa, G., Escalona, S.S., Orduñez, R.M. & Cervantes, A.D.M. Measurements of VOCs in Mexico City (1992-2001) and evaluation of VOCs and CO in the emissions inventory. *Atmospheric Environment* **38**, 2523-2533 (2004).

Barletta, B., et al. Mixing ratios of volatile organic compounds (VOCs) in the atmosphere of Karachi, Pakistan. *Atmospheric Environment* **36**, 3429-3442 (2002).

Bossert, J.E. An investigation of flow regimes affecting the Mexico City region. *J. Applied Meteorology* **36**, 119-140 (1997).

Chameides, W.L., Kasibhatla, P.S., Yienger, J. & Levy II, H. Growth of continental-scale metro agro-plexes, regional ozone pollution, and world food production. *Science* **264**, 74-77 (1994).

Decker, E.H., Elliot, S., Smith, F.A., Blake, D.R. & Rowland, F.S. Energy and material flow through the urban ecosystem. *Annu. Energy Environ*. **25**, 685-740 (2000).

Dockery, D.W., et al. An association between air pollution and mortality in six US cities. *New England Journal of Medicine* **329(24)**, 1753-1759 (1993).

Dorsey, J.R. et al. Direct measurements and parameterization of aerosol flux, concentration and emission velocity above a city. *Atmospheric Environment* **36**, 791-800 (2002).

Evans, J., et al. in *Quality in the Mexico Megacity: an integrated assessment* (ed. Molina, L.T. & Molina M.J.) 105-136 (Kluwer Academic Publishers, Netherlands, 2002).

Finlayson-Pitts, B.J. & Pitts, J.N. Chemistry of the upper and lower atmosphere. (Academic Press, USA 2000).

Fujita, E.M., et al. Comparison of emission and ambient concentration ratios of CO, NOx, and NMOG in California's south coast air basin. *Journal of Air and Waste Management Association* **42**, 264-276 (1992).

Gauss, M., et al. Radiative forcing in the 21st century due to ozone changes in the troposphere and the lower stratosphere. *Journal of Geophysical Research* **108**, 4292 (2003).

Gobierno del Distrito Federal (GDF). Informe del Estado de la Calidad del Aire y Tendencias 2003 para la Zona Metropolitana del Valle de México. (Dirección General de Gestión Ambiental del Aire. México, D.F., 2004).

Goldan, P.D. et al. Measurements of hydrocarbons, oxygenated hydrocarbons, carbon monoxide, and nitrogen oxides in an urban basin in Colorado: implications for emission inventories. *Journal of Geophysical Research* **100**, 22771-22783 (1995).

Grimmond, C.S.B., King, T.S., Cropley, F.D., Nowak, D.J. & Souch, C. Local-scale fluxes of carbon dioxide in urban environments: methodological challenges and results from Chicago. *Environmental Pollution* **116**, 243–254 (2002).

Grimmond, C.S.B., Salmond J.A., Oke, T.R., Offerle, B. & Lemonsu, A. Flux and turbulence measurements at a densely built-up site in Marseille: heat, mass (water and carbon dioxide), and momentum. *Journal of Geophysical Research* **109**, 24101-24120 (2004).

Guenther, A. & Hills, A. Eddy covariance measurement of isoprene fluxes. *Journal of Geophysical Research* **103**, 13145-13152 (1998).

Guenther, A. et al. Isoprene fluxes measured by enclosure, relaxed eddy accumulation, surface layer gradient, mixed layer gradient, and mixed layer mass balance techniques. *Journal of Geophysical Research* **101**, 18555-18567 (1996).

Gurjar, B.R. & Lelieveld, J. New directions: megacities and global change. *Atmospheric Environment* **39**, 391-393 (2005).

Intergovernmental Panel on Climate Change (IPCC). Climate Change 2001: The scientific basis. Contribution of working group I to the third assessment report of the intergovernmental panel on climate change. (Cambridge University Press, Cambridege, UK, 2001).

Jacob, D.J., Logan, J.A. & Murti, P.P. Effect of rising Asian emissions on surface ozone in the United States. *Geophysical Research Letters* **26**, 2175-2178 (1999).

Karl, T.G. et al. Virtual disjunct eddy covariance measurements of organic compound fluxes from a subalpine forest using proton transfer reaction mass spectroscopy. *Atmospheric Chemistry and Physics* **2**, 279-291 (2002).

Kiehl, J.T., Schneider, T.L., Portmann, R.W. & Solomon, S. Climate forcing due to tropospheric and stratospheric ozone. *Journal of Geophysical Research* **104**, 31239-31254 (1999).

Lindinger, W., Hansel, A. & Jordan, A. On-line monitoring of volatile organic compounds at pptv levels by means of proton-transfer-reaction mass spectroscopy (PTR-MS): Medical applications, food control and environmental research. *International Journal of Mass Spectrometry Ion Processes* **173**, 191-241 (1998).

McGaughey, G.R., Desai, N.R., Allen, D.T., Seila, R.L., Lonneman, W.A., Fraser, M.P., Harley, R.A, Pollack, A.K., Ivy, J.M. & Price, J.H. Analysis of motor vehicle emissions in a Houston

tunnel during the Texas Air Quality Study 2000. *Atmospheric Environment* **38**, 3363-3372 (2004).

Molina, L.T., Molina, M., Favela, R., Fernandez, A., Slott, R. & Zavala, M. in *Quality in the Mexico Megacity: an integrated assessment* (ed. Molina, L.T. & Molina M.J.) 21-55(Kluwer Academic Publishers, Netherlands, 2002).

Molina, M.J. & Molina L.T. Megacities and atmospheric pollution. *Air and Waste Management Association* **54**, 644-680 (2004).

Molina, M.J., Molina, L.T., West J., Sosa G., Sheibaum C. in *Quality in the Mexico Megacity: an integrated assessment* (ed. Molina, L.T. & Molina M.J.) 137-202 (Kluwer Academic Publishers, Netherlands, 2002).

Moriwaki, R. & Kanda, M. Seasonal and diurnal fluxes of radiation, heat, water vapor, and carbon dioxide over a suburban area. *Journal of Applied Meteorology* **43**, 1700-1710 (2004).

Nemitz, E., Hargreaves, K.J., Mcdonald, A.G., Dorsey, J.R. & Fowler, D. Micrometeorological measurements of the urban heat budget and CO_2 emissions on a city scale. *Environmental Science and Technology* **36(14)**, 3139-3146 (2002).

Parrish, D.D. & Fehsenfeld, F.C. Methods for gas-phase measurements of ozone, ozone precursors and aerosol precursors. *Atmospheric Environment* **34**, 1921-1957 (2000).

Pressley, S., Lamb, B., Westberg, H., Flaherty, J. & Chen, J. Long-term isoprene mesurements above a northern hardwood forest. *Journal of Geophysical Research* **110**, doi:10.1029/2004JD005523 (2005).

Prinn, R.G., et al. Evidence for substantial variations of atmospheric hydroxyl radicals in the past two decades. *Science* **282**, 1882-1998 (2001).

Rinne, H.J.I, Guenther, A., Warneke, C., de Gouw, J.A. & Luxembourg, S.L. *Geophysical Research Letters* **28**, 3139-3142 (2001).

Rusell, A., et al. Urbane ozone control and atmospheric reactivity of organic gases. *Science* **269**, 491-495 (1995).

Sawyer, R.F. et al. Mobile sources critical review : 1998 NARSTO assessment. *Atmospheric Environment* **34**, 2161-2181 (2000).

Secretaria del Medio Ambiente del Gobierno del Distrito Federal (SMA-GDF). Inventario de emisiones de la Zona Metropolitana del Valle de México (Draft). Available at: http://www.sma.df.gob.mx (2005).

Shaw, W.J., Spicer, C.W. & Kenny, D.V. Eddy correlation fluxes of trace gases using a tandem mass spectrometer. *Atmospheric Environment* **32**, 2887-2898 (1998).

Sillman, S. The relation between ozone, NO_x, and hydrocarbons in urban and polluted rural environments. *Atmospheric Environment* **33**, 1821-1845 (1999).

Singer, B.C. & Harley, R.A. A fuel-based motor vehicle emission inventory. *Journal of the Air and Waste Management Association* **46**, 581–593 (1996).

Soegaard, H. & Møller-Jensen, L. Towards a spatial CO_2 budget of a metropolitan region based on textural image classification and flux measurements. *Remote Sensing of Environment* **87**, 283-294 (2003).

Spirig, C., Neftel, A., Ammann, C., Dommen, J., Grabmer, W., Thielmann, A., Schaub, A., Beauchamp, J., Wisthaler, A. & Hansel, A. Eddy covariance flux measurements of biogenic VOCs during ECHO 2003 using proton transfer reaction mass spectrometry. *Atmospheric Chemistry and Physics* **5**, 465–481 (2005).

Trainer, M., Parrish, D.D., Goldan, P.D., Roberts, J. & Fehsenfeld, F.C. Review of observation-based analysis of the regional factors influencing ozone concentrations. *Atmospheric Environment* **34**, 2045–2061 (2000).

United Nations (UN). *World Urbanization Prospects. The 2003 Revision.* Avialable at: http://www.un.org/esa/population/publications/wup2003/2003WUPHighlights.pdf (2004).

Velasco, E., Lamb, B., Pressley, S.., Allwine, E., Westberg, H., Jobson, B.T., Alexander, M., Prazeller, P., Molina, L. & Molina, M. Flux measurements of volatile organic compounds from an urban landscape. *Geophysical Research Letters* **32(20)**, L20802, doi:10.1029/2005GL023356 (2005a).

Velasco, E., Pressley, S., Allwine, E., Westberg, H., Lamb, B. Measurements of CO_2 fluxes from the Mexico City urban landscape. *Atmospheric Environment* **39(38)**, 7433-7446 (2005b).

Watson, J.G., Chow, J.C. & Fujita, E. Review of volatile organic compound source apportionment by chemical mass balance. *Atmospheric Environment* **35**, 1567-1584 (2001).

West, J.J. et al. Modeling ozone photochemistry and evaluation of hydrocarbon emissions in the Mexico City Metropolitan Area. *Journal of Geophysical Research* **109**, 19312 (2004).

Westberg, H. & Zimmerman, P. Analytical methods used to identify nonmethane organic compounds in ambient atmospheres. *Advances in Chemistry Series* **232**, 275-290 (1993).

Westberg, H. et al. Measurement of isoprene fluxes at the PROPHET site. *Journal of Geophysical Research* **106**, 24347-24358 (2001).

CHAPTER 2

DISTRIBUTION, MAGNITUDES, REACTIVITIES, RATIOS AND DIURNAL PATTERNS OF VOLATILE ORGANIC COMPOUNDS IN THE VALLEY OF MEXICO DURING THE MCMA 2002 & 2003 FIELD CAMPAIGNS

2.1. Abstract

A wide array of volatile organic compound (VOC) measurements was conducted in the Valley of Mexico during the MCMA-2002 and 2003 field campaigns. Study sites included locations in the urban core in, a heavily industrial area and at boundary sites in rural landscapes. Four distinct analytical techniques were used: whole air canister samples with gas chromatography / flame ionization detection (GC-FID), on-line chemical ionization using a Proton Transfer Reaction Mass Spectrometer (PTR-MS), continuous real-time detection of olefins using a Fast Olefin Sensor (FOS), and long path measurements using UV differential optical absorption spectrometers (DOAS). The simultaneous use of these techniques provided a wide range of individual VOC measurements with different spatial and temporal scales. The VOC data were analyzed to understand concentration and spatial distributions, diurnal patterns, origin and reactivity in the atmosphere of Mexico City. On the basis of concentrations given in ppbC, the VOC burden was dominated by alkanes (60%), followed by aromatics (15%) and olefins (5%). The remaining 20% was a mix of alkynes, halogenated hydrocarbons, oxygenated species (esters, ethers, etc.) and other unidentified VOCs. However, in terms of ozone production, olefins were the most relevant hydrocarbons. Elevated levels of toxic hydrocarbons, such as 1,3-butadiene, benzene, toluene and xylenes were also observed. Various analytical techniques have demonstrated that vehicle exhaust is the main source of VOCs in urban areas and that diurnal patterns depend on vehicular traffic. Finally, examination of the VOC data in terms of lumped modeling VOC classes and comparison to the VOC emissions reported in the

available Mexican inventory derived for purposes of photochemical air quality suggests that some, but not all, classes are underestimated in the inventory by factors of 2 or 3.

2.2. Introduction

Volatile Organic Compounds (VOCs) play a key role in photochemical air quality in urban atmospheres. In the presence of sunlight and nitrogen oxides (NO_x), VOC oxidation produces secondary products including radicals (e.g., hydroxyl, hydroperoxy, organoperoxy), oxygenated organics (e.g., aldehydes, ketones, acids, nitrates, peroxides), and inorganics (e.g., carbon monoxide, ozone, hydrogen peroxide, nitric acid) (Finlayson-Pitts and Pitts, 1997). It has been demonstrated that many of these secondary compounds may have direct health impacts (Evans et al., 2002), and that some individual VOCs are extremely toxic pollutants (e.g., the carcinogens benzene and 1-3-butadiene). In a short-term study such as reported in this manuscript, it is not possible to quantify the health impacts from exposure to air toxic species because health benchmarks are measured in terms of annual averages. Long term measurements of VOCs are needed for understanding air toxic issues in urban areas, especially in megacities such as Mexico City, where millions of people are exposed to high concentrations of VOCs and other pollutants (Molina and Molina, 2004).

Mexico City with a population of 19 million, is a good example of a megacity with severe air pollution problems. It is situated in the Valley of Mexico and is the capital city of a developing country. Mexico City is in the subtropical zone as are most of the world's fastest growing cities. Many of the most populated Latin-American urban areas, like Mexico City are at high altitude which makes combustion processes less efficient leading to enhanced VOC emissions. Mexico City's high altitude (~2240 m) and low latitude (19^o 25' N), subtropical weather and intense solar radiation accentuate the VOC evaporative emissions from a variety of sources such as storage and distribution of gasoline, cleaning, painting, and industrial processes. However the main contributors to high VOC concentrations in Mexico City are the extensive presence of aged industrial operations (more than 53,000 industries) and a relatively old vehicle

fleet (more than 3.5 million vehicles with an average age of ~9 years). The elevated anthropogenic emissions, the intense solar radiation and area's topography with mountains to the west, east and south of the valley (see Figure 1) produce elevated levels of photochemical pollutants that are trapped in the basin on a daily basis.

Many researchers have addressed the VOC pollution problem in Mexico City. Ambient VOC concentrations have been evaluated since the early 90's (see papers cited by Raga et al., 2001). All studies have consistently reported high concentrations of propane, butane and other low molecular weight alkanes, which have been attributed to liquefied petroleum gas (LPG) leakage during handling, distribution and storage. LPG is the main fuel for cooking and water heating in Mexican households. High ambient concentrations of photochemical reactive VOCs, such as olefins and aromatics have been reported, as well (Mugica et al., 2002; Arriaga et al. 1997). These two VOC groups have been identified to be the main species responsible for the ozone and secondary organic aerosol formation in Mexico City (Gasca et al., 2004; Mugica et al., 2002). High exposure levels to aromatics hydrocarbons, particularly to toluene, benzene and xylenes have been detected in different microenvironments and public transport of Mexico City (Shiohara et al., 2005, Gomez-Perales et al., 2004; Cruz-Nuñez et al., 2003; Bravo et al., 2002; Ortiz et al., 2002; Meneses et al., 1999).

From source apportionment studies, it has been determined that motor-vehicles, especially gasoline-vehicles are the main source of those aromatic hydrocarbons (Mugica et al., 2003). Emissions profiles for motor-vehicles in on-road conditions have been obtained from tunnel and remote sensing studies (Schifter et al., 2003; Mugica et al., 1998). However, many uncertainties exist about vehicular emissions in Mexico City as consequence of the lack of reliable emission factors and daily activity levels of the fleet (Gakenheimer et al., 2002). VOC emission profiles are also available for food cooking, asphalt application and painting operations, among other types of sources in Mexico City (Vega et al., 2000; Mugica et al. 2001). The biogenic component in the VOC emission burden has been estimated to contribute no more than 7% in the Valley of Mexico (Velasco, 2003).

During the last decade, a number of policies and actions have been enacted to decrease VOC emissions in Mexico City, among them, the enforcement of vapor recovery systems in fuel service stations, the banning of leaded gasoline and heavy oil fuels, the availability of diesel with reduced sulfur content and the substantial reduction of olefins, benzene, and other aromatic hydrocarbons content in gasoline. Arriaga-Colina et al. (2004) reported that, as result of these emission control measures, ambient VOC concentrations have stabilized and possibly decreased, despite the growth in the vehicular fleet and other activities. However, ambient VOC levels still remain high and the national air quality standard for ozone (110 ppb/1 hour average) is exceeded 70% of the days (GDF, 2004).

Although some advances have been achieved, it is clear that a better understanding of the photochemical pollution in the complex urban ecosystem of Mexico City is needed to support effective control strategies. In this context, a number of US and Mexican institutions and agencies participated in the Mexico City Metropolitan Area 2002 and 2003 (MCMA-2002 & MCMA-2003) field campaigns. The first was an exploratory campaign performed in February 2002, and the second an intensive five week field study during April and May, 2003. The goals of both field studies were to update and improve the emissions inventory of Mexico City, and to gain a better understanding of the chemistry and transport processes driving atmospheric pollution in the valley. As part of the investigation to meet these goals, a wide array of VOC measurements was conducted at airshed boundary sites, central urban core sites, and downwind urban receptor sites. Four different analytical methods were used: VOC speciation by gas chromatographic analysis using flame ionization detection (GC-FID), olefin detection with a Fast Olefin Sensor (FOS), determination of a number of oxygenated and aromatic VOCs by Proton Reaction Transfer Mass Spectroscopy (PTR-MS), and measurements of selected VOCs using Differential Optical Absorption Spectroscopy (DOAS). Key aspects of these VOC measurements were the number of individual species measured and the variety of spatial and temporal scales employed in the measurements.

This manuscript presents a summary of results from the different VOC measurements in terms of the distribution, magnitudes, and diurnal patterns of selected VOCs. The use of ratios of individual VOC species is used to characterize different sites, to investigate the relative reactivity of different species and to determine their origins through comparisons with source signatures, in particular with vehicle exhaust profiles. In addition, the ambient VOC data has been compared to the lumped VOC emissions classes in the Mexican emissions inventory used for photochemical air quality modeling. It has been suggested that VOC emissions are underestimated in the official emissions inventory by a factor of 3 from analysis of the VOC/NO_x ratio (Arriaga-Colina et al., 2004) and from ozone modeling exercises (West et al., 2004). However, eddy covariance flux measurements of selected VOCs during the MCMA-2003 campaign suggest that for the VOC classes measured, the VOC emissions reported in the emissions inventory are generally correct (Velasco et al., 2005).

2.3. Monitoring sites

During the MCMA-2002 field campaign only instantaneous canister samples were collected from five different sites. For the MCMA-2003 study, new sites were included and diverse measurement techniques were implemented. Figure 1 shows a map of the Valley of Mexico indicating the VOC sites in both campaigns. Overall, eight sites were employed, four corresponded to urban sites with different characteristics (La Merced, Constituyentes, Pedregal and CENICA), one to an industrial section of the city (Xalostoc), and three to boundary sites in rural areas (La Reforma, Teotihuacan and Santa Ana Tlacotenco). Table 1 lists a summary of these sites and VOC measurement methods used during the MCMA-2002 and MCMA-2003 field campaigns.

2.4. Instrumentation

2.4.1. Gas chromatography separation and flame ionization detection (GC-FID)

Ambient VOC samples were collected from all monitoring sites in Summa® electro-polished stainless-steel canisters. During the MCMA-2002 study, 46 samples were filled instantaneously, while for the MCMA-2003 study, 184 samples were collected with (usually) a three hour averaging interval using automated samplers. From both studies, 64% of the samples were collected during the morning rush traffic period (6:00 to 9:00 h) when VOC concentrations are strongly related to anthropogenic emissions and before the photochemical processing has begun. The remaining samples were collected during the late morning and early afternoon hours.

Samples were collected and analyzed by two different research groups: Washington State University (WSU) and the Mexican Petroleum Institute (IMP). WSU collected and analyzed 78% of the samples. During the MCMA-2003 study, WSU collected all its samples with a XonTech, Inc. Air Sampler model 910PC. Half of the samples were analyzed on-site within 24 hours of collection to minimize storage losses before analysis. IMP collected samples only in 2003 using an AVOCS Anderson Automated Sampler with a Viton diaphragm pump. Both groups analyzed their samples using methodology similar to the US EPA compendium methods TO-14/15 (US-EPA, 1999). The GC analysis utilized cryogenic pre-concentration by drawing air from the canisters through a stainless-steel loop containing glass beads (60/80 mesh) and cooled to liquid oxygen temperature. WSU employed a Hewlett-Packard 6890 Series chromatograph. The GC was equipped with a 30-m fused silica DB-1 column (0.32 mm i.d. and 1 μm film thickness) with a 2 ml min^{-1} carrier flow. Prior to sample injection, the oven was cooled to -50ºC. During analysis, the oven temperature was raised at 4ºC min^{-1} to a final temperature of 150ºC. The total analysis time was approximately one hour. Detector response was calibrated with NIST traceable 2,2-dimethylbutane standard. A minimum detection limit of 20 pptC was determined. Individual species were identified by retention times.

IMP conducted their analysis using a Hewlett-Packard 5890 Series II chromatograph containing a 60-m Quadrex fused silica glass capillary column (0.32 mm i.d. and coated with a 1

μm film thickness) at a flow of 2 ml min^{-1}. The oven temperature started at -50ºC and was heated up to 200ºC at a rate of 8ºC min^{-1}. The FID response was calibrated with a certified high-purity propane standard from Praxair. The detection limit was determined to be 1 ppbC. Individual species were identified by retention times using a mixture of 55 hydrocarbons (Scott Specialty Gases NIST Traceable), and a certified mixture of 33 halogen-containing compounds (Spectra Gases, with 10% analytical accuracy).

2.4.2. The Proton Transfer Reaction Mass Spectrometry (PTR-MS)

The Proton Transfer Reaction Mass Spectrometry identifies VOCs in ambient air as their molecular mass plus one. This technique creates ions by transferring a H^+ from H_3O^+ to the VOCs followed by mass spectroscopy detection of the product ions (Lindinger et al., 1998). The PTR-MS does not employ a column, so response times are short (seconds) and automated, continuous measurements can be made over extended periods of time. Specificity in the PTR-MS is achieved by the soft ionization (minimal fragmentation) and response is limited to species with a greater proton affinity than water. In cases where several VOCs produce the same M+1 ion, individual species quantitation is not possible. For example, the signal at mass 121 (C_3-benzenes) is comprised of i and n-propylbenzene, three ethyltoluene and three trimethylbenzenes isomers. Validation of PTR-MS measurements have been performed by de Gouw et al. (2003) and Warnake et al. (2003) to determine the set of VOCs that are suitable for measurements with this technique.

During the MCMA-2003 field campaign, two PTR-MS instruments were used. One was operated at the CENICA site by the Pacific Northwest National Laboratory (PNNL), and the second PTR-MS instrument, belonging to Montana State University (MSU), was housed in a mobile laboratory used primarily for vehicle chase experiments. During selected periods the mobile laboratory was employed as a fixed monitoring station at La Merced, Santa Ana Tlacotenco and Pedregal sites. This manuscript presents only PTR-MS fixed-site measurements. The species monitored by PTR-MS included benzene, toluene, styrene, C_2-benzenes, C_3-

benzenes, naphthalene, phenol, cresols, methanol, acetaldehyde, acetone and acetonitrile. The C_2-benzenes are represented by mass 107, which has contributions from ethylbenzene, o,m & p-xylene, and benzaldehyde (de Gouw et al., 2003).

Both PTR-MS instruments were calibrated in the field using a multi-component gas standard that contained the species reported here. The calibration standard was diluted with humidified zero air in order to generate a multipoint calibration curve over the 1 to 50 ppbv range. Calibrations were performed every 2–3 days. The instrument background was automatically recorded every 3 hours by switching the sample flow to a humid zero air stream. Zero air was continuously generated by passing ambient air through a Pt-catalyst trap heated to 300 ˚C. Background count rates were subtracted from the ambient data.

2.4.3. Fast Olefin Sensor (FOS)

Continuous real-time measurements of olefin concentrations were made at the CENICA site during the MCMA-2003 study by WSU using a FOS. The FOS is a fast isoprene sensor (Guenther and Hills, 1998) based on chemiluminescent that occurs when an olefinic bond reacts with ozone. The chemiluminescent response varies considerably for individual olefins. In an urban atmosphere where numerous olefins are present, it is necessary to evaluate the FOS response to as many olefins as possible. For Mexico City, we determined response characteristics for five olefins (propylene, ethylene, isoprene, 1-butene and 1-3 butadiene). Since NO levels are known to be high in the Mexico City atmosphere, we investigated potential interferences due to its reaction with ozone. Nitric oxide gave no response in this test. Response results for the olefins are shown in Table 2 along with their corresponding relative sensitivities to propylene. It was found that the FOS is more sensitive to 1-3-butadiene and isoprene than to propylene; however, their ambient concentrations were much lower than the ambient levels of propylene. In contrast, species with a lower sensitivity than propylene, but with high concentrations in urban atmospheres (e.g. ethylene) can produce large signals.

During the campaign, the FOS was calibrated 3 times per day using dilutions from a propylene standard (Scott Specialty Gases, 10.2 ppm, ±5% certified accuracy). The linear slope of instrument response versus propylene concentration and the zero level exhibited relatively little drift during the study period, 14% and 9%, respectively.

2.4.4. Differential Optical Absorption Spectrometry (DOAS)

During the MCMA-2003 field campaign, three DOAS instruments were employed to measure ambient VOC concentration. DOAS is based on the UV-molecular absorption of atmospheric gases and measures continuously concentrations of a number of trace gases averaged over a long optical path. The Massachusetts Institute of Technology (MIT) deployed a DOAS system 16 m above the surface with a path length of 960 m to measure benzene, styrene, m-xylene, p-xylene, ethylbenzene, benzaldehyde, phenol, cresols, naphthalene and formaldehyde at the CENICA site. A second DOAS (L = 860 m, H = 70 m) was employed by the MIT group to measure special trace gases such as glyoxal and HONO. A third DOAS system (L = 426 m, H = 20 m) was deployed at La Merced by the National Autonomous University of Mexico (UNAM) to measure benzene and toluene.

2.5. Ambient air inter-comparison of GC, PTR-MS and DOAS measurements for selected VOCs

Table 1 shows that at 50% of the monitored sites, two or more different techniques were used to measure VOCs. This provides the opportunity to inter-compare data to verify that they yield consistent results. Since no single technique can provide speciated measurements of all the VOCs needed for photochemical modeling, different measurement techniques are often used in combination to provide information for as many species as possible.

Figures 2a and 2b show time series of benzene and toluene mixing ratios measured by GC-FID (WSU), PTR-MS (MSU) and DOAS (UNAM) at the La Merced site. Both figures show generally good temporal agreement for benzene and toluene. Some differences between

concentration levels measured by DOAS and the other two methods are to be expected. The DOAS signal represents average concentrations over an open path distance of about 426 m while the PTR-MS and GC data are from measurements at a specific location. The PTR-MS technique is the most sensitive to transient plumes from close-by sources because it measures in real-time with no averaging. This feature can be seen in Figure 2a where benzene concentrations determined by the PTR-MS are much more variable than those from DOAS or GC, for example the hourly standard deviations of concentrations measured by the PTR-MS are twice those measured by DOAS. Furthermore, it is evident in this figure that the GC results agree better with the PTR-MS than with DOAS. Benzene levels measured by DOAS appear to exceed the concentrations determined by the other two techniques, especially during the afternoon hours. This may indicate that the point measurements (GC and PTR-MS) underestimate the regional benzene abundance and/or the DOAS measurement of benzene is subject to an interference during the midday period. It's unusual to see a benzene peak in the 10-16:00 time period.

The toluene time series shows better agreement between techniques and a more normal urban pattern of high nighttime and early morning concentrations and much lower levels during the midday period. Jobson et al. (2005) present a more detailed inter-comparison with the same three techniques at the CENICA site. They found that the level of agreement between point and long path techniques is influenced by wind direction, but in general terms they also found relatively good agreement between GC, PTR-MS and DOAS techniques.

Figure 3 shows time series plots of C_2-benzenes and C_3-benzenes measured by the MSU PTR-MS together with GC-FID samples collected during the same time periods at the Pedregal, Santa Ana Tlacotenco and La Merced sites. At La Merced and Pedregal sites, good agreement between methods for the two aromatic groups was observed. Temporal variability correlate well and GC-FID mixing ratios were always within the one standard deviation range of the PTR-MS measurements. Agreement was not as good at the Santa Ana Tlacotenco site. GC-FID C_3-benzenes concentrations were quite often above the one standard deviation range of the PTR-MS concentrations. Note that concentrations at this site were one order of magnitude smaller than

concentrations at the other sites. Benzene agreement between GC and PTR-MS was not as good at the rural Santa Ana Tlacotenco site as at the urban sites. GC-FID measurements of benzene were always near the lower limit of the one standard deviation range of the PTR-MS concentrations. However, toluene concentrations agreed closely at all three sites.

Analytical consistency was examined for the two GC techniques by collecting parallel samples using WSU and IMP samplers. WSU reported 57 hydrocarbons up to 10 carbons, while IMP quantified 104 VOCs up to 12 carbons, including oxygenated and halogenated species. The extra 47 species determined by IMP represented less than 10% of the total VOC burden. Halogenated species comprised about 2.5% of the total VOC total. Analytical results for the each of the 57 compounds directly compared during four different sampling periods showed a VOC_{WSU}/VOC_{IMP} ratio between 0.9 and 1.10.

A comparison of the FOS response to the sum of olefins as measured simultaneously with the canister sampling system suggests that the total olefin level detected by the FOS is larger than the sum of identified olefins from canister samples. The ratio between the sum of olefins measured by canisters and the FOS signal showed a median of 48%. This suggests that 52% of olefins detected by the FOS remain unknown or that the use of propylene as the calibration standard does not adequately represent the urban olefin mix. Additional laboratory studies are needed resolve this uncertainty. However, it can be affirmed that the FOS measures a mix of VOCs responding as propylene and can be used to provide a continuous and fast response measurement of the olefinic VOC mix in an urban atmosphere.

2.6. Results and discussion

2.6.1. Diurnal patterns of various VOCs at selected sites

Although the VOC time series shown in Figures 2 and 3 only cover a few days, they provide insight concerning the diurnal pattern of VOCs at sites with different characteristics in the Valley of Mexico. For example, at the La Merced site, concentrations of benzene, toluene, C_2-benzenes and C_3-benzenes reach their highest level during the morning rush hour at 7:00 h. The

accumulation of these species in the surface-based layer starts in the evening of the previous day. During the night the stability of the surface-based layer increases, and trapps pollutants emitted near the surface. Near sunrise, the VOC concentrations increase due to the beginning of the daily vehicular traffic. Between 10 and 11:00 h, concentrations decrease significantly because the nighttime surface inversion erodes with consequent growth of the boundary layer. The typical mixing height changes from less than 500 m in the early morning to heights above 2000 m at noon (Whiteman et al., 2000).

It is interesting that no late afternoon peak in VOC concentration was observed at the La Merced site, in contrast to the Pedregal site, where morning and late afternoon VOC peaks were observed. The late peak at Pedregal was observed to occur during the evening between 18 and 22:00 h. This difference between the La Merced and Pedregal sites appears to be due to different diurnal traffic patterns. Traffic counts performed during the MCMA-2003 campaign on avenues close to the two sites indicated that at La Merced had a single traffic peak that begins at 6:00 h and extends until late evening. On avenues near the Pedregal site, the typical morning and afternoon traffic peaks could be identified. Note that VOC concentrations were higher at La Merced than at Pedregal by a factor of ~3. The La Merced site was located immediately next to a number of avenues, while the Pedregal site was more distant from main roadways.

Santa Ana Tlacotenco is a rural site located in a mountain gap in the southeast corner of the Valley of Mexico through which pollutants are advected to the contiguous Valley of Cuautla. This drainage usually occurs during nighttime and the morning. During afternoons and early evenings air flow through this gap is in the opposite direction. The air coming back into the Valley of Mexico may contain diluted concentrations of pollutants that originated there at an earlier time. This drainage effect has been described in detail by Doran and Zhong (2000) and Jazcilevich et al. (2003). For this reason is difficult to find a diurnal pattern in our VOC time series at this site (see Figures 3e and 3f). In general, concentrations of benzene, toluene, C_2-benzenes and C_3-benzenes were lower than 1 ppbv during the entire diurnal cycle. However, a

number of spikes with higher concentrations were observed, possibly due to local sources, such as burning of agricultural debris.

The FOS provided an alternative method to measure concentrations of olefins at real time at the CENICA site during the MCMA-2003 study. As shown in Figure 4, the diurnal average pattern of olefinic VOCs detected by the FOS exhibits a similar pattern to what would be expected for typical pollutants emitted by mobile sources (INE, 2000). The highest olefin concentrations were measured at 7:00 h and ranged from 30 to 87 ppbv, with 58 ppbv as average. This morning peak is attributed to the release of anthropogenic emissions into a shallow mixed layer as the work day. Low olefin concentrations were observed during the afternoon, with an average of 6.6 ppbv, when dilution through the deep mixed layer was large and emissions were reduced compared to morning periods. The diurnal olefin pattern was relatively constant during the entire study. The MCMA-2003 field campaign included the Holy Week (April 14 – 20), a period in which the vehicular traffic is reduced as many of the city residents leave for the holiday period. By taking measurements before, during and after this period, we expected to obtain data to help determine the influence of vehicular emissions upon atmospheric pollution. The FOS reported a small difference of 6 ppbv in the olefin mixing ratio during the early morning peak between Holy Week and the other two measurement weeks.

A comprehensive analysis of the diurnal patterns of benzene and toluene measured at La Merced by DOAS is provided by Grutter and Flores (2004), while Jobson et al. (2005) describe in detail the diurnal course of a number of VOCs measured by PTR-MS at the CENICA site.

2.6.2. Ambient mixing ratios and hydrocarbon reactivity

We have described that the highest ambient mixing ratios of VOCs in the atmosphere of Mexico City occur during the morning rush hours (6:00 to 9:00 h). An analysis of the canister sampling from the four urban monitored sites (Pedregal, La Merced, CENICA and Constituyentes) during this morning period will provide a description of the VOC species that contribute to photochemical ozone and haze production in Mexico City. On the basis of average

concentrations, the 10 most abundant VOCs for those sites were in decreasing order: propane (113 ppbv), n-butane (43), ethylene (19), i-butane (16), i-pentane (16), ethane (15), toluene (13), acetylene (12), n-pentane (7), and MTBE (6). In general, VOC mixing ratios observed in this study are slightly lower than those reported in previous studies (Arriaga et al., 1997; Mugica et al., 2002), which is consistent with Arriaga et al. (2004) conclusions that ambient VOC concentrations have reach a stabilization level or have decreased. The elevated levels of low molecular weight alkanes measured here are consistent with those reported in the first VOC study in Mexico City (Blake and Sherwood, 1995), and they are attributable mainly to the widespread use of LPG, as discussed previously.

It is useful to examine the VOC distribution in an urban area in terms of reactivity with the hydroxyl radical (OH), which in fact represents the contribution of each VOC specie to the OH loss rate. Such an OH loss rate is a measure of the initial peroxy radical formation rate, which is frequently the rate-limiting step in ultimate ozone formation. The actual amount of ozone produced by a given hydrocarbon depends on their particular oxidation mechanism, the abundance of other hydrocarbons, and NO_x concentrations (Carter, 1994). While realizing that this approach does not account for the full atmospheric chemistry of the compounds considered, it provides a useful approximation of their relative contributions to daytime photochemistry. For this purpose, Table 3 lists the major hydrocarbons in the atmosphere of the Valley of Mexico by reactivity with OH along with their average ambient concentrations during the morning rush hour. Average reactivity levels and concentrations are shown in columns according to the site type: urban, rural (Santa Ana Tlacontenco, La Reforma and Teotihuacan) and industrial (Xalostoc). For urban and rural sites, the reactivity values were calculated independently for each monitored site but, as the results were quite similar, only the reactivity values calculated for the average concentrations of each type of site are presented. VOCs are sorted in descendent order according to their reactivity in urban sites. The OH reaction rate coefficients shown in Table 3 correspond to the coefficients published by Atkinson (1994, 1997) at 298 K and 1 atm.

Where no information was available, the OH reaction rate coefficient was estimated from information from similar compounds.

The ten most important hydrocarbons in the urban atmosphere of the Valley of Mexico in terms of ozone production include two aromatics, five olefins and three alkanes: ethylene, propylene, propane, n-butane, m,p-xylenes, i-butene, toluene, 2-methyl-1-butene, 2-methyl-2-butene and i-pentane. It is important to point out that the two most reactive VOCs at urban sites were also the top two VOCs reported for the industrial site. These species were olefins mainly emitted by vehicles with high concentrations and high reaction rate coefficients. Also, it is important to highlight that the elevated concentrations of propane and n-butane are sufficient to rank these two alkanes among the top 5 VOCs, even though their reactivity rate coefficients are small compared to those for olefins and aromatics.

Overall, major VOCs in terms of ozone production in the Valley of Mexico correspond to VOCs of anthropogenic origin. Biogenic VOCs seem to be relatively insignificant. Isoprene concentrations were low (0.36 ppbv in urban sites) and were assumed to have their origin more in vehicle exhaust than in vegetation. Vegetation was sparse at the three monitored rural sites, and therefore isoprene concentrations were also low (0.05 ppbv). At rural sites, low molecular weight alkanes were the most abundant species, having their origin in LPG leakages as it has been discussed before. At rural sites, the most reactive hydrocarbon was styrene, with ambient concentrations similar to those observed at urban sites (0.51 ppbv). The presence of styrene in these rural environments is attributed to local biomass and trash burning.

A comparison of the reactivity levels between the urban and industrial sites indicates that on average the industrial location is 1.8 times more reactive than an urban atmosphere. Half of the measured VOCs at the industrial site had reactivity levels between 1.4 and 2.1 times higher than at the urban sites. A similar comparison between urban and rural sites shows that an urban atmosphere is 5.9 times more reactive than a rural atmosphere in the Valley of Mexico.

2.6.3. Distribution of VOCs by groups

Figure 5 shows the VOC distributions by groups during the morning (6:00 to 9:00 h) and afternoon (12:00 to 15:00 h). Note that concentrations are in ppbC. Hereafter all contribution fractions are based on ppbC, as well. The data shown in Figure 5 were derived from canister samples collected and analyzed by the WSU and IMP groups. In the morning, the entire valley experiences a relatively homogeneous mix of VOCs consisting of ~60 % alkanes, ~15 % aromatics, ~5 % olefins and a remaining 20% of alkynes, halogenated hydrocarbons, oxygenated species (esters, ethers, etc.) and other unidentified VOCs. In our study, concentrations of total VOCs in the industrial area were 1.6 times higher than at urban sites during the morning period, while concentrations at rural sites were about one-sixth of those measured at the urban locations. In the afternoon, distributions were different with a higher contribution of unidentified VOCs at the urban sites. The total VOC concentration was 2.4 times lower in the afternoon compared to the morning at urban sites. However, not all VOC groups showed the same reduction, alkanes were reduced 70%, olefins 60%, aromatics 53%, and unidentified VOCs 20%. Lower afternoon concentrations are normally ascribed to increased dispersion and photochemical oxidation during the midday period. However, employing these mechanisms alone is insufficient because the relatively unreactive alkane group showed the largest proportional loss. Emission rates must be a factor, as well, with a large decrease in alkane emissions relative to aromatics and olefins. Santa Ana Tlacotenco, a rural downwind boundary site, showed an opposite pattern. Transport from the urban region resulted in afternoon VOC concentrations 2.4 higher than in the morning.

Hydrocarbons. At urban and industrial sites during the morning period, hydrocarbons with four or less carbons represent the major fraction of the alkanes and alkenes. The main contributors are propane, n-butane, ethylene, propylene, and the sum of i-, t-2- and -c-2 butenes. 1,3-butadiene is a four-carbon diene that is considered to be a carcinogenic and reproductive toxicant to humans, whose main source is vehicle exhaust (USEPA, 1999). 1,3-Butadiene is of concern in Mexico City because of its relatively elevated concentrations: 0.48 and 0.63 ppbv at urban and industrial sites, respectively.

The most abundant aromatics were the BTEX species (benzene, toluene ethylbenzene and the xylene isomers). They average about 75% of the aromatic burden. Toluene showed an average concentration of 13.1 ppbv at urban sites and concentrations up to about 33 ppbv in the industrial area. Total xylene concentrations averaged 14.5 ppbv at the industrial site and about half that (7. 4 ppbv) in the urban area. Ethylbenzene had average concentrations about the same as the individual xylene isomers with urban concentrations 1.5 ppbv in the urban area and about 3 ppbv in the industrial region. Benzene averaged 5.1 and 2.9 ppbv at the industrial and urban sites. The urban benzene concentration determined in this study is similar to that reported by Bravo et al. (2002) for residential areas in southwest Mexico City.

Oxygenated hydrocarbons. Methyl tertiary-butyl ether (MTBE) is the only oxygenated VOC listed in Table 3. MTBE is used as an additive in unleaded gasoline to enhance the combustion efficiency. MTBE contributes no more than 2 % to the total VOC burden of the Valley of Mexico. Ethyl tertiary butyl ether (ETBE) was another oxygenated VOC identified in the samples analyzed by IMP. ETBE is not included in Table 3 because it was measured at only half of the sites (Xalostoc, Pedregal, CENICA and La Merced). Average ETBE concentrations were 0.3 and 0.6 ppbv at urban and industrial sites, respectively. Both, MTBE and ETBE have their origin in vehicle exhaust due to incomplete combustion and gasoline leakage from fueling stations.

Halogenated hydrocarbons. The GC-FID technique can be used to identify halogenated VOCs, but not to quantify precisely their concentration, since halogenated VOCs contain other atoms besides carbon and hydrogen. However, IMP quantified approximately the ambient concentrations of 14 halogenated VOCs in ppbC at the Xalostoc, Pedregal, CENICA and La Merced sites. Table 4 shows that the halogenated species contribute less than 2.5% to the total VOC burden. Many of them are classified as toxic and carcinogenic species, and others, such as the vinyl chloride, are suspected to cause congenital malformation. Another concern is the very long atmospheric residence times of chlorofluorocarbons such as Freon 113. They can eventually diffuse into the stratosphere where photolysis produces chorine radicals, which

catalytically destroy ozone and indirectly contribute to the greenhouse effect. All halocarbons listed in Table 4 are emitted from anthropogenic sources in urban atmospheres. Even though the use of chlorofluorocarbons as refrigerants is not allowed anymore, most release of chlorofluorocarbons occurs during the disposal of refrigeration units and, in developing cities such as Mexico City, leakage from old residential refrigerators may be a significant source, also. This may be the reason why ambient concentrations of Freon-113 were higher for urban sites than for the industrial site.

2.6.4. Comparison of ambient VOC concentrations to vehicles exhaust signatures

Since roadway vehicle emissions are normally the dominant VOC source in urban areas (Watson et al., 2001), it was of interest to compare the mixing ratios obtained from canister sampling at the urban sites to the vehicle exhaust source signature measured during mobile vehicle chase experiments.

In brief, vehicle chase measurements were made using the Aerodyne mobile laboratory equipped with several instruments to characterize emissions from vehicles under actual driving conditions (see Herndon et al., 2005). In chase mode, the Aerodyne van was driven immediately behind a selected vehicle for approximately 10 to 20 minutes. Vehicle plume samples were collected with an auto-sampling system that included a fast response CO_2 sensor (LICOR LI-7000). Distinct peaks in the CO_2 mixing ratio during a vehicle chase indicated interception of the exhaust plume. When the CO_2 levels were elevated above a selected threshold, a conditional VOC sampler was activated to sample into a "chase" canister and when CO_2 levels were below the threshold, air was channeled into an "urban background" canister.

For the comparison between ambient and vehicular emission data, it is necessary to remove the impact of photochemical aging on source signatures. This is achieved by regressions between species with similar atmospheric lifetimes. The source ratio is preserved for species with similar lifetimes because photochemical loss and mixing will result in similar rates of concentration change (Parrish et al., 1998). This procedure allowed all of the ambient data to be

used including afternoon data when mixing ratios were typically lower due to mixing and photochemical removal. The slope obtained in ambient data plots defines the source ratio that can be directly compared to the vehicular chase measurements and literature values. In practice, there are a limited number of species that can be employed in this analysis because photochemical loss rates must be similar. We have constrained the hydrocarbon pairings such that OH rate coefficients differ by 20% or less. The exception is the regression between propene and ethene where rate constants differ by a factor of three.

Correlations between selected alkenes, alkanes and aromatics are shown in Figures 6, 7 and 8, respectively. The average ratios from the vehicular chase data and from the ambient sampling at urban, rural and industrial sites are tabulated in Table 5. In addition, Table 5 shows average exhaust ratios for Mexican gasoline and diesel vehicles from a tunnel study conducted in Mexico City (Mugica et al., 2001). An average vehicle exhaust ratio for light duty vehicles calculated by Jobson et al. (2004) from six published tunnel studies conducted in the 1990s in US and Canada is included in the table, as well.

In the alkene group, t-2-pentene versus c-2-pentene exhibits excellent agreement between the ambient and vehicular emission ratios. The ambient concentrations span three orders of magnitude due to atmospheric processing and variations in source strength. In general, the highest concentrations were recorded during vehicular chase experiments. In a few cases, ambient industrial and urban samples approached vehicle chase concentrations. The very good agreement between the exhaust emission and ambient ratios for the 2-pentenes clearly implies a vehicle exhaust source signature. The t-2-butene versus the c-2-butene correlation shows reasonable agreement between vehicular chase emissions, ambient ratios and literature values. The similarity of the ambient and vehicle exhaust ratios for these species suggests vehicle exhaust as their primary source. For 1-hexene and 1-pentene, ambient data showed considerable scatter suggesting that each site is impacted by a mix of different sources, and that sources and emission rates of 1-hexene are not strongly correlated with sources and emission rates of 1-pentene. The propylene:ethylene ratio displays a fair correlation but contains considerable

scatter. The vehicle emission ratio (0.58±0.37) bisects the ambient data, but the large amount of scatter about this ratio is indicative of multiple independent sources. The emissions ratio itself has a high degree of scatter, suggesting that the emission relation of these species may vary considerably within the Mexican fleet. As indicated previously, propylene and ethylene rate constants vary much more than for the other alkene pairs, which may contribute also to the poor correlations observed for these species.

Alkane ratios for i-butane:n-butane showed excellent agreement between the ambient, vehicular emission and literature values. Note that the average ratios in Table 5 for ambient (0.38 industrial and 0.37 urban) and vehicle exhaust (0.36) are essentially equal. Mugica et al. (2001) reported exhaust emission ratios of 0.32 and 0.48 for gasoline and diesel vehicles in Mexico. These results suggest that vehicle exhaust is an important source of n-butane and i-butane, besides residential LPG usage. Through a source apportionment analysis, Mugica et al. (2002) determined that vehicle exhaust contributes ~20% to the presence of these two alkanes, while handling and distribution of LPG contributes ~65%. Although LPG powered vehicles represent less than 1% of the total fleet, they should be considered also as important sources. Schifter et al. (2000) evaluated the LPG vehicles program implemented in Mexico City and found that 95% of them exceed the required environmental regulations. The LPG fleet is composed mainly by vehicles of intensive use (light- and heavy duty trucks, and small buses with a 20 passenger capacity). Gasca et al. reported that tailpipe and evaporative emissions of i-butane contribute 16 and 28%, respectively to the total VOC emissions from LPG vehicles, and 17 and 21% of n-butane.

Good agreement between 2-methylpentane:3-methylpentane ambient, vehicle chase and literature ratios imply vehicle exhaust emissions as the primary source of these VOCs in the Mexico City atmosphere. For the other alkane pairs listed in Table 5, agreement between ambient and vehicle exhaust ratios was not as good. The ambient ratios generally followed the vehicular emissions line, but with considerable scatter. This suggests that species such as

isopentane, n-pentane, hexane, cyclohexane, n-heptane, n-nonane and n-octane are emitted by vehicles, but also by a variety of other anthropogenic sources.

As illustrated in Figure 8, the ratios of i-propylbenzene and styrene with other aromatics displayed significant scatter suggesting the importance of other anthropogenic sources, such as industries and trash burning, for these two VOCs. The xylenes showed excellent agreement with vehicle exhaust ratios, in fact they showed the best agreement between all correlated VOCs, indicating clearly that their source is vehicle exhaust. The ethylbenzene:toluene average ratios from vehicle exhaust and ambient measurements agreed quite well although there was more scatter in the data. The toluene versus benzene ratio violates the assumption of similar OH reactivity, but is shown to illustrate the variability. It varied from 3.7 at rural sites to 9.2 at the industrial site. The median ratio at urban sites (4.9) was similar to the ratio published by Bravo et al. (2002) for residential areas of Mexico City.

Another method of comparing the ambient data to the roadway vehicle exhaust signature is to compare ratios using a tracer species as a reference. In this case, we compared hydrocarbon abundances relative to acetylene since acetylene is known to be a good marker for vehicular fuel combustion (Barletta et al., 2002). The use of ratios compresses the large differences in concentration that exist between the various environments and provides a direct comparison of hydrocarbon distribution patterns. To eliminate changes in the ratio due to chemical aging, the ambient data were restricted to the morning period between 6:00 and 9:00 h. Figure 9 shows the median values of the VOC/acetylene ratios together with the 10^{th} and 90^{th} percentile ranges. A good correlation can be seen between vehicle exhaust and ambient ratios at urban sites with all exhaust ratios falling within the 10-90 percentile confidence interval. Species with the highest OH reactivity showed bigger deviations from the exhaust ratio suggesting that, even in samples collected during the early morning hours, a chemical aging bias may affect the data. Reactive species such as 1,3-butadiene, isoprene, 1-pentene, 1,2,4-trimethylbenzene and 1,3,5-trimethylbenzene had median ratios that were between 30 and 45% of the exhaust values. For example, while the abundances of 1,3-butadiene and 1,3,5-trimethylbenzene relative to acetylene

at urban sites were 31 and 44% those of the chasing samples, the ambient MTBE and toluene ratios with acetylene agreed well with the exhaust ratio. This would support a chemical age argument because 1,3-butadiene and 1,3,5-trimethylbenzene are about ten times more reactive with OH than MTBE and toluene. It is important to highlight that the C_2-C_4 alkanes (ethane, propane, i-butane and n-butane), and ethyl acetate showed higher ratios compared to exhaust values at urban sites. This is what would be expected if other anthropogenic sources contribute to low molecular weight alkane emissions. All olefin and aromatic ratios were lower than the vehicle chase ratios, which is consistent with an ageing bias. Interesting, the 90th percentile ambient ratio boundary agrees very well with the vehicle chase ratio. The 90th percentile data perhaps reflects fresher emissions and less aging bias.

2.6.5. Comparison of ambient VOC concentrations to the emissions inventory

The ambient VOC data can be compared to the distribution of VOC classes represented in the most recent emissions inventory derived for air quality modeling in Mexico City (West et al., 2004). This emissions inventory was based on annual emissions reported in 1998 (CAM, 2001). The official inventory was created by local government authorities using bottom-up methods and emissions factors which were either measured locally or taken from elsewhere. The VOC speciation was based on the SAPRC-99 chemical mechanism for VOC reactivity assessment (Carter, 2000) and a standard mixture of hydrocarbons in urban atmospheres in the United States (Jeffries et al., 1989). The speciation was determined for each source category using emissions profiles measured in Mexico City (Mugica et al., 1998, 2002; Vega et al., 2000). These profiles were adjusted to include species and source categories not measured in Mexico City using emissions profiles from the SPECIATE database (EPA, 1993).

The median ambient data are lumped into the inventory modeling classes in Table 6. For comparison, the total emissions by each class are also included in the table along with the corresponding percentage of the total. The comparison was limited to the morning period between 6:00 and 9:00 h when concentrations are strongly related to anthropogenic emissions

before the photochemistry's beginning. The column showing the adjustment factor, which takes into account the molecular weight of each class, reflects the degree of change needed to yield the same distribution in the emissions inventory as observed in ambient VOC concentrations. This comparison of early morning ambient data and gridded total emissions suggests that some, but not all, classes are underestimated in the inventory by factors of 1.1 to 3.1, in contrast to other species that are overestimated, such as some aromatic and olefin classes (ARO1, ARO2, OLE1 and OLE2). The extreme adjustment factors of 10.8 and 0.05 for butadiene and isoprene, respectively, are due to their small ambient concentrations compared to other VOC classes. Overall, the emissions inventory appears to underestimates the contribution of alkanes and overestimates the contributions of olefins and aromatics. These results do not support the idea that all VOC emissions reported in the official inventory are underestimated by a factor of 3 (Arriaga et al., 2004; West et al., 2004), however this is a relatively simplistic comparison that does not fully account for the spatial and temporal distribution of emissions, the small number of monitoring sites, or for any early morning chemistry that might affect the ambient levels.

2.6.6. Comparison of olefin concentrations measured by FOS to olefin concentrations calculated by the CIT model

The high resolution and continuous data from instruments such as the FOS provide a basis for comparison with grid model simulations of selected VOCs. For example, results are shown in Figure 10 for olefin mixing ratios measured at the CENICA site during the MCMA-2003 field campaign by FOS and modeled with the California Institute of Technology (CIT) airshed model. This model was used by West et al. (2004) to model ozone photochemistry in Mexico City. Concentrations of ethene, isoprene, and groups OLE1 and OLE2 in the CIT model were weighted according to their contribution to the hydrocarbon mix used by the SAPRC99 chemical mechanism and their corresponding FOS response factor.

The modeled concentrations closely follow the measured concentrations. This result was unexpected because of all the assumptions and uncertainties involved in the model and the FOS response. An evaluation of the fractional error defined by:

$$Fractional\ \ Error = \frac{1}{N}\sum_{i=1}^{N}\frac{\left|\left(c_{m_i} - c_{o_i}\right)\right|}{\frac{1}{2}\left(c_{m_i} - c_{o_i}\right)}(100\%) \qquad (1)$$

where c_m and c_o represents the modeled and measured concentrations, respectively, showed a median error of 51% for the entire MCMA-2003 field campaign. During the daytime (6:00 - 19:00 h) the fractional error was smaller than at night (19:00 – 6:00 h), 48% versus 56%. Figure 10a shows there were periods when modeled and measured levels matched very well (day 105), and other periods when the FOS reported higher or lower concentrations than the model. In general, the model tends to under-predict concentrations at night and to over-predict during the day. Figure 10b shows that the major discrepancy occurs during the rush hour when the model over-predicts the morning peak. This peak is predicted by the model to occur one hour later than observed in the ambient measurements. Overall, the estimated olefin concentrations are in good agreement with the measured concentrations, since modeled concentrations are in the one standard deviation range of the measured concentrations.

This result is consistent with our conclusions drawn from the comparison with the emissions reported in the emissions inventory, and from eddy covariance flux measurements of selected VOCs performed during the MCMA-2003 (Velasco et al., 2005). These analyses suggest that emissions of some VOC classes reported in the official emissions inventory are essentially correct, while others are underestimated by factors between 1.1 and 3. If this is correct, previous suggestions that poor agreement between modeled and measured ozone levels in Mexico City was due to a threefold underestimation of total VOC emissions (Arriaga-Colina et al., 2004; West et al., 2004) may not be correct. Quite possibly other factors, such as incorrect NO_x emissions or an erroneous evolution of the boundary layer may be causing the poor ozone agreement.

2.7. Summary and conclusions

A number of independent methods were used to measure ambient VOC concentrations in the Valley of Mexico during the MCMA 2002 and 2003 field campaigns. The use of different techniques allowed a wide range of individual species to be measured with different spatial and temporal scales, providing confidence in the data, as well as a basis for comparison with grid model simulations of selected VOCs. The VOC concentrations were analyzed to understand better their distribution, diurnal pattern, origin and reactivity in the atmosphere of Mexico City. All data have been valuable to evaluate the Mexican emissions inventory, as well to support effective control strategies. The following points summarize the main findings and conclusions of this work.

- Ambient air inter-comparison of GC, PTR-MS and DOAS measurements for selected VOCs reported good agreement. This allows to combine data into a single comprehensive data set including measurements of VOCs concentrations of different spatial and temporal scales.
- At urban sites, the ambient concentration of VOCs depends strongly on the vehicular activity. At La Merced, no late afternoon peak in VOC concentration was observed, while at the Pedregal site the morning and late afternoon VOC peaks were observed. At both sites, the VOC peaks corresponded to the vehicular traffic peaks during the morning and afternoon rush hours.
- At boundary sites, the diurnal profiles of ambient VOC concentrations depend mainly on wind patterns. These sites correspond to rural landscapes, where burning of agriculture debris and trash is common. Biomass burning was observed to produce spikes on ambient concentrations of selected VOCs, such as styrene.
- In general, VOC concentrations reported here are smaller than concentrations reported in the last decade. This finding is consistent with Arriaga et al. (2004), who state that ambient VOC concentrations have stabilized and possibly decreased. This is a good indicator that enacted policies and actions to control VOC emissions have shown success, despite the growth in the vehicular fleet and other activities.

- In the morning, the entire valley experiences a relatively homogeneous mix of VOCs consisting of ~60 % alkanes, ~15 % aromatics, ~5 % olefins and a remaining 20% of alkynes, halogenated hydrocarbons, oxygenated species and other unidentified VOCs. Contributions are based on ppbC. In the afternoon, distributions were different with a higher contribution of unidentified VOCs at the urban sites.
- In terms of ozone production, olefins are the hydrocarbons of major concern in Mexico City; ethylene and propylene are the two most reactive VOCs. The elevated concentrations of propane and n-butane are sufficient to rank these two alkanes among the top 5 VOCs, even though their reactivity rate coefficients are small compared to those for olefins and aromatics.
- Elevated levels of toxic VOCs, such as 1,3-butadiene, vinyl chloride and the BTEX hydrocarbons were observed. These VOCs are of public health concern.
- The ratios between ambient concentrations of two hydrocarbons of similar lifetime and the ratios of each different VOC with acetylene demonstrated that many olefins and aromatics have their main origin in vehicle exhaust, such as the xylenes, toluene, ethylbenzene, t-2-pentene, c-2-pentene, etc., as well as MTBE and some alkanes, such as 2-methylpentane and 3-methylpentane. Besides, the ratios with acetylene showed that vehicle exhaust contributes to the emission of all VOC species, including alkanes of light molecular weight that have been widely related with the use of residential LPG, particularly propane and n-butane.
- Examination of the VOC data in terms of the relative distribution of lumped modeling VOC classes and comparison to the emissions inventory suggests that the inventory underestimates the contribution of some alkanes and overestimates the contributions of some olefins and aromatics.
- The comparison between ambient concentrations of olefins measured by FOS and olefins predicted by the CIT model at the CENICA site showed relatively good agreement. This finding does not support the statement that the emissions inventory underestimates the emissions of VOCs by a factor of 3.

Although some pollutants have been successfully controlled in Mexico City during the last decade, other pollutants are still reporting elevated concentrations. Among these pollutants are

several VOCs discussed in this manuscript. Effective control strategies to reduce ambient VOC concentrations need to consider both, the VOC reactivity in terms of production of ozone and other secondary pollutants, and the toxic potential. These control strategies must be focused in improve fuels quality and vehicle technology, since there are strong evidence that vehicle exhaust is the main source of many hydrocarbons. However, they are not going to solve by themselves the air pollution problem in Mexico City, where not all population have access to efficient transport and clean technology for basic daily activities, such as cooking and water heating. The economic necessities of the major population need to be solved, and the actual style of life needs to be modified, as well. Private cars cannot continue being the main transport mode, new types of massive public transport with excellent quality need to be implemented to promote the less use of private cars. A good example is the system of confined buses to unique lanes in main avenues simulating subways lines above the surface, such as the "Metrobus system" in Mexico City, which requires a relatively inexpensive infrastructure compared to other systems. Also, new policies promoting environmental education, the use of bicycle and a greater support to environmental research are needed to reduce the harmful VOC levels reported here, and overall, the air pollution problem in Mexico City.

2.8. References

Arriaga, J.L., Escalona, S., Cervantes, A.D., Orduñez, R. & Lopez, T. Seguimiento de COV en aire urbano de la ZMCM 1992-1996. In Contaminación Atmosférica, vol. 2, edited by L.G. Colin and J.R. Varela, pp 67-98, UAM, Mexico D.F., 1997.

Arriaga-Colina, J.L., West, J.J., Sosa, G., Escalona, S.S., Orduñez, R.M. & Cervantes, A.D.M. Measurements of VOCs in Mexico City (1992-2001) and evaluation of VOCs and CO in the emissions inventory. *Atmospheric Environment* **38**, 2523-2533 (2004).

Atkinson, R. Gas-phase tropospheric chemistry of organic compounds. *Journal of Physical and Chemical Reference Data Monographs* **2**, 11-216 (1994).

Atkinson, R. Gas-phase tropospheric chemistry of volatile organic compounds. *Journal of Physical and Chemical Reference Data Monographs* **26**, 215-290 (1997).

Barletta, B., Meinardi, S., Simpson, I.J., Khwaja, H.A., Blake, D.R. & Rowland, F.S. Mixing ratios of volatile organic compounds (VOCs) in the atmosphere of Karachi, Pakistan. Atmospheric Environment **36**, 3429-3443 (2002).

Blake, D.R. & Sherwood, F. Urban leakage of liquefied petroleum gases and its impact on Mexico City air quality. *Science* **269**, 953-956 (1995).

Bravo, H., Sosa, R., Sanchez, P., Bueno, E. & Gonzalez, L. Concentration of benzene and toluene of the southwestern area at the Mexico City Metropolitan Zone. *Atmospheric Environment* **36**, 3843-3849 (2002).

Carter, W. P. L. Development of ozone reactivity scales for volatile organic compounds, *Journal of Air & Waste Management Association* **44**, 881– 899 (1994).

Carter, W.P.L. Documentation of the SAPRC-99 Chemical Mechanism for VOC reactivity assessment, final report to California Air Resources Board, contracts 92-329 and 95-308. (Calif. Air Res. Board, Sacramento, California 2000, available at www.cert.ucr.edu/~carter).

Comisión Ambiental Metropolitana (CAM). Inventario de emisiones a la atmósfera, Zona Metropolitana del Valle de México, 1998. (Comisión Ambiental Metropolitana, México, D.F. 2001).

Conner, T.L., Lonneman, W.A. & Seila, R.L. Transportation related volatile hydrocarbon source profiles measured in Atlanta. *Journal of Air & Waste Management Association* **45**, 383–394 (1995).

Cruz-Nuñez, X., Hernandez-Solis, J.M. & Ruiz-Suarez, L.G. Evaluation of vapor recovery systems efficiency and personal exposure in service stations in Mexico City. *The Science of the Total Environment* **309**, 59-68 (2003).

de Gouw, J.A., Goldan, P.A., Warnake, C., Kuster, W.C., Roberts, J.M., Marchewka, M., Bertman, S.B., Pszenny, A.A.P. & Keene, W.C. Validation of proton transfer reaction-mass spectrometry (PTR-MS) measurements of gas-phase organic compounds in the atmosphere during the New England Air Quality Study (NEAQS) in 2002. *Journal of Geophysical Research* **108**, 4682-4199 (2003).

Doran, J.C. & Zhong, S. Thermally driven gap winds into the Mexico City basin. *Journal of Applied Meteorology* **39**, 1330-1340 (2000).

Evans, J., *et al*. in *Quality in the Mexico Megacity: an integrated assessment* (ed. Molina, L.T. & Molina M.J.) 105-136 (Kluwer Academic Publishers, Netherlands, 2002).

Finlayson-Pitts, B.J. & Pitts, J.N. Chemistry of the upper and lower atmosphere. (Academic Press, USA 2000).

Fraser, M.P., Cass, G.R., & Simoneit, B.R.T. Gas-phase and particle-phase organic compounds emitted from motor vehicle traffic in a Los Angeles roadway tunnel. *Environmental Science and Technology* **32**, 2051–2060 (1998).

Gakenheimer, R., Molina, L.T., Sussman, J., Zegras, C., Howitt, A., Makler, J., Lacy, R., Slott, R. & Villegas A. The MCMA transportation system: mobility and pollution. In Air Quality in the Mexico Megacity: An Integrated Assessment., edited by Molina, L.T. & Molina M.J., pp 213-284. Kluwer Academic Publishers, Netherlands, 2002.

Gasca, J., Ortiz, E., Castillo, H., Jaimes, J.L. & Gonzalez, U. The impact of liquefied petroleum gas usage on air Quality in Mexico City. *Atmospheric Environment* **38**, 3517-3527 (2004).

Gobierno del Distrito Federal (GDF). Informe del Estado de la Calidad del Aire y Tendencias 2003 para la Zona Metropolitana del Valle de México. (Dirección General de Gestión Ambiental del Aire. México, D.F., 2004).

Gomez-Perales, J.E., et al. Commuters' exposure to $PM_{2.5}$, CO, and benzene in public transport in the metropolitan area of Mexico City. *Atmospheric Environment* **38**, 1219-1229 (2004).

Grutter, M. & Flores, E. Air pollution monitoring with two optical remote sensing techniques in Mexico City. Proceedings of SPIE 5571, Gran Canaria, Spain, 13-16 of September (2004).

Guenther, A. & Hills, A. Eddy covariance measurement of isoprene fluxes. *Journal of Geophysical Research* **103**, 13145-13152 (1998).

Herndon, S.C., Kolb, C.E., Lamb, B., Westberg, H., Allwine, E., Velasco, E., Knighton, B., Zavala, M., Molina, L. & Molina, M. Conditional sampling of volatile organic compounds in on-road vehicle plumes. *In preparation* (2005).

Instituto Nacional de Ecología (INE). Almanaque de datos y tendencias de la calidad del aire en ciudades mexicanas. (INE-SEMARNAT. México, D.F., 2000).

Jazcilevich, A.D., Garcia, A.R. & Ruiz-Suarez, L.G. A study of air flow patterns affecting pollutant concentrations in the Central Region of Mexico**.** *Atmospheric Environment* **37**,183-193 (2003).

Jeffries, H.E., Sexton, K.G., Arnold, J.R. & Kale T.L. Validation testing of new mechanisms with outdoor chamber data, Volume 2: analysis of VOC data for the CBA and CAL photochemical mechanisms, final report EPA-600/3-89-010b. (Environmental Protection Agency, Research Triangle Park, N.C. 1989).

Jobson, B.T., Alexander, M.L., Prazeller, P., Berkowitz, C.M., Westberg, H., Velasco, E., Allwine, E., Lamb, B., Volkamer, R., Molina, L. & Molina, M. Intercomparison of volatile organic carbon measurements techniques and data from the MCMA 2003 field experiment. *In preparation* (2005).

Jobson, B.T., Berkowitz, C.M., Kuster, W.C., Goldan, P.D., Williams, E.J., Fesenfeld, F.C., Apel, E.C., Karl, T., Lonneman, W.A. & Riemer, D. Hydrocarbon source signatures in Houston, Texas: influence of the photochemical industry. *Journal of Geophysical Research* **109**, D24305,doi10.1029/2004JD004887 (2004).

Kirchstetter, T.W., Singer, B.C., Harley, R.A., Kendall, G.R. & Chan W. Impact of oxygenated gasoline use on California light duty vehicle emissions, *Environmental Science and Technology* **30**, 661– 670 (1996).

Lindinger, W., Hansel, A. & Jordan, A. On-line monitoring of volatile organic compounds at pptv levels by means of proton-transfer-reaction mass spectroscopy (PTR-MS): Medical applications, food control and environmental research. *International Journal of Mass Spectrometry Ion Processes* **173**, 191-241 (1998).

Meneses, F., Romieu, I., Ramirez, M., Colome, S., Kochy, F., Ashley, D. & Hernandez-Avila, M. A survey of personal exposures to benzene in Mexico city. *Archives of Environmental Health* **54**, 359-363 (1999).

Molina, M.J. & Molina, L.T. Megacities and atmospheric pollution. *Air and Waste Management Association* **54**, 644-680 (2004).

Mugica, V., Ruiz, M.E., Watson, J. and Chow, J. Volatile aromatic compounds in Mexico City atmosphere: levels and source apportionment. *Atmósfera* **16**, 15-27 (2003).

Mugica, V., Vega, E., Arriaga, J.L. & Ruiz, M.E. Determination of motor vehicle profiles for non-methane organic compounds in the Mexico City Metropolitan Area. *Journal of Air & Waste Management Association* **48**, 1060-1068 (1998).

Mugica, V., Vega, E., Chow, J., Reyes, E., Sanchez, G., Arriaga, J.L., Egami, R. & Watson, J. Speciated non-methane organic compounds emissions from food cooking in Mexico. *Atmospheric Environment* **35**, 1729-1734 (2001).

Mugica, V., Vega, E., Ruiz, H., Sanchez, G., Reyes, E. & Cervantes, A. Photochemical reactivity and sources of individual VOCs in Mexico City. In Air pollution X (ed. Brebbia, C.A. & Martin-Duque, J.F.) WIT Press, UK 2002.

Mugica, V., Watson, J.,Vega, E., Reyes, E., Ruiz, M.E. & Chow, J. Receptor model source apportionment of nonmethane hydrocarbons in Mexico City. *The Scientific World Journal* **(2)**, 844– 860 (2002).

Ortiz, E., Alemon, E., Romero, D., Arriaga, J.L., Olaya, P., Guzman, F. & Rios, C. Personal exposure to benzene, toluene and xylene in different microenvironments at the Mexico City metropolitan zone. *The Science of the Total Environment* **287**, 241-248 (2002).

Parrish, D.D., Trainer, M., Young, V., Goldan, P.D., Kuster, W.C., Jobson, B.T., Fehsenfeld, F.C., Lonneman, W.A., Zika, R.D., Farmer, C.T., Riemer, D.D. & Rodgers, M.O. Internal consistency tests for evaluation of measurements of anthropogenic hydrocarbons in the troposphere. *Journal of Geophysical Research* **103**, 22339–22359 (1998).

Raga, G.B., Baumgardner, D., Castro, T., Martinez-Arroyo, A. & Navarro-Gonzalez, R. Mexico City air quality: a qualitative review of gas and aerosol measurements (1960-2000). *Atmospheric Environment* **35**, 4041-4058 (2001).

Rogak, S.N., Pott, U., Dann, T. & Wang D. Gaseous emissions from vehicles in a traffic tunnel in Vancouver, British Columbia. *Journal of Air & Waste Management Association* **48**, 604–615 (1998).

Sagebiel, J.C., Zielinska, B., Pierson, W.R. & Gertler, A.W. Real world emissions and calculated reactivities of organic species from motor vehicles. *Atmospheric Environment* **30**, 2287–2296 (1996).

Schifter, I., Diaz, L., Duran, J., Guzman, E., Chavez, O. & Lopez-Salina, E. Remote sensing study of emissions from motor vehicles in the Metropolitan Area of Mexico City. *Environmental Science and Technology* **37**, 395-401 (2003).

Schifter, I., Diaz, L., Lopez-Salinas, E., Rodriguez, R., Avalos, S. & Guerrero, V. 2000. An evaluation of the LPG vehicles program in the metropolitan area of Mexico City. *Journal of the Air and Waste Management Association* **50**,301–309 (2000).

Shiohara, N., Fernández-Bremauntz, A., Blanco-Jiménez, S. & Yanagisawa Y. The commuters' exposure to volatile chemicals and carcinogenic risk in Mexico City. *Atmospheric Environment* **39**, 3481-3489 (2005).

US Environmental Protection Agency (USEPA). Compendium method TO-14a. Determination of volatile organic compounds (VOCs) in ambient air using specially prepared canisters with subsequent analysis by gas chromatography (EPA/625/R-96/010b). Compendium of methods for the determination of toxic organic compounds in ambient air, 2nd Edition. US EPA, Cincinnati, OH, 1999.

US Environmental Protection Agency (USEPA). Integrated Risk Information System (IRIS) on 1,3-Butadiene. (National Center for Environmental Assessment, Office of Research and Development, Washington, DC. 1999).

US Environmental Protection Agency (USEPA). SPECIATE, VOC/PM speciation data system, version 1.50. (Environmental Protection Agency and Radian Corporation, Research Triangle Park, N.C. 1993).

Vega, E., Mugica, M., Carmona, R. & Valencia, E. Hydrocarbon source apportionment in Mexico City using the chemical mass balance receptor model. *Atmospheric Environment* **34**, 4121-4129 (2000).

Velasco, E. Estimates for biogenic non-methane hydrocarbons and nitric oxide emissions in the Valley of Mexico. *Atmospheric Environment* **37**, 625-637 (2003).

Velasco, E., Lamb, B., Pressley, S., Allwine, E., Westberg, H., Jobson, T., Alexander, M., Prazeller, P., Molina, L. & Molina, M. Flux measurements of volatile organic compounds from an urban landscape. *Geophysical Research Letters **32**(20) L20802,* (2005).

Warneke, C., de Gouw, J.A., Kuster, W.C., Goldan, P.D. & Fall, R. Validation of atmospheric VOC measurements by proton transfer reaction mass spectroscopy using a gas

chromatographic preseparation method. *Environmental Science and Technology* **37**, 2494-2501 (2003).

Watson, J.G., Chow, J.C. & Fujita, E.M. Review of volatile organic compound source apportionment by chemical mass balance. *Atmospheric Environment* **35**, 1567– 1584 (2001).

West, J., Zavala, M.A., Molina, L.T., Molina, M.J., San Martini, F., McRae, J., Sosa, G. & Arriaga-Colina, J.L. Modeling ozone photochemistry and evaluation of hydrocarbon emissions in the Mexico City metropolitan area. *Journal of Geophysical Research* **109**, 19312-19327 (2004).

Whiteman, C.D., Zhong, S., Bian, X., Fast, J.D. & Doran, J.C. Boundary layer evolution and regional-scale diurnal circulations over the Mexico Basin and Mexican plateau. *Journal of Geophysical Research* **106(D8)**, 10081-10102 (2000).

Table 2.1. Description of the VOC monitoring sites during the MCMA-2002 and 2003 field campaigns

Site #	Site and position	Year	Site description	Method
1	CENICA (N19.358º, W99.073º)	2003	MCMA-2003 super site located in the Autonomous Metropolitan University campus Iztapalapa at the southeast of the city in a mixed area with residences, light and medium industries, services and commerce. The traffic is heavy and composed by old and new vehicles on paved roads.	Canister sampling and GC-FID analysis. PTR-MS. FTIR & DOAS. FIS.
2	Constituyentes (N19.400º, W99.210º)	2002	Western suburban neighborhood close to Chapultepec park. Heavy traffic on paved roads composed by private cars and heavy-duty diesel buses.	Canister sampling and GC-FID analysis.
3	La Merced (N19.424º, W99.119º)	2002 & 2003	Central city section composed by a mix of residences, small and medium commerce, light industries and a busy market. Heavy traffic on paved roads with private cars, light–duty vehicles and modern heavy-duty diesel buses.	Canister sampling and GC-FID analysis. PTR-MS. FTIR & DOAS.
4	La Reforma (N19.976º, W98.697º)	2003	Southwestern downwind site from Pachuca, city with 245,000 inhabitants located to the northeast of Mexico City. Rural site close to urban areas with reduced vehicular traffic on paved and unpaved roads.	Canister sampling and GC-FID analysis.
5	Pedregal (N19.325º, W99.204)	2002 & 2003	Southwestern suburban neighborhood with paved residential roads lightly traveled. This site is in the prevailing downwind direction from the center of the city.	Canister sampling and GC-FID analysis. PTR-MS.
6	Santa Ana Tlacotenco (N19.177º, W98.99º)	2003	Rural site to the southwest of Mexico City, close to the gap in the mountains at Amecameca. Paved and unpaved roads with minimum traffic.	Canister sampling and GC-FID analysis. PTR-MS.
7	Tehotihucan (N19.688º, W98.870º)	2002	Northern upwind boundary site of Mexico City with pollution influence from a large power plant and large industries around the region.	Canister sampling and GC-FID analysis.
8	Xalostoc (N19.527º, W99.076º)	2002 & 2003	North-eastern industrial section of the city with light to medium industries. Heavy traffic on paved and unpaved roads formed by a mix of new and old gasoline and diesel vehicles.	Canister sampling and GC-FID analysis.

Table 2.2. Sensitivities and average concentrations measured during selected days throughout the MCMA-2003 campaign between 6 and 10 am by a canister sampling system and GC-FID analysis, FOS responses to those average concentrations, and relative sensitivities to propylene for six compounds

Compound	Sensitivity (photons ppb^{-1} s^{-1})	Average conc., 6–10 am (ppb)	Average FOS response (photons s^{-1}) [c]	Relative sensitivity to propylene [d]
Propylene	25.4	7.50	191	1.00
Isoprene	74.7	0.304	23	2.94
Ethylene	17.7	20.7	366	0.70
1-3 Butadiene	49.8	0.791	39	1.96
1-Butene	7.9	3.90 [a]	31	0.31
NO	~0.0	61.2 [b]	0	~0.0

[a] As i-butene
[b] From continuous monitoring during the entire campaign.
[c] Average response = (sensitivity)(average conc.) + (zero value)
[d] Relative sensitivity = (compound sensitivity) / (propylene sensitivity)

Table 2.3. OH reactivity and average ambient concentrations of major VOCs measured during the MCMA-2002 and 2003 studies at urban (Pedregal, La Merced, CENICA and Constituyentes), rural (Santa Ana Tlacotenco, Teotihuacan and La Reforma) and industrial (Xalostoc) sites of the Valley of Mexico. Data correspond to the morning rush hours (6:00 to 9:00 h)

Species	Group	OH reaction rate coeff.*	OH reactivity[§]			Ambient concentration (ppbv)		
			Urban	Rural	Industrial	urban	rural	Industrial
Ethylene	olefin	8.52	3.91	0.28	6.72	18.7	1.32	32.1
Propylene	olefin	26.3	3.43	0.53	6.06	5.30	0.81	9.37
Propane	alkane	1.15	3.20	0.46	4.53	113	16.4	160
n-butane	alkane	2.54	2.71	0.38	3.81	43.4	6.08	61.4
m,p-xylene	aromatic	18.9	2.53	0.26	4.93	5.44	0.56	10.6
i-butene	olefin	31.4	2.13	0.46	4.08	2.75	0.60	5.28
Toluene	aromatic	5.96	1.93	0.20	4.81	13.2	1.37	32.8
2-methyl-1-butene	olefin	61.0	1.67	0.08	3.70	1.11	0.05	2.47
2-methyl-2-butene	olefin	86.9	1.57	0.16	2.37	0.74	0.08	1.11
i-pentane	alkane	3.70	1.42	0.37	2.61	15.6	4.05	28.7
1,2,4-trimethylbenzene	aromatic	32.5	1.41	0.22	2.76	1.76	0.28	3.45
t-2-butene	olefin	64.0	1.33	0.42	3.14	0.85	0.27	2.00
t-2-pentene	olefin	67.0	1.00	0.15	2.18	0.61	0.09	1.32
c-2-butene	olefin	56.4	0.94	0.29	1.73	0.68	0.21	1.25
Isoprene	olefin	101	0.88	0.13	0.68	0.36	0.05	0.27
i-butane	alkane	2.19	0.87	0.14	1.30	16.1	2.54	24.1
1,3,5-trimethylbenzene	aromatic	57.5	0.82	0.17	1.51	0.58	0.12	1.07
1,3-butadiene	olefin	66.6	0.79	0.18	1.03	0.48	0.11	0.63
Styrene	aromatic	58.0	0.69	0.72	1.63	0.49	0.51	1.14
o-xylene	Aromatic	13.7	0.66	0.06	1.31	1.96	0.18	3.88
n-pentane	alkane	3.94	0.66	0.06	0.86	6.80	0.65	8.85
2-methylpentane	alkane	5.60	0.64	0.06	1.25	4.66	0.47	9.07
Hexane	alkane	5.61	0.61	0.03	1.30	4.39	0.23	9.44
c-2-pentene	olefin	65.0	0.50	0.27	1.08	0.31	0.17	0.68
MTBE	oxygenated	2.90	0.45	0.03	0.59	6.30	0.41	8.32
3-methylpentane	alkane	5.70	0.42	0.04	0.88	3.00	0.32	6.30
1-pentene	olefin	31.4	0.39	0.19	1.98	0.50	0.24	2.57
3-methylhexane	alkane	7.20	0.38	0.07	0.45	2.14	0.41	2.53
2,3-dimethylbutane	alkane	5.99	0.35	0.03	0.53	2.40	0.18	3.57
Methylcyclopentane	alkane	8.80	0.31	0.04	0.55	1.41	0.18	2.55
m-ethyltoluene	aromatic	19.2	0.30	0.03	0.65	0.65	0.06	1.37
Acetylene	alkyne	0.91	0.27	0.01	0.35	12.1	0.62	15.7
Ethylbenzene	aromatic	7.10	0.27	0.03	0.52	1.54	0.17	2.98
n-heptane	alkane	7.15	0.26	0.02	0.38	1.50	0.12	2.13
2-methylhexane	alkane	6.80	0.26	0.04	0.37	1.55	0.26	2.20

*OH reaction rate coefficients at 298 K and 1 atm (cm^3 $molecule^{-1}$ s^{-1}) × 10^{-12}, (Atkinson, 1994; Atkinson, 1997).

[§]Products of mean individual VOC concentrations and OH reaction rate coefficients.

Continuation table 2.3								
Species	**Group**	**OH reaction rate coeff.***	**OH reactivity[§]**			**Ambient concentration (ppbv)**		
			Urban	**Rural**	**Industrial**	**urban**	**rural**	**Industrial**
i-octane	alkane	3.57	0.25	0.02	0.48	2.86	0.23	5.45
ethyl acetate	ester	8.00	0.25	0.02	0.00	1.27	0.10	0.00
p-ethyltoluene	aromatic	12.1	0.22	0.03	0.32	0.72	0.09	1.08
2,3,4-trimethylpentane	alkane	7.00	0.21	0.01	0.31	1.19	0.05	1.82
Cyclohexane	alkane	7.49	0.17	0.03	0.37	0.90	0.17	2.02
1-hexene	olefin	37.0	0.16	0.15	0.44	0.17	0.17	0.48
2,3-dimethylpentane	alkane	7.20	0.16	0.02	0.20	0.89	0.09	1.11
o-ethyltoluene	aromatic	12.3	0.15	0.04	0.28	0.50	0.13	0.93
2,4-dimethylhexane	alkane	8.60	0.13	0.01	0.16	0.63	0.05	0.73
Methylcyclohexane	alkane	10.4	0.13	0.02	0.24	0.49	0.09	0.93
n-octane	alkane	8.70	0.12	0.02	0.30	0.56	0.10	1.38
2,2-dimethylbutane	alkane	2.59	0.10	0.01	0.17	1.62	0.13	2.61
n-decane	alkane	11.2	0.10	0.02	0.23	0.37	0.08	0.85
Ethane	alkane	0.27	0.10	0.01	0.28	14.9	1.26	41.8
Nonane	alkane	10.0	0.10	0.01	0.24	0.39	0.04	1.00
Benzene	aromatic	1.23	0.09	0.02	0.15	2.86	0.53	5.05
2-methylheptane	alkane	8.20	0.08	0.02	0.16	0.40	0.10	0.77
Propyne	alkyne	5.90	0.08	0.04	0.15	0.52	0.25	1.04
n-propylbenzene	aromatic	6.00	0.06	0.01	0.10	0.39	0.05	0.67
2,5-dimethylhexane	alkane	8.30	0.05	0.13	0.00	0.26	0.61	0.00
1,2,4 trimethyl cyclohexane	alkane	7.50	0.04	0.01	0.08	0.23	0.04	0.42
Cyclopentane	alkane	5.02	0.04	0.00	0.02	0.34	0.04	0.13

*OH reaction rate coefficients at 298 K and 1 atm (cm^3 $molecule^{-1}$ s^{-1}) × 10^{-12}, (Atkinson, 1994; Atkinson, 1997).

[§]Products of mean individual VOC concentrations and OH reaction rate coefficients.

Table 2.4. Ambient average concentrations of halogenated VOCs measured during the MCMA-2003 study at urban (Pedregal, La Merced and CENICA) and industrial (Xalostoc) sites of the Valley of Mexico

Species	Urban sites (ppbC)		Industrial site (ppbC)	
	6-9 am	12-15 h	6-9 h	12-15 h
p-dichlorobenzene	5.53	2.26	5.94	2.80
Trichloroethylene	4.15	1.56	4.44	1.48
1,2-dichloropropane	3.51	2.82	0.00	0.00
c-1,3-dichlopropene	3.20	1.67	6.03	3.96
1,2-dichloroethane	3.17	2.27	0.52	0.00
o-dichlorobenzene	2.96	0.39	4.60	0.00
1,1-dichloroethane	1.69	2.01	1.40	2.28
Chloroform	1.36	0.37	3.47	0.93
t-1,3-dichloropropene	0.92	0.26	1.46	0.30
Freon113	0.90	0.94	0.52	0.00
Perchloroethylene	0.51	0.34	0.92	0.28
Chlorobenznene	0.11	0.01	0.20	0.73
Vinyl chloride	0.00	0.35	0.52	0.86
m-dichlorobenzene	0.00	0.67	0.00	0.00
Subtotal halogens	**28.01**	**15.94**	**30.02**	**13.62**
Halogens percent between unidentified VOCs	**11.4**	**8.2**	**11.3**	**3.6**
Halogens percent between total VOCs	**1.8**	**2.4**	**1.2**	**0.9**

Table 2.5. Hydrocarbon molar ratios (ppbC/ppbC) measured at the industrial, urban and rural sites and from vehicle chase operation during the MCMA-2002 and 2003 field studies. Also ratios from vehicles exhaust studies in North America are shown for comparison

	Industrial		Urban		Rural		Vehicular chases		Mexican gasoline vehicles[§]	Mexican diesel vehicles[§]	US & Canada light duty vehicles[#]
	Average*	Median	Average*	Median	Average*	Median	Average*	Median	Average	Average	Average*
Alkene ratios											
t-2-butene/c-2-butene	1.69±0.91	1.25	1.44±0.83	1.21	1.63±0.66	1.48	1.16±0.50	1.10	1.17	1.00	1.27±0.33
t-2-pentene/c-2-pentene	1.82±0.51	1.91	2.05±0.53	2.07	1.83±0.51	1.89	1.98±0.46	1.98	---	9.33	1.78±0.19
1-hexene/1-pentene	0.63±0.46	0.52	0.67±0.48	0.59	---	---	---	---	---	---	0.49±0.25
1,3-butadiene/t-2-pentene	1.13±0.58	1.14	0.89±0.52	0.77	0.67±0.47	0.64	1.16±0.97	0.96	---	---	1.36±0.51
propene/ethane	0.52±0.30	0.44	0.59±0.47	0.42	0.47±0.28	0.44	0.58±0.37	0.50	0.55	0.71	0.30±0.04
Alkane ratios											
i-butane/n-butane	0.38±0.04	0.37	0.37±0.03	0.37	0.41±0.07	0.41	0.36±0.04	0.36	0.32	0.48	0.19±0.08
i-pentane/n-pentane	3.64±0.69	3.62	3.06±1.41	2.59	9.03±6.61	8.08	2.80±1.69	2.36	2.63	4.27	2.97±0.57
2-methylpentane/3-methylpentane	1.38±0.19	1.41	1.67±1.80	1.54	1.74±0.78	1.59	1.49±0.14	1.47	1.67	1.18	1.69±0.11
Hexane/2-methylpentane	1.15±0.31	1.11	0.80±0.40	0.72	0.90±0.83	0.69	0.65±0.15	0.65	0.78	1.02	0.52±0.05
cyclohexane/n-heptane	1.06±1.03	0.50	0.70±0.60	0.50	1.02±0.74	0.91	0.73±0.63	0.54	0.86	0.29	0.43±0.17
n-octane/nonane	0.87±0.38	1.01	1.56±0.82	1.29	1.26±0.62	1.12	1.36±0.43	1.28	1.04	0.55	1.49±0.05
Aromatic ratios											
Toluene/benzene	9.17±4.57	8.81	5.42±2.32	4.89	3.74±1.35	3.45	4.14±1.34	3.80	2.78	5.05	1.59±0.28
ethylbenzene/toluene	0.10±0.04	0.09	0.13±0.05	0.13	0.16±0.07	0.15	0.15±0.05	0.15	0.21	0.30	0.17±0.03
Isopropylbenzene/toluene	0.014±0.005	0.014	0.020±0.008	0.020	---	---	---	---	0.027	0.016	0.020±0.008
o-xylene/m,p-xylene	0.36±0.03	0.36	0.41±0.07	0.39	0.40±0.11	0.40	0.39±0.05	0.39	0.39	0.36	0.38±0.02
Styrene/1,3,5-trimethylbenzene	1.08±0.68	0.98	1.78±1.67	1.22	4.28±3.58	3.10	0.66±0.42	0.55	0.37	0.84	0.81±0.21
1,2,3-trimethylbenzene/1,2,4-trimethylbenzene	0.39±0.09	0.36	0.41±0.13	0.37	---	---	---	---	---	---	0.25±0.07

* Average ± 1 standard deviation.

[§] From vehicle emission profiles measured in Mexico City in 1998 (Mugica et al., 2001).

[#] Average vehicle exhaust ratio calculated by Jobson et al. (2004) from six tunnel studies conducted in the 1990s (Conner et al., 1995; Kirchstetter et al., 1996; Sagebiel et al., 1996; Fraser et al., 1998; Rogak et al., 1998).

Table 2.6. Comparison between ambient VOC concentrations measured at urban sites during the morning period (6:00 to 9:00 h) and the corresponding VOC emissions from the most recent emissions inventory for modeling purposes

Model species	Ambient [VOC] (ppbC)	% of total	Inventory $\times 10^3$ (tons/yr)	% of inventory in C moles	Adjustment factor to correct the inventory
ETHANE	29.7	2.3	3.3	1.0	2.3
PROPANE	339.5	25.7	50.1	15.1	1.7
ALK1	470.8	35.7	36.2	11.7	3.1
ALK2	91.5	6.9	78.3	22.5	0.3
ACETYLENE	24.3	1.8	4.2	1.4	1.3
ETHYLENE	37.3	2.8	7.9	2.50	1.1
OLE1	29.5	2.2	15.8	5.2	0.4
OLE2	20.8	1.6	22.9	7.5	0.2
BUTADIENE	1.9	0.2	0.04	0.01	10.8
ISOPRENE	1.8	0.1	7.8	2.5	0.05
BENZENE	17.2	1.3	3.3	1.1	1.1
ARO1	95.5	7.2	40.1	13.0	0.6
ARO2	127.5	9.7	42.8	13.1	0.7
MTBE	31.5	2.4	12.7	3.2	0.8
Total	1318.8	100.0	325.5	100.0	

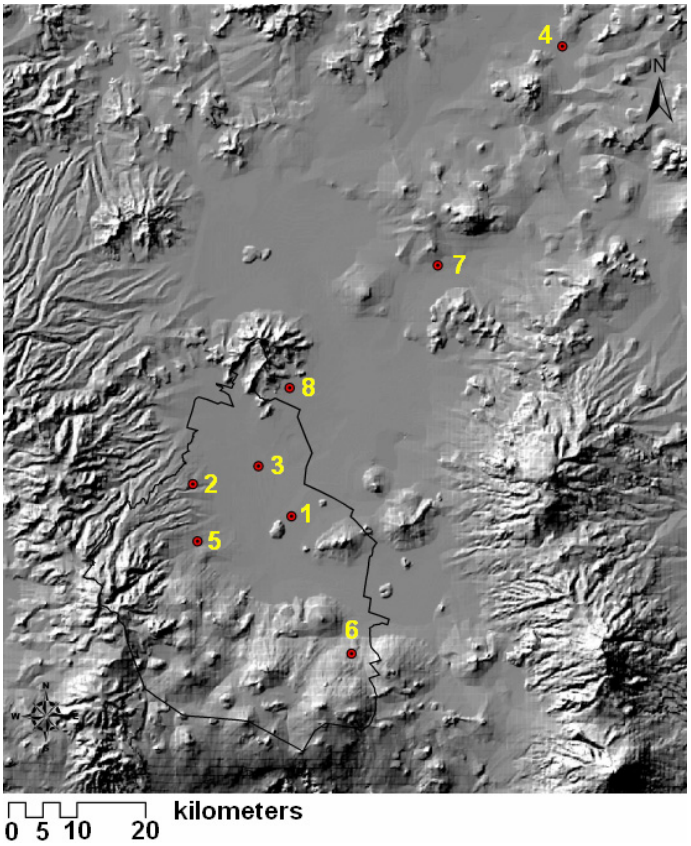

Figure 2.1. Sampling sites during MCMA-2002 and MCMA-2003 field campaigns. Points indicate the location of the sampling sites and numbers correspond to the sites listed in Table 1. The gray scale shows the orography of the Valley of Mexico and the black contour limits the Federal District.

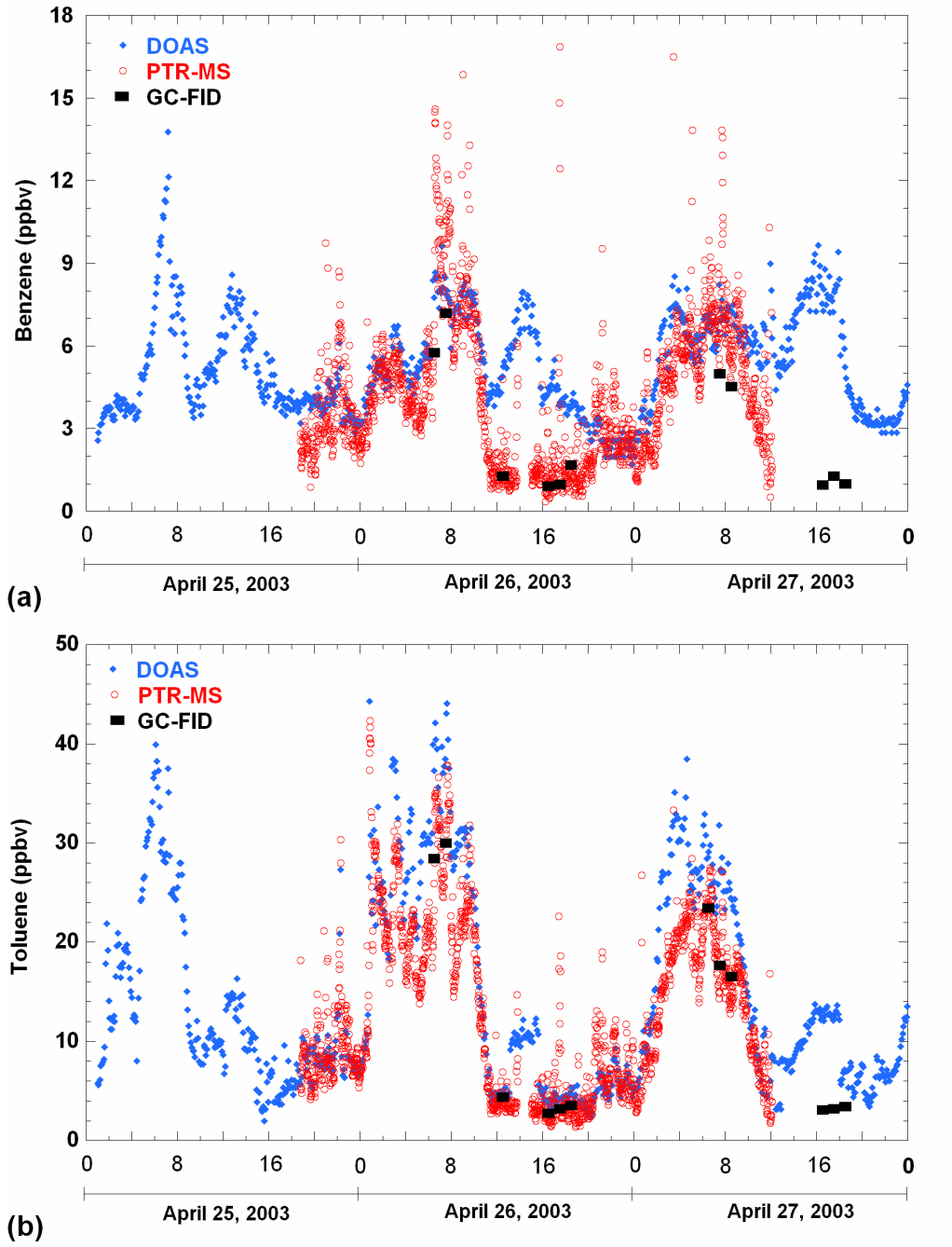

Figure 2.2. Time series of benzene (a) and toluene (b) mixing ratios measured by DOAS, PTR-MS and GC-FID. The resolution time for DOAS was 5 minutes and for PTR-MS ~30 sec. PTR-MS points correspond to 1 minute averages. Samples collected by canisters and analyzed by GC-FID correspond to 1 hour averages. Short term spikes were commonly observed with PTR-MS indicating local sources.

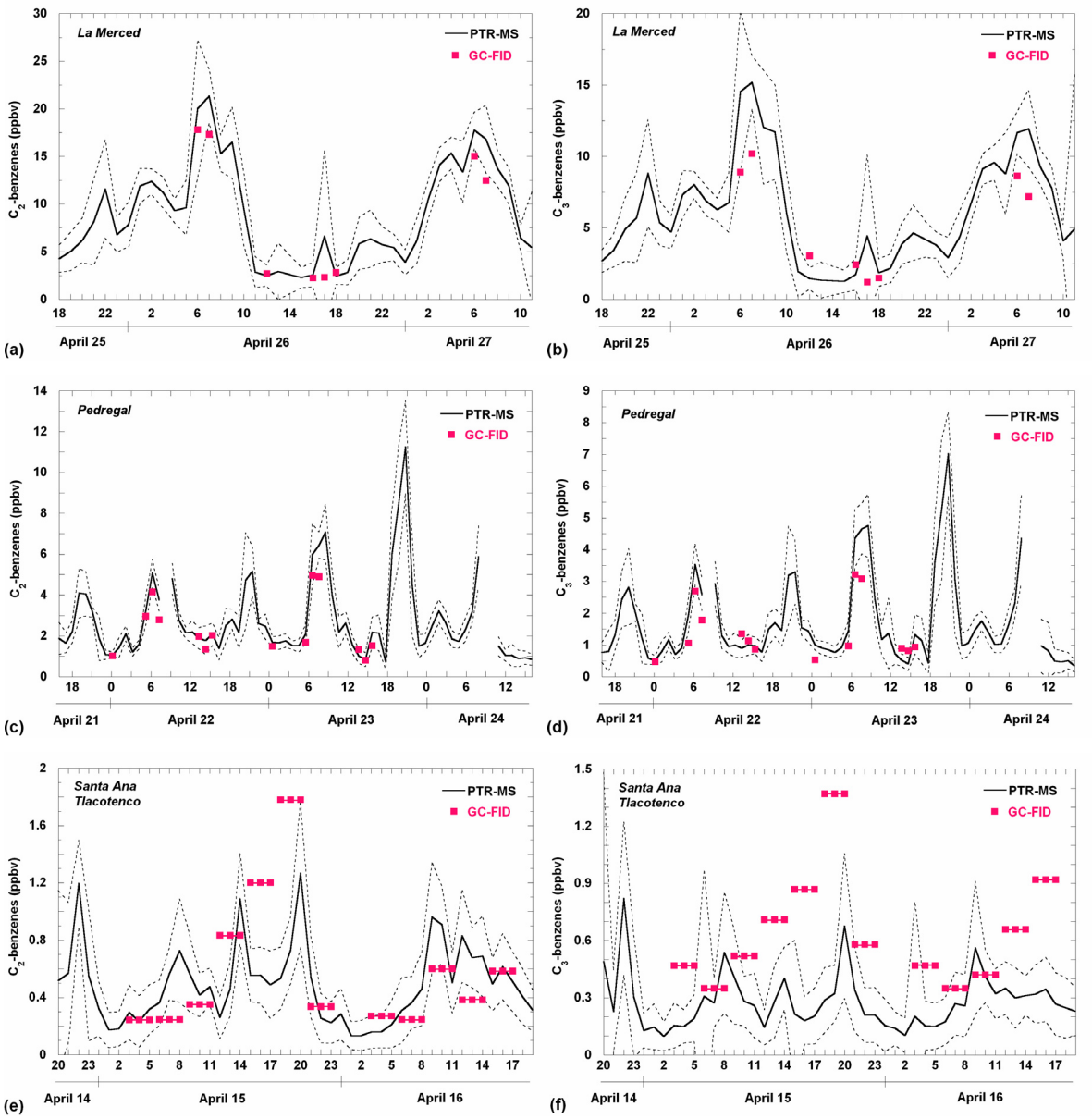

Figure 2.3. Time series of C_2-benzenes and C_3-benzenes measured by the PTR-MS together with GC-FID samples collected in parallel at La Merced (a, b), Pedregal (c, d) and Santa Ana sites (e, f). PTR-MS concentrations represent hourly averages. GC-FID samples were collected in hourly periods at La Merced and Pedregal sites, and in 3-hours periods at Santa Ana Tlacotenco. The dashed lines indicate ±1 standard deviation of the PTR-MS concentrations.

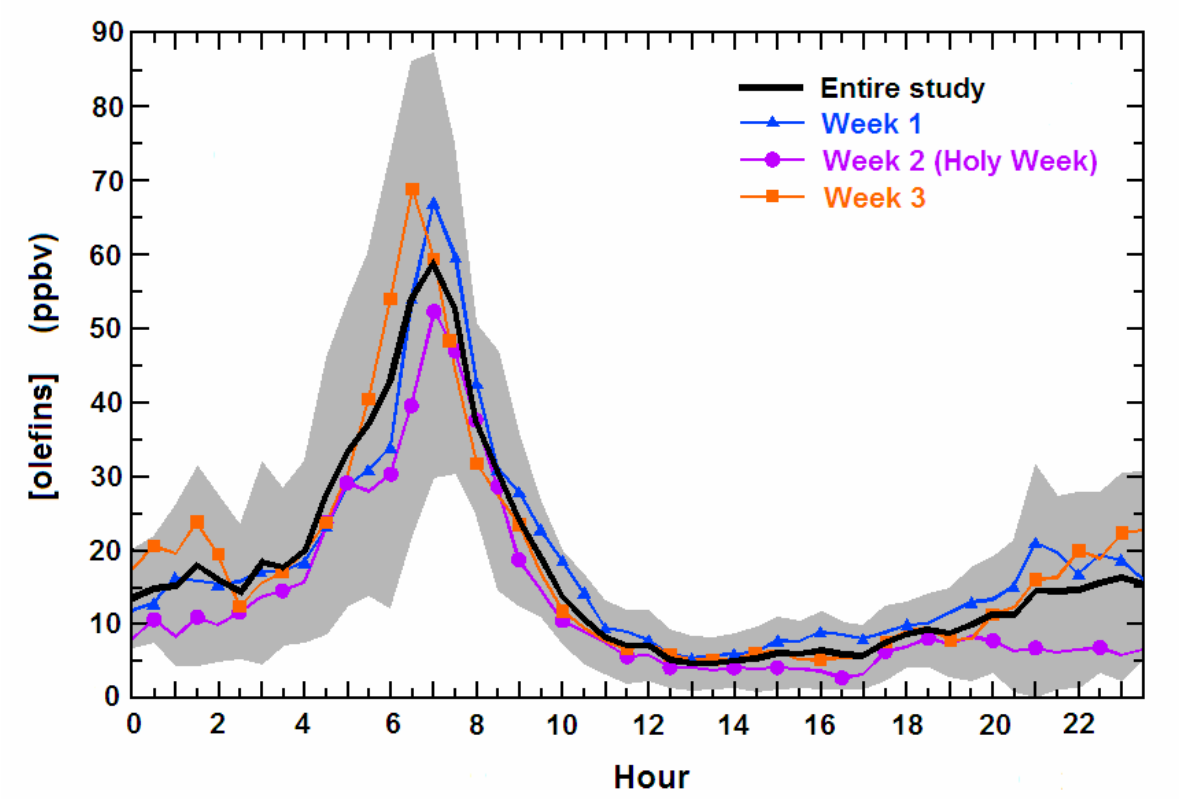

Figure 2.4. Average diurnal pattern of the olefinic mixing ratio (as propylene) detected by the FOS for 23 days during the MCMA-2003 study (black line) and for individual weeks. The gray shadow represents the one standard deviation range, and gives and indication of the day-to-day variability in each phase of the daily cycle.

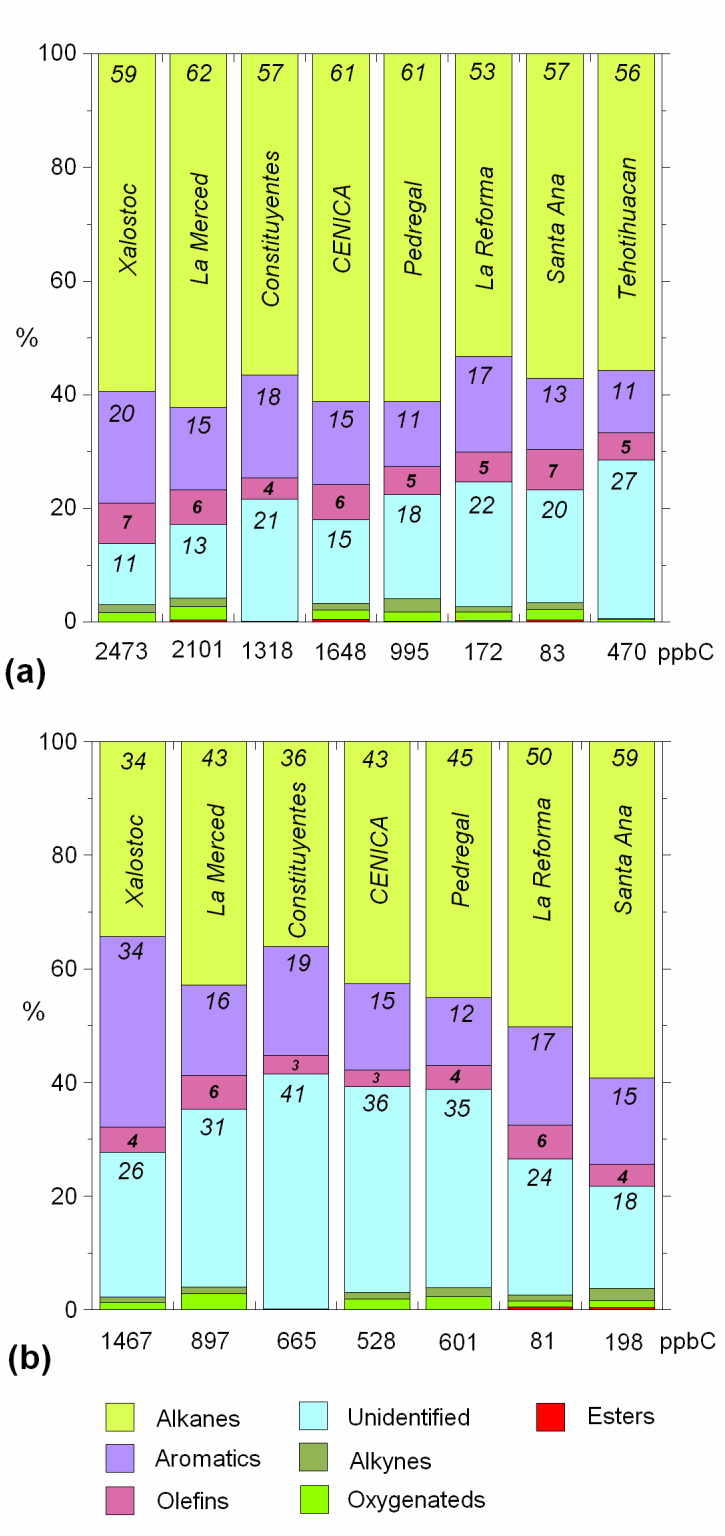

Figure 2.5. VOC distribution by groups during the morning (a) and afternoon (b). Numbers in the columns indicate the percent contribution of each VOC group to the total VOC concentration, which is displayed at the bottom of each column in ppbC.

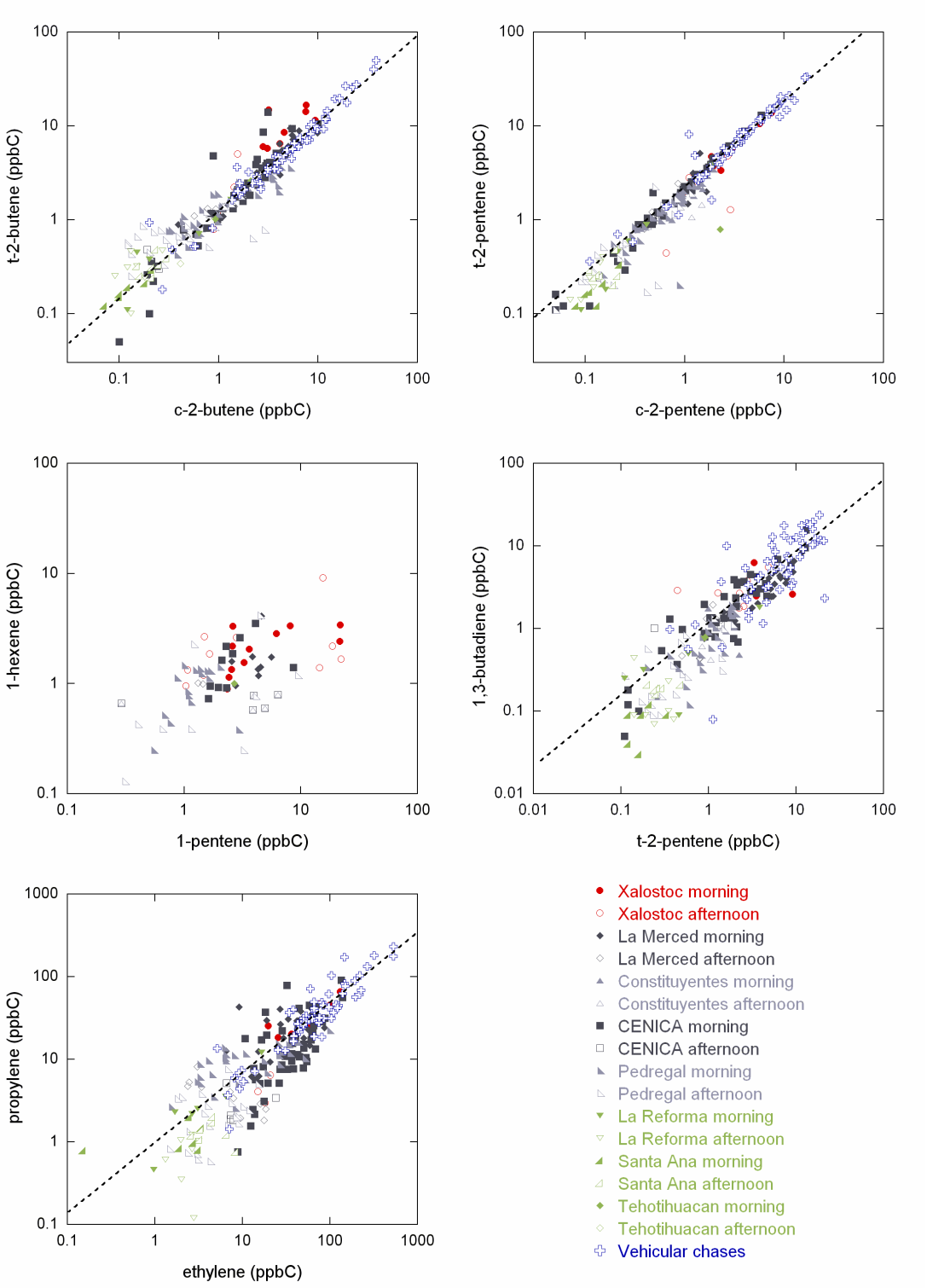

Figure 2.6. Correlations between alkenes comparing ambient data to vehicle chase samples. Ambient data correspond to all canister samples and the dashed line indicates the regression line for vehicular emissions.

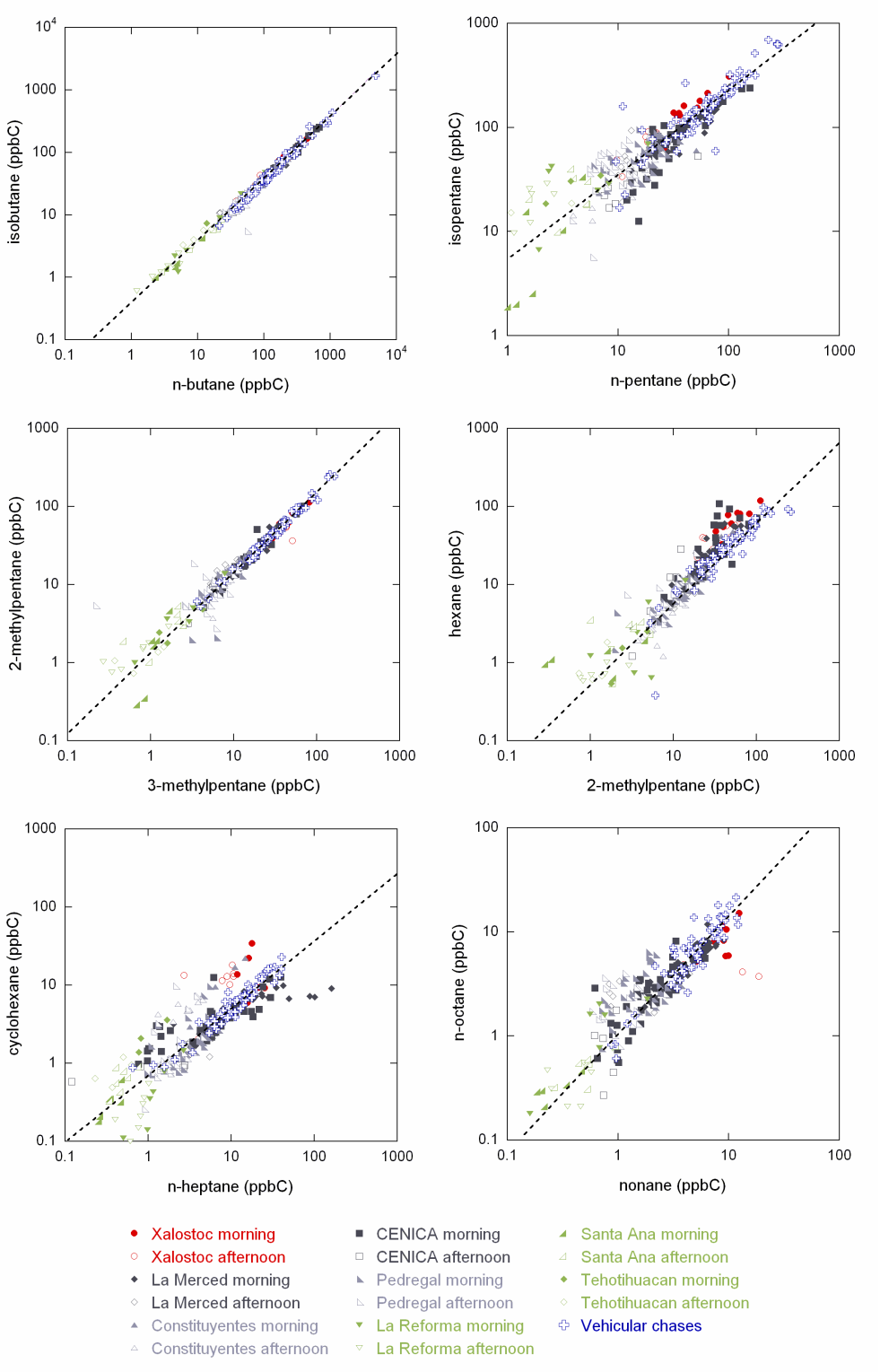

Figure 2.7. Correlations between alkanes comparing ambient data to vehicle chase samples. Ambient data correspond to all canister samples and the dashed line indicates the regression line for vehicular emissions.

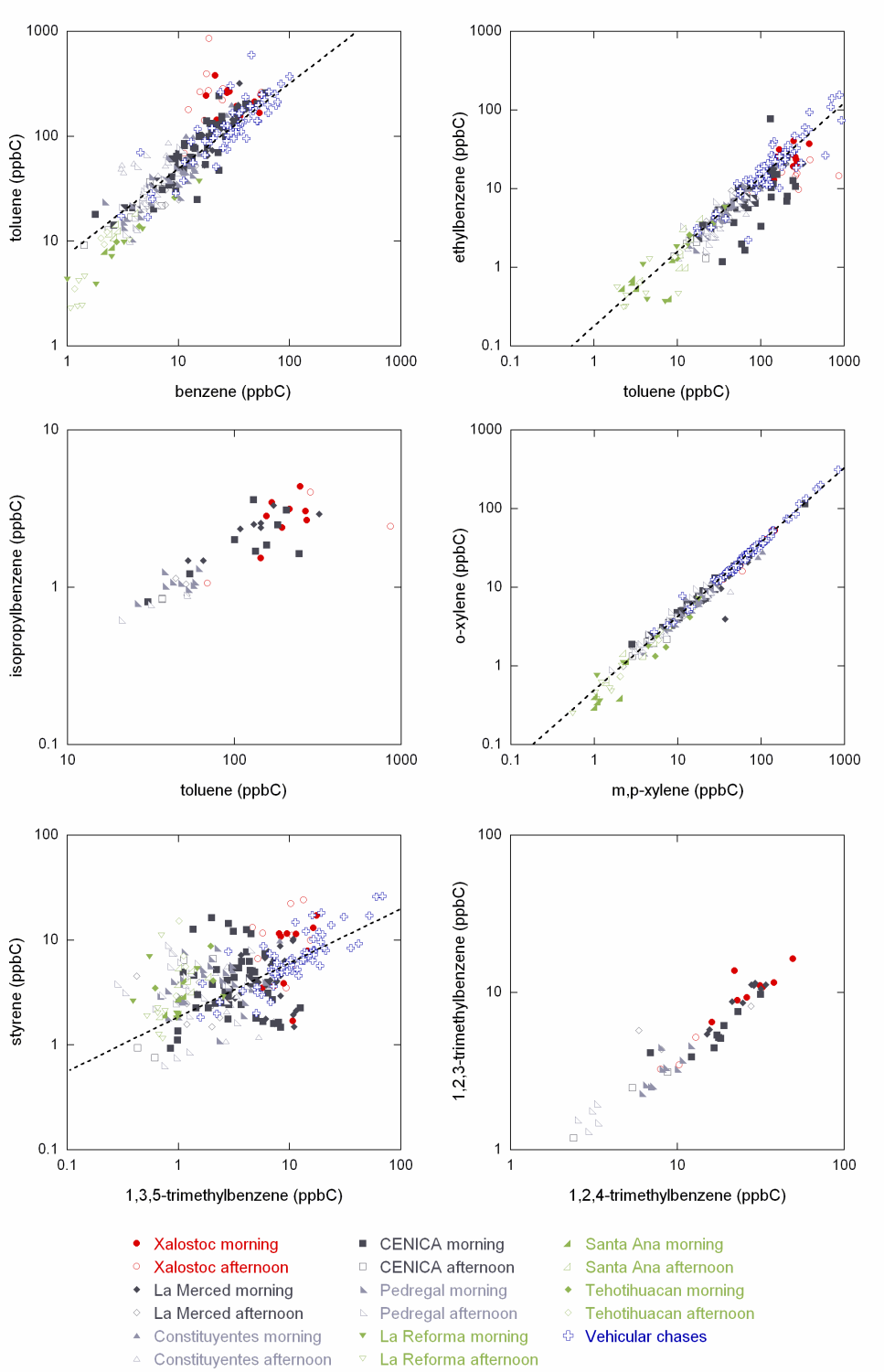

Figure 2.8. Correlations between aromatics comparing ambient data to vehicle chase samples. Ambient data correspond to all canister samples and the dashed line indicates the regression line for vehicular emissions.

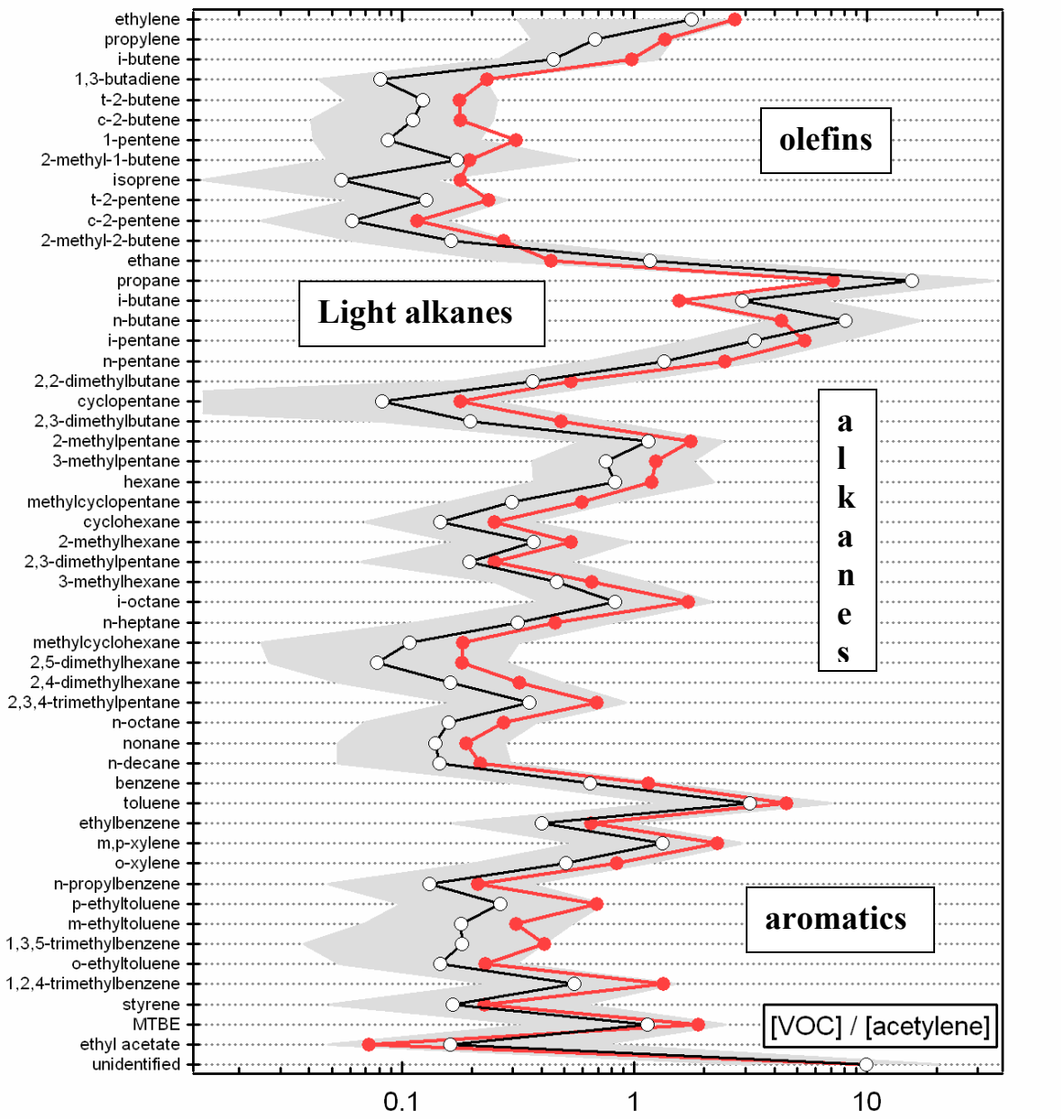

Figure 2.9. Comparison of urban and vehicle exhaust hydrocarbon abundances relative to acetylene in (ppbC/ppbC). The closed circles indicate the median values for vehicle exhaust, while the open circles indicate the median values for urban data collected from urban sites (Pedregal, La Merced and CENICA) between 6 and 9:00 h. The gray shading encloses the 10th and 90th percentiles of the urban values.

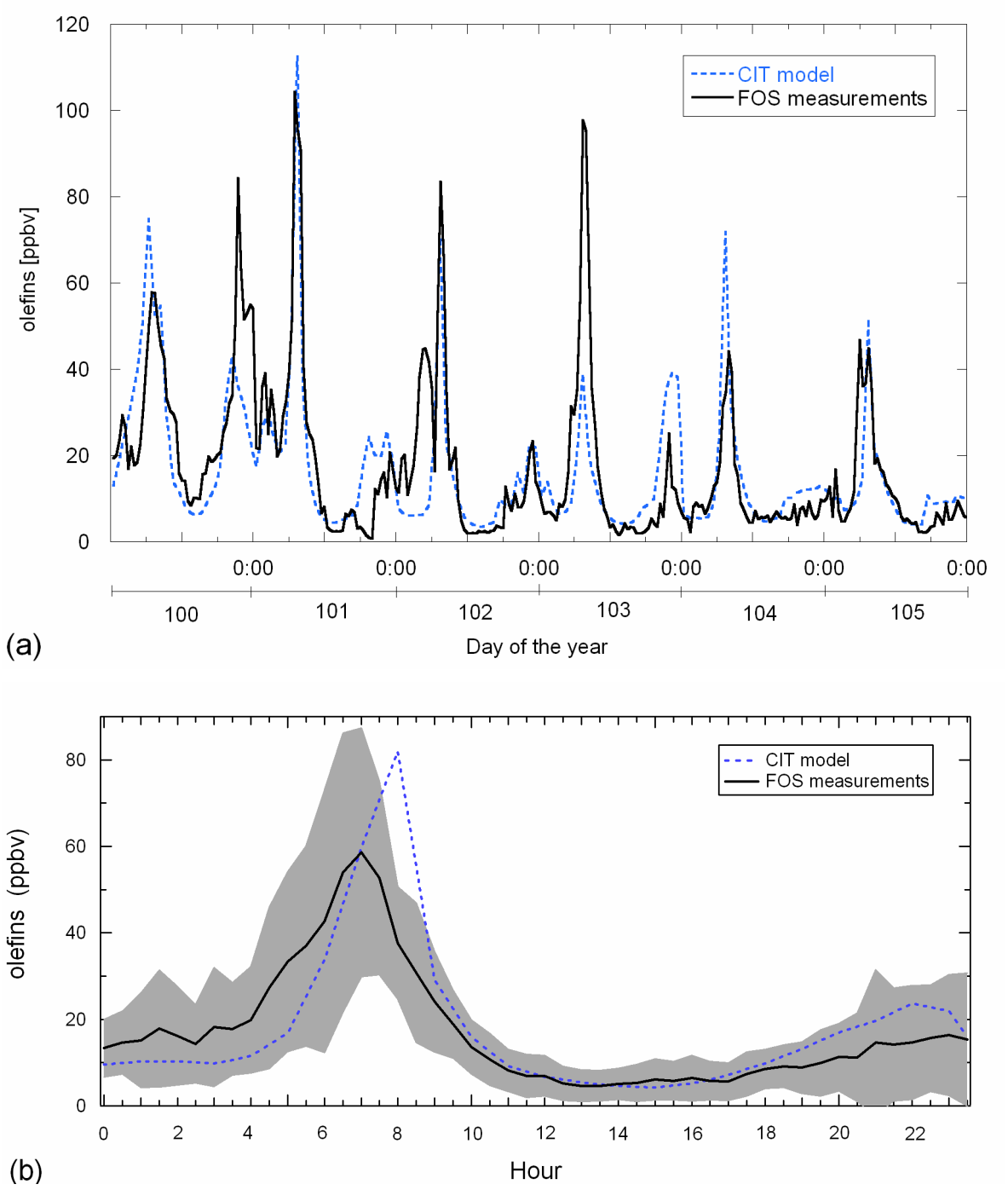

Figure 2.10. Olefins concentration measured by the FOS and calculated by the CIT model (a) during 5 days and (b) average concentrations measured during the entire MCMA-2003 field campaign at the CENICA site. The gray shading indicates the ±1 standard deviation range from the FOS measurements.

CHAPTER 3

FLUX MEASUREMENTS OF VOLATILE ORGANIC COMPOUNDS FROM AN URBAN LANDSCAPE*

3.1. Abstract

Direct measurements of volatile organic compound (VOC) emissions that include all sources in urban areas are a missing requirement to evaluate emission inventories and constrain current photochemical modelling practices. Here we demonstrate the use of micrometeorological techniques coupled with fast-response sensors to measure urban VOC fluxes from a neighbourhood of Mexico City, where the spatial variability of surface cover and roughness is high. Fluxes of olefins, methanol, acetone, toluene and C_2-benzenes were measured and compared with the local gridded emissions inventory. VOC fluxes exhibited a clear diurnal pattern with a strong relationship to vehicular traffic. Recent photochemical modelling results suggest that VOC emissions are significantly underestimated in Mexico City, but for the olefin class, toluene, C2-benzenes, and acetone fluxes measured in this work, the results show general agreement with the gridded emissions inventory. While these measurements do not address the full suite of VOC emissions, the comparison with the inventory suggests that other explanations may be needed to explain the photochemical modelling results.

3.2. Introduction

Emission inventories provide the foundation for testing our understanding of atmospheric chemistry at urban, regional and global scales. For VOC emissions, it has been a frequent practice to adjust anthropogenic VOC emissions by factors between 1 and 4 to obtain matches between photochemical model simulations and observations of ozone [*Solomon et al*., 2000]. This calibration of models using adjusted emissions can hide critical modelling issues that

* Velasco, E., Lamb, B., Pressley, S., Allwine, E., Westberg, H., Jobson, T., Alexander, M., Prazeller, P., Molina, L. & Molina, M. Flux measurements of volatile organic compounds from an urban landscape. *Geophysical Research Letters* ***32****(20) L20802,* (2005).

prohibit the development of a true picture of atmospheric chemistry. One way to address this problem is to make direct measurements of VOC emissions and to use these data for an explicit evaluation of gridded VOC emission inventories. We recently completed a set of micrometeorological measurements of VOC fluxes as part of the Mexico City Metropolitan Area 2003 field campaign (April 7-29) in a densely populated district of Mexico City. We employed a tall urban tower instrumented with a Fast Olefin Sensor (FOS), a Proton Transfer Reaction-Mass Spectrometer (PTR-MS) and appropriate meteorological sensors. Fluxes of olefins were measured with the FOS and computed by the eddy covariance technique (EC), while fluxes of toluene, C_2-benzenes, methanol and acetone were measured by the PTR-MS and calculated using the disjunct eddy covariance method (DEC).

The applicability of micrometeorological techniques to a potentially inhomogeneous area, such as a city with diverse emission sources (motor vehicles, industrial process, solvents evaporation, food cooking, etc.), is confined to conditions, such that the tower height exceeds the blending height at which the small scale heterogeneity merge into a net exchange flux above the city. The left side of Figure 3.1 illustrates how the emissions from different sources are blended by the turbulence produced in the roughness sub-layer by the influence of buildings, trees, and the urban surface heating. Instruments must be mounted in the constant flux-layer, which is at least twice the mean height of the roughness elements [Grimmond and Oke, 1999], to measure fluxes fully representative of the underlying surface. Our measurements fulfilled both constraints with a 37 m tower, a height 3 times the height of surrounding buildings and below a tenth of the minimal atmospheric boundary height in Mexico City (~400 m).

3.3. Experimental methods

To instrument the flux tower, a 3-d sonic anemometer was attached to a 3 m boom near the top of the tower. Signal/power cables and a Teflon sampling line were run from the sensors to a shelter on the roof-top. Inlet lines to the FOS and PTR-MS were connected to the sampling line near the roof-top instrument shelter. The lag time for sampling at the shelter was determined

from a covariance analysis between the vertical wind speed and the FOS signal. In operation, the flux system collected data at 10 Hz. The data were used to calculate 30 min average fluxes.

The EC method calculates the flux of a trace gas (F_χ) as the covariance between the instantaneous deviation of the vertical wind velocity (w') and the instantaneous deviation of the trace gas (c_χ') for time periods no longer than one hour [*Aubinet et al*., 2000]. The DEC method is similar to EC, but with a slower sampling rate, and therefore the flux is calculated from a smaller subset of samples.

The quality of flux measurements is difficult to assess, because there are various sources of errors that range from failure to satisfy any of a number of theoretical assumptions to failure of the technical setup. Systematic and random errors are estimated to restrict the accuracy of an individual turbulent flux measurement to within 10% to 20% [*Montcrieff et al*., 1996]. It has been suggested there are certain plausibility criteria that EC flux methods should fulfil [*Aubinet et al*., 2000]. We investigated three criteria: the statistical characteristics of the raw instantaneous measurements, the frequency resolution of the eddy covariance system through the spectra and cospectra of the measured variables, and the stationarity of the measurement process. These criteria were satisfied more than 70% of the time for our flux measurements. Details are given in the auxiliary material.

Additional uncertainties in the olefins flux are due to analytical uncertainties. The FOS is a chemiluminescent detector calibrated with propylene, but known to have different sensitivities to a variety of olefins [*Guenther and Hills*, 1998]. We evaluated the FOS response and found that, on average, 52% of the olefins detected by the FOS remained unknown. Additional analysis would be needed to identify these unknown species. However, we can affirm that the FOS measures a mix of VOC responding as propylene and can be used to provide a continuous and fast response measurement of the olefinic VOC mix in an urban atmosphere.

The PTR-MS is a more specific sensor compared to the FOS. The PTR-MS detection is based on mass spectroscopy of ions produced in proton-transfer reactions of H_3O^+ with selected aromatic and oxygenated VOCs [*Lindinger et al.*, 1998]. However, the fluxes of these species

involve uncertainties due to the use of the DEC technique. The PTR-MS operated with a resolution varying from 1.2 to 3.6 s. Although DEC gives more time to process the samples, it increases the statistical uncertainty of the fluxes. We evaluated this uncertainty and found the potential error to range from 9% to 40%, with a median of 30% due to the longer time resolution.

The height of the tower in conjunction with the surface roughness and atmospheric stability determines the footprint (upwind source area) of the measured flux. For an inhomogeneous surface, such as an urban area, the measured signal depends on which parts of the surface have the strongest influence on the sensor, and thus the location and size of the source footprint. To evaluate the footprint we applied a hybrid Lagrangian model [*Hsieh et al*., 2000] to all of the 30-minute periods from the campaign. For a footprint that encompasses 80% of the total flux, the longest footprints (~ 5 km) correspond to stable conditions, which prevail at nighttime; while the smaller footprints (500 m) correspond to unstable conditions, characteristic of morning and early afternoon (Figure 3.1). The average footprint was 1.3 km, which approaches the grid scale (i.e. 2 km x 2 km) of the emissions inventory.

3.4. Results and discussion

The diurnal profile of olefin fluxes in Figure 3.2 shows that fluxes remained positive during our study, which indicates that the urban surface is always a net source of olefins. The highest fluxes occurred after sunrise, between 6:30 and 8 a.m., and lower fluxes were observed during the night. Fluxes ranged from zero to 1.4 μg m^{-2} s^{-1}, with an average of 0.36 μg m^{-2} s^{-1}. The morning peak coincided with the rush hour. Olefin fluxes were lower on the weekends than on weekdays, and on weekends the morning rush hour peak was not observed. On average, the daily flux on weekdays was 21% higher than during weekends. This effect is directly related to changes in vehicular traffic and to industrial and commercial activities.

In an urban area, it is important to determine the magnitude of the fluxes as a function of the upwind direction to identify the strongest sources. Figure 3.3 shows the olefin flux footprint superimposed on a map of the neighborhood. Fluxes were consistently lower when winds were

from areas with fewer streets, such as north of the tower site. A high density of streets indicates a residential area, while regions with few streets are occupied by factories and stores. Thus, we can infer that residential areas and streets are the major contributor to the olefin flux in this section of the city. The largest olefin fluxes were associated with winds from the east and southeast directions. These sectors are densely inhabited and include the avenue #3 in Figure 3.3, the street with the highest traffic near the measurement site.

Figure 3.4 shows the fluxes of methanol, acetone, toluene and C_2-benzenes. All showed similar diurnal patterns, with highest fluxes during the morning and lowest fluxes during night. In general, fluxes for these species were always positive. Fluxes of acetone were negative in early morning, which suggests that deposition of acetone may occur before sunrise. The average flux for each of these species was lower than the average olefin flux. The mean daily flux of 0.29 $\mu g\ m^{-2}\ s^{-1}$ for methanol was 19% lower than the mean olefin flux. For toluene, the mean daily flux was 0.23 $\mu g\ m^{-2}\ s^{-1}$, while mean fluxes of acetone and C_2-benzenes were 0.11 and 0.13 $\mu g\ m^{-2}\ s^{-1}$, respectively. The spike observed with the olefin fluxes after sunrise was not recorded for these species; this suggests that they may arise from different sources. Fluxes of these four species increased after sunrise at 7 a.m., remained relatively constant during the morning, decreased at noon, and then remained constant during the afternoon. On average, the fluxes for these compounds were reduced by 53% in the afternoon relative to the morning. In some cases, these decreases were related to wind direction variations, when the upwind changed from highly inhabited areas before noon to areas mainly occupied by factories and stores in the afternoon.

We compared our flux measurement to the most recent emissions inventory derived for air quality modelling [West *et al*., 2004]. The annual emissions inventory developed for Mexico City was gridded using landuse, traffic pattern and industrial data, as well as population, commercial, or other distributions, as appropriate. Speciation of the VOC emissions for the SAPRC-99 chemical mechanism was primarily based upon Mexican emission profiles [Vega *et al*., 2000]. Further details for this inventory are presented in the auxiliary material. The diurnal patterns for calculated and measured olefin fluxes for the tower location are in good agreement

as shown in Figure 3.2. The measured flux of olefins was slightly higher than predicted by the emissions inventory during early morning hours. Then, during the rest of the day, the inventory emissions exceeded the measured fluxes by no more than 30%. The only significant discrepancy is a smaller morning rush hour peak in the emissions inventory compared to the peak observed in the measured fluxes. Thus, the results for this site and for the olefin class of VOC do not support the idea that the inventory is underestimated by a factor of 3 as suggested in the modelling study of *West et al*. [2004]. For toluene, we found that estimated emissions were generally greater than the measured average flux, but the inventory emissions were within one standard deviation of the measured value for most of the diurnal period. For C_2-benzenes, we observed relatively poor agreement between measured fluxes and the reported emissions. During the entire day, emissions in the inventory were more than 2 times higher than the measured flux profile. Finally, for acetone, we found that the inventoried rates were within one standard deviation of the measured average flux throughout the diurnal period. Methanol was not specified in the emissions inventory so a comparison was not possible.

These comparisons indicate that inventoried olefin, toluene, and C_2-benzene emissions agree with or exceed measured fluxes in this district of Mexico City. If this is true for other VOC classes and in other sections of the city, it implies that factors other than an underestimation of VOC emissions may be causing poor agreement between modelled and measured ozone levels. At the same time, it is important to note that the species we measured do not account for a majority of the VOC emissions which tend to be dominated by alkane species. For this reason, it is important to extend these direct VOC flux measurements to include other compounds and to also make measurements in other parts of the city.

During the study, traffic counts were performed at two intersections (roads 1 and 2; roads 2 and 3 in Figure 3.3). The typical morning and afternoon traffic peaks in urban areas were not identified at either intersection; instead an abrupt increase in traffic was observed at 6 a.m., with constant traffic counts during the day and, declining counts at night. Additionally, fluxes of CO_2 were also measured from the tower. A comparison of the diurnal pattern of traffic counts against

the fluxes of olefin and CO_2 showed a significant relationship. The average diurnal ratio between fluxes of olefins and CO_2 was 0.85, suggesting that both species are emitted by the same sources. If we accept this hypothesis and assume that 61% of CO_2 emissions are due to transportation as indicated in *Sheinbaum et al.* [2000], we find that transportation sources account for 46% to 76% of the olefin flux. This range coincides with the official emissions inventory [*SMA-GDF*, 2004] and a recent study based upon a chemical mass balance model [*Vega et al*., 2000]. For the modeling grid cell where the flux tower was located, the distribution of sources in the emissions inventory shows that mobile sources contribute 59% of the emissions for both olefins and C_2-benzenes, and 45% and 9% of the emissions for toluene and acetone, respectively. Emissions from painting buildings, cleaning surfaces, and solvent consumption are the most important acetone emission sources. This distribution of source types is similar to other sections of the city dominated by poor neighbourhoods (~70% of Mexico City).

3.5. Concluding remarks

Micrometeorological techniques have not previously been used in urban areas to measure VOC fluxes because of the lack of fast-response VOC sensors and the uncertainties involved with flux measurements in a city, where the spatial variability of surface cover, emission sources and roughness is high. However, in this field study, we have demonstrated the use of EC and DEC techniques to perform VOC flux measurements in an urban area using state of the art VOC sensors. The capability to evaluate emissions inventories using micrometeorological techniques, as we have described in this work, is a valuable, new tool for improving air quality management. Results from these direct flux measurements reduce the degrees of freedom available to match typical photochemical grid modeling results with observations and thus suggest that unresolved uncertainties should be sought in other aspects of urban atmospheric chemistry.

3.6. Acknowledgements

This study was supported by the Integrated Program on Urban, Regional and Global Air Pollution from the Massachusetts Institute of Technology and the Metropolitan Commission of Environment of Mexico City. The authors thank the assistance of the National Center for Environmental Research and Training as host of this study. The authors are also grateful to Chuck Kolb of Aerodyne for comments on the manuscript, and Miguel Zavala and Benjamin Foy of MIT, who supplied the emissions data.

3.7. References

Aubinet, M. et al. (2000), Estimates of the annual net carbon and water exchange of forests: the EUROFLUX methodology. *Advances in Ecological Research, 30*, 113-175.

Grimmond, C. S. B., and T. R. Oke (1999), Aerodynamic properties of urban areas derived from analysis of surface form, *J. Applied Meteor., 38*, 1262-1292.

Guenther, A. B., and A. Hills (1998). Eddy covariance measurement of isoprene fluxes. *J. Geophys. Res., 103(D11)*, 13145-13152.

Hsieh, C.I., G. Katul, and T. Chi (2000), An approximate analytical model for footprint estimation of scalar fluxes in thermally stratified atmospheric flows. *Advances in Water Resources, 23*, 765-772.

Lindinger, W., A. Hansel, and A. Jordan (1998), On-line monitoring of volatile organic compounds at pptv levels by means of proton-transfer-reaction mass spectroscopy (PTR-MS): Medical applications, food control and environmental research. *Int. J. Mass Spectrom.*, 173, 191-241.

Montcrieff, J. B., Y. Malhi, and R. Leuning (1996), The propagation of errors in long-term measurements of land-atmosphere fluxes of carbon and water, *Global Change Biology,* 2, 231-240.

Sheinbaum, C., L. V. Ozawa, O. Vasquez, and G.Robles (2000), Inventario de emisiones de gases de efecto invernadero asociados a la producción y uso de energía en la Zona Metropolitana del Valle de México. Reporte Final del Grupo de Energía y Ambiente, Universidad Nacional Autónoma de México, México, D.F.

SMA-GDF (2004), *Inventario de emisiones a la atmósfera. Zona Metropolitana del Valle de México,* Secretaria del Medio Ambiente del Gobierno del Distrito Federal, México D.F.

Solomon, P. A., E. B. Cowling, G. M. Hidy, and C. S. Furiness (2000), Comparison of scientific findings from major ozone field studies in North America and Europe. *Atmos. Environ., 34*, 1885-1920.

Vega, E., V. Mugica, R. Carmona, and E. Valencia (2000), Hydrocarbon source apportionment in Mexico City using the chemical mass balance receptor model. *Atmos. Environ. 34*, 4121-4129.

West, J. J., M. A. Zavala, L. T. Molina, M. J. Molina, F. San Martini, G. J. McRae, G. Sosa, and J. L. Arriaga-Colina (2004), Modeling ozone photochemistry and evaluation of hydrocarbon emissions in the Mexico City Metropolitan Area, *J. Geophys. Res., 109*, 19312, doi: 10.1029/2004JD004614.

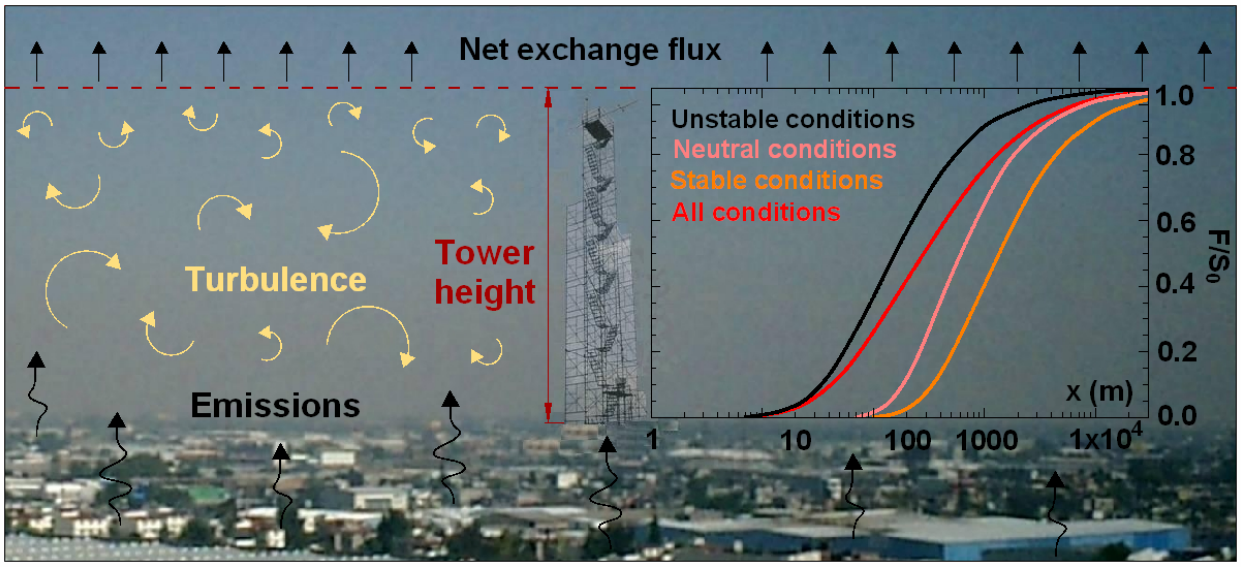

Figure 3.1. Left side: emissions from different sources are blended by the turbulence generated in the roughness sub-layer, producing a net exchange flux in the constant flux layer where the flux is measured. Right side: fraction of the flux measured (F/S_0) at the tower height versus the upwind distance or effective source footprint (x). F is the flux and S_0 the source strength.

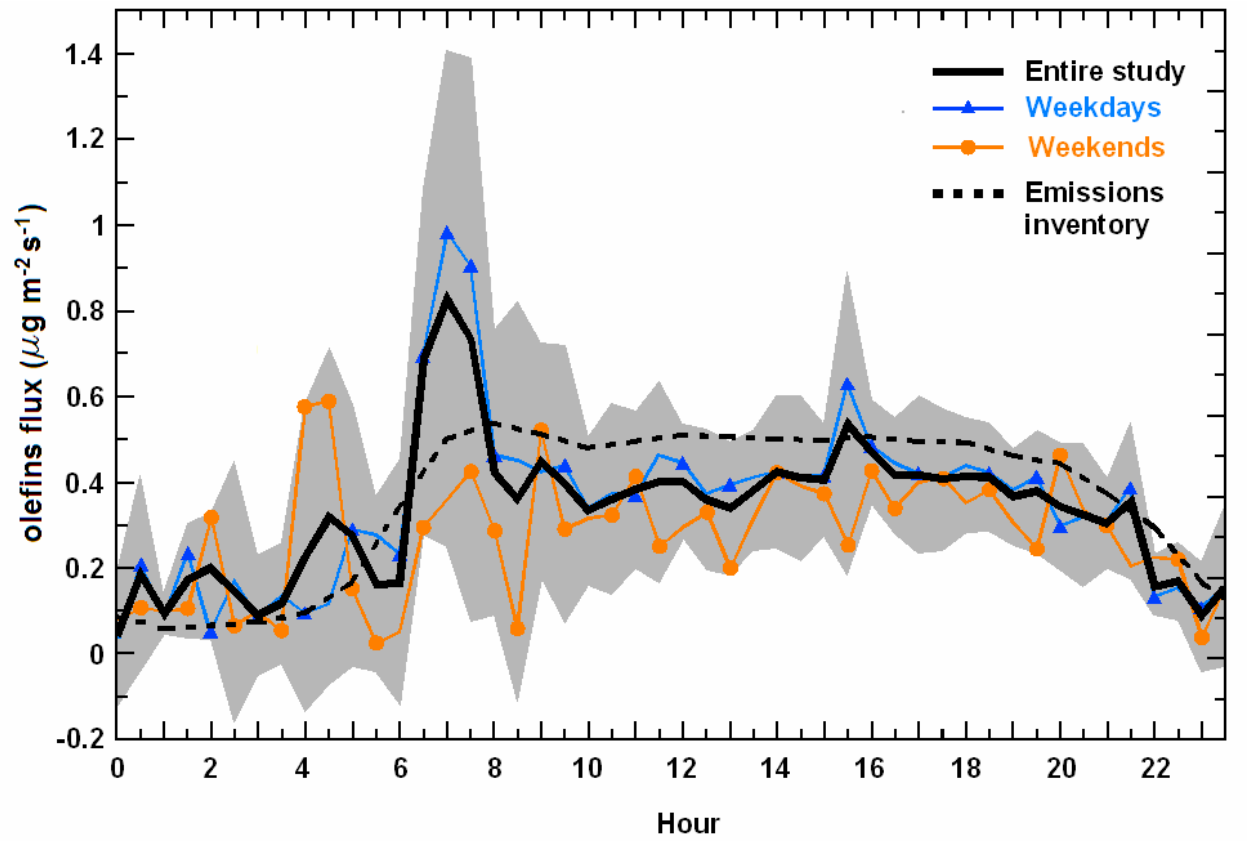

Figure 3.2. Average diurnal pattern of olefin fluxes predicted and measured for the 23-day study, and for weekdays and weekends. The dashed line indicates the sum of olefinic VOC emissions reported in the emissions inventory for the grid cell where the flux system was located. The grey shadow represents ±1 standard deviation from the total average.

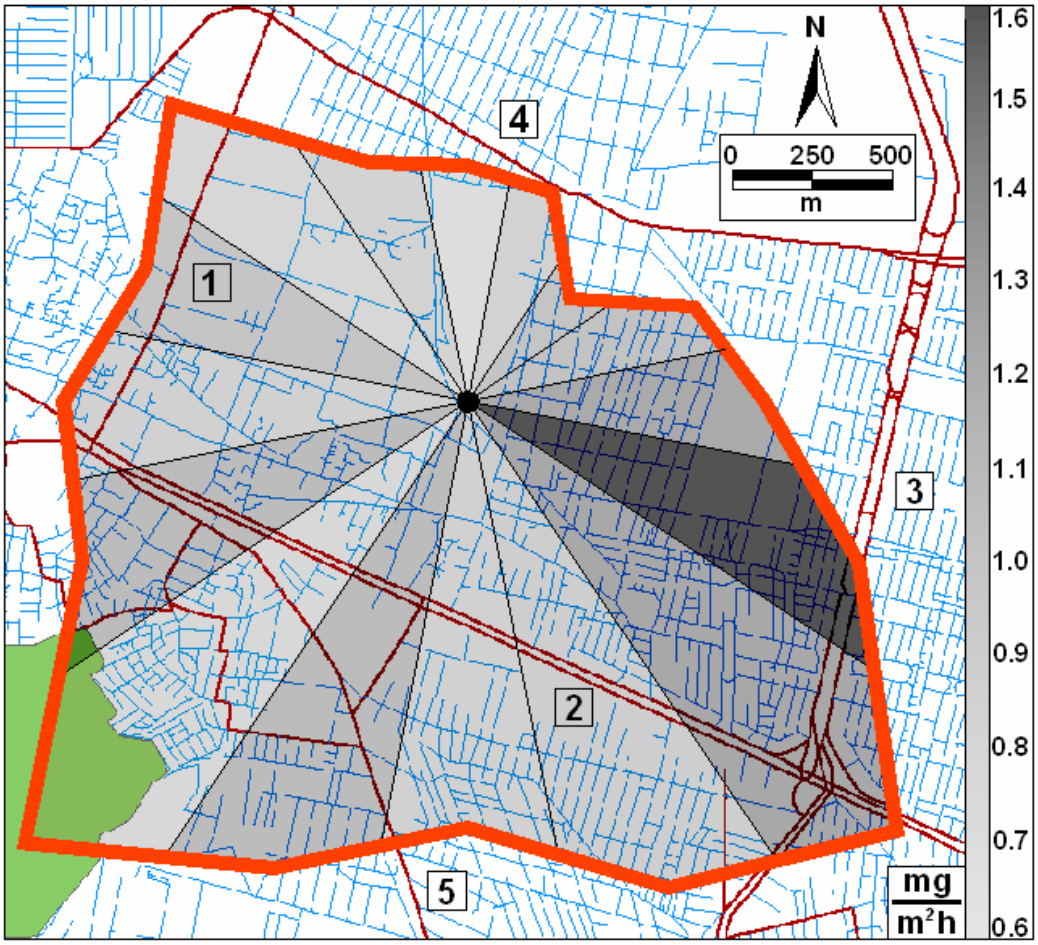

Figure 3.3. Olefin flux distribution as a function of the upwind direction during the entire study. The contour indicates the footprint that is estimated to encompass 80% of the total flux. Flux intensity is shown in grey scale.

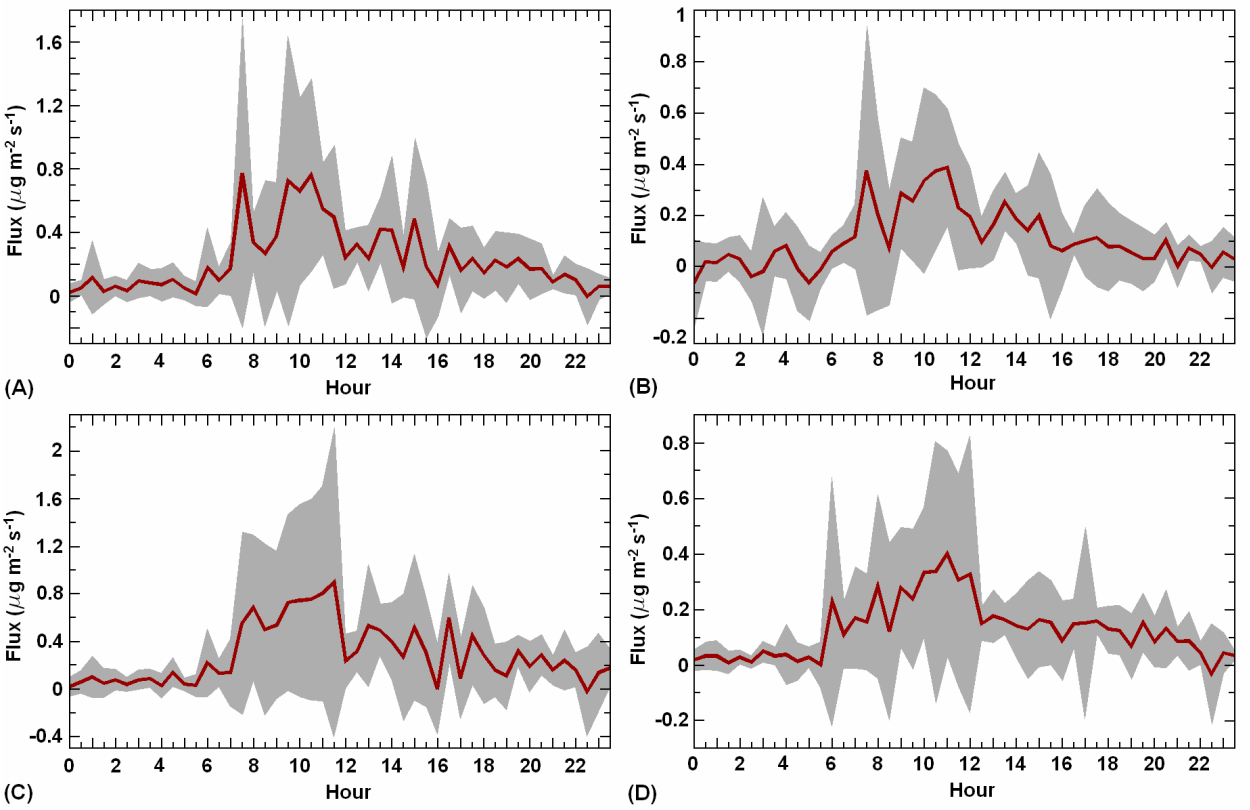

Figure 3.4. Average diurnal patterns of the flux of (A) methanol, (B) acetone, (C) toluene and (D) C_2-benzenes measured by the PTR-MS during ten days of the study. The grey shadows represent ±1 standard deviation from the total averages.

3.A. Auxiliary material

3.A.1. Evaluation of emission inventories

Generally, emissions inventories are evaluated through ambient measurements. The most direct evaluation has been to compare measured concentrations of NO_x and VOC with model results [West et al., 2004; Sillman, 1999; Trainer et al., 2000]; using this approach input emissions in models are modified to obtain the closest possible agreement with ambient measurements, with the assumption being that all errors come from the emissions inventory and not from model or measurements uncertainties. Other evaluation methods are based on measured ratios between species [Goldan et al., 1995]; for example, the morning VOC/NO_x ratio has been demonstrated to be useful for this purpose because chemical losses are relatively small during the morning and ambient concentrations reflect the ratio of directly emitted species [Sillman, 1999; Arriaga-Colina et al., 2004]. The chemical mass balance receptor model has also been successfully applied to evaluate and improve emissions inventories by identifying the relative contribution of different sources to measured VOC fingerprint [Watson et al., 2001]. For the case of emissions inventories from mobile sources, emissions have also been evaluated using open path sensors positioned across roads and from tunnel studies. Tunnel studies have proved to be a useful tool to measure emissions from in-use vehicles operating under real-world conditions [Sawyer et al., 2000].

3.A.2. Micrometeorological techniques to measure fluxes of trace gases

Micrometeorological techniques have been successfully used to measure biogenic hydrocarbon emissions from woodlands and agricultural fields. Biogenic VOC (BVOC) fluxes have been measured by techniques such as surface layer gradient, relaxed eddy accumulation (REA), EC and DEC [Guenther et al., 1996; Westberg et al., 2001; Karl et al., 2002]. The first two are indirect measurements of flux that rely on empirical parameterizations. EC is a direct flux measurement technique that requires a sampling rate of approximately 5 Hz. Fast-response sensors have recently become available so that EC methods can be used to measure VOC fluxes

above a forest canopy [Guenther and Hills, 1998] and over crop lands [Shaw et al., 1998]. The capabilities of the PTR-MS have been expanded to allow direct flux measurements of a number of BVOC through DEC [Karl et al., 2002; Rinne et al., 2001]. This method calculates fluxes using measurements at a lower frequency compared to EC; the sample interval can be as long as 30 s. This makes it possible to use relatively slow sensors for flux measurements. In urban areas, micrometeorological approaches have previously been applied to measure fluxes of momentum, heat and CO_2 [Grimmond et al., 2004; Oke et al., 1999; Moriwaki and Kanda, 2004; Soegaard and Møller-Jensen, 2003; Nemitz et al., 2002], and aerosols [Dorsey et al., 2002].

3.A.3. Field experiment

The flux measurements were conducted in a suburb at the southeast of Mexico City (19º21'29'' N, 99º04'24'' W) in spring 2003. Here we describe the site, equipment used and details of the post-processing of the data.

3.A.3.1. The CENICA super site

The CENICA super site is located in the Iztapalapa suburb, which is the suburb with the highest population in Mexico City (1,771,673 inhabitants) and highest density (12,000 inhabitants km^2) [INEGI, 2000]. Mexico City was selected for this experiment because it is a megacity known for severe photochemical air pollution problems, and because the urban VOC concentrations are among the highest in the world [Arriaga-Colina et al., 2004]. VOC emissions from combustion sources are accentuated by the high elevation of the city (2240 m.s.l.), which makes combustion processes less efficient. VOC evaporative emissions from a variety of sources such as cleaning, painting, and industrial processes are large due to the subtropical weather, temperatures of over 20ºC and intense solar radiation all the year round. Finally, the main contributor to high VOC concentrations in Mexico City is the extensive presence of aged industrial operations and a relatively old vehicle fleet.

A 25 m tower was installed on the rooftop of the 12 m tall CENICA laboratory. The instruments were mounted at a height 3 times taller than the surrounding buildings, this was assumed to be a sufficient height to be in the constant flux layer. The flux measurements were representative of the local scale ($10^2 – 10^4$ m), and integrated different neighbourhoods, with different combinations of built and vegetated cover.

3.A.3.2. The study period

The measurements of fluxes of olefins, CO_2 and energy were performed during 23 days during the dry season in April 2003 (days of the year: 97 – 119). The study period included the Holy Week (April 14 – 20), a period in which the vehicular traffic is reduced as many of the city residents leave for the holiday period. By taking measurements before, during and after this period, we expected to obtain data to help determine the influence of vehicular emissions upon atmospheric pollution. Fluxes of olefins were measured continuously with a FOS, while fluxes of methanol, acetone, toluene and C_2-benzenes were measured using a PTR-MS during selected days, including a continuous period between April 9 and April 16. During the other portions of the study, the PTR-MS was operated in a VOC scan mode to help identify the full range of VOC present in the Mexico City atmosphere.

This experiment was part of a large field campaign conducted in Mexico City (MCMA-2003), whose main objectives were to update and improve the Mexican emissions inventory, as well as to improve the current knowledge of the chemistry, dispersion and transport processes of pollutants emitted to the atmosphere.

3.A.3.3. Instrumentation

To instrument the flux tower (Figure 3.A.1), a 3 m boom was attached to the tower and a three axes sonic anemometer (Applied Technologies, Inc., model SATI-3K), an open-path infrared gas analyzer (IRGA) to monitor CO_2 and water vapour, were attached at the end of the boom. The length of the boom was enough to minimize the effects of flow distortion from the tower, and the

sensors were arranged to be as aerodynamic as feasible. Signal/power cables were run from the sensors to a shelter on the roof-top where the pc data acquisition system was operated through LabView software specifically designed for this experiment. A Teflon sampling line (5/8 inch O.D.) was positioned from the boom down the tower to a large pump. Inlet lines to the FOS and PTR-MS were connected to the sampling line near the roof-top instrument shelter. The lag time for sampling at the shelter was determined from a covariance analysis between the vertical wind speed and raw data from the FOS. The covariance was calculated for 0 to 100 s lags; the maximum correlation occurred for a lag time of 4.3 s. In operation, the flux system collected data at 10 Hz. The data were used to calculate 30 min average fluxes using the EC mode for the olefins, CO_2 and heat fluxes, and the DEC mode for the fluxes evaluated through the PTR-MS.

3.A.3.4. The Fast Olefin Sensor

The FOS is a Fast Isoprene Sensor calibrated with propylene instead of isoprene. Detection is based on chemiluminescent reaction between alkenes and ozone, and the detector responds with different sensitivity to a variety of olefins. Also there are reactions between ozone and other trace gases that could be potential interferences. Instrument response factors for a number of compounds have been previously reported [Guenther and Hills, 1998]. To analyze the FOS response in the atmosphere of Mexico City we evaluated the sensitivity of 5 olefins (propylene, ethylene, isoprene, 1-butene and 1-3 butadiene) and nitric oxide. All of the olefins exhibited a response. Nitric oxide gave no response in this test. Sensitivities for these species are shown in Table 3.A.1 with their corresponding relative sensitivities to propylene and FOS responses to average concentrations measured during selected days throughout the campaign between 6 and 10 am from the sampling line of the eddy covariance system by a canister sampling system. We found that the FOS has a more sensitive response to 1-3 butadiene and isoprene than to propylene; however, their ambient concentrations were much lower than the ambient levels of propylene. In comparison, species with a lower sensitivity than propylene, but with high concentrations in urban atmospheres (e.g. ethylene) can produce large signals. Figure 3.A.2

compares the FOS response to the sum of olefins as measured simultaneously with the canister sampling system. Results suggest that generally the total olefins level detected by the FOS is larger than the sum of identified olefins from canister samples. In only 3 of the 21 sample periods compared was the FOS response less than the sum of olefins measured in canister samples. With these periods removed, the ratio between the sum of olefins measured by canisters and the FOS signal shows a median of 48%. This indicates that 52% of olefins detected by the FOS remain unknown. Additional analysis is needed to identify these unknown species.

During the campaign the FOS was calibrated 3 times per day using propylene as standard (Scott Specialty Gases, 10.2 ppm, ±5% certified accuracy). The linear slope of instrument response versus propylene concentration and the zero level exhibited relatively little drift during the study period, 14% and 9%, respectively. Their possible influence in the assignment of absolute ambient propylene concentrations was corrected through frequent calibrations.

3.A.3.5. The Proton Transfer Reaction Mass Spectrometer

The Proton Transfer Reaction Mass Spectrometry is a novel technique capable of accurate, selective, and fast-response measurement of a subset of important VOC. This subset includes hydrocarbons from anthropogenic origin, such as aromatic and oxygenated species [de Gouw et al., 2003]. The PTR-MS has been described in detail elsewhere [Lindinger et al., 1998]. Briefly, H_3O^+ ions, which are produced in a hollow cathode discharge, are injected into a conventional ion drift tube. The air to be analyzed acts as the buffer gas and is continuously introduced at the front end of the drift tube. H_3O^+ ions will only react with trace components in the air having higher proton affinities than H_2O:

$$R + H_3O^+ \xrightarrow{k} RH^+ + H_2O \qquad (1)$$

The major constituents of air, N_2, O_2, CO_2, CH_4 and noble gases do not react with H_3O^+. A small portion of the flow through the reaction chamber is sampled by a quadrupole mass spectrometer where the RH^+ and H_3O^+ ions are mass filtered and detected by an ion multiplier.

The density of analyte R can be determined from the H_3O^+ and RH^+ count rates, the rate constant for the ion-molecule reaction, a fixed reaction time calculated from known mobility values of H_3O^+ in air, and the relative ion transmission efficiencies. In practice we calibrated the instrument sensitivity in the field using a multi-component gas standard that contained the analytes reported here. The calibration gas was diluted with a humid zero air flow and a multipoint calibration curve determined over the 1 to 50 ppbv range. Calibrations were performed every 2–3 days. The instrument background was automatically recorded every 3 hours by switching the sample flow to a humid zero air stream. Zero air was continuously generated by passing ambient air through a Pt-catalyst trap heated to 300 ºC. Background count rates were subtracted from the ambient data.

We operated the PTR-MS in a selective ion mode measuring up to 6 compounds of interest with dwell times of 0.2 or 0.5 s per compound to produce a disjunct time series with a resolution between 1.2 and 3.6 s, depending on the number of analyzed compounds. Four species, namely methanol (m/z 33), acetone (m/z 59), toluene (m/z 93) and C_2-benzenes (m/z 107) were targeted for this study. The m/z 107 contains contributions from ethyl benzene, three xylene isomers, and benzaldehyde [de Gouw et al., 2003]. The signal at m/z 59 is a composite of acetone and propanal. Based upon previous measurements of acetone and propanal in urban areas, acetone is likely to dominate (~90%) the response at this mass. The PTR-MS data was recorded on a separate computer from the computer used for the other sensors. The meteorological raw data and the data from the PTR-MS were continuously synchronized using a flag sent by the PTR-MS acquisition system.

3.A.3.6. The open-path InfraRed Gas Analyzer (IRGA)

The IRGA is an instrument specially designed for fast response measurements of CO_2 and H_2O fluctuations. A detailed description of it is given elsewhere [Auble and Meyers, 1992]. This instrument is quite robust, and we found that the response is relatively constant. For CO_2 it was calibrated twice per week using two CO_2 standard gas mixtures (327 and 402 ppm). We

compared the water vapor response to the Vaisala relative humidity sensor on the tower as a basis for calibrating the H_2O signal.

3.A.4. Eddy covariance flux technique

The flux of a trace gas (F_χ) is calculated according to the EC technique as the covariance between the instantaneous deviation of the vertical wind velocity (w') and the instantaneous deviation of the trace gas (c_χ') from their 30 minutes mean (equation 2). Fundamental aspects of EC have been widely discussed elsewhere [McMillen, 1988; Aubinet et al., 2000].

$$F_\chi = \overline{w' c_\chi'} = \frac{1}{t_2 - t_1} \int_{t_1}^{t_2} w'(t) c'(t) dt \qquad (2)$$

Because an urban surface is not flat and smooth, the data from the eddy covariance system is post-processed using archived 30 min raw data files to test that each period meets requirements for stationarity. Post-processing includes the following steps:

1) Convert raw data signal to scientific units, apply FOS and IRGA calibration coefficients, remove hard spikes and identify data gaps. Hard spikes can be caused by random electronic spikes or sonic transducer blockage (e.g. during precipitation). Data gaps may occur as a result of system breaks for routine maintenance or calibration, inadequacy of the meteorological conditions or complete system failures. A period is rejected if it does not fulfill 83% of the readings.

2) Identify and remove soft spikes, large short-lived departures from the period means [Schmid et al., 2000].

3) Perform coordinate rotation on three-dimensional velocity components. Its aim is to eliminate errors due to sensor tilt relative to the terrain surface or aerodynamic shadow due to the sensor or tower structure [Aubinet et al., 2000].

4) Calculate the mean and standard deviation for each variable.

5) Remove means from each signal to obtain fluctuations (prime quantities).

6) Apply a low pass filter to all the variables processed to eliminate the presence of a possible trend in the 30 min time series. We used a recursive digital filter [Kaimal and Finnigan, 1994].

7) Calculate 30 minute average vertical fluxes for momentum, sensible heat, latent heat, CO_2 and olefins. For olefins, the lag time needs to be applied.

9) Account for the effects of density fluctuations upon the fluxes, applying the Webb corrections [Webb et al., 1980] to water vapor, CO_2 and olefin fluxes.

10) Apply a correction to the olefin flux for high frequency loss due to damping of fluctuations within the sampling tube and due to instrument response time. This is done using a low-pass filtered heat flux [Massman and Lee, 2002].

11) Apply a second phase of quality control. All measured or derived variables (30 min averages) are submitted to a plausibility test and are rejected if they fall outside statically defined constraints for each variable (e.g. wind speed not to exceed 25 m s^{-1}).

3.A.5. Disjunct eddy covariance technique

The DEC technique employs instantaneous measurements, but with a slower frequency compared to the EC method. The flux is calculated as an average of a smaller subset of samples:

$$F_\chi = \overline{w' c_\chi'} = \frac{1}{N}\sum_{i=1}^{N} w'(t_i)c'(t_i) \qquad (3)$$

In equation 3, the time interval between samples is longer than in equation 2, thus the sum in 3 is an ensemble average rather than a time average. This technique gives more time to process

the samples, but increases the statistical uncertainty of the fluxes. DEC does not increase the statistical uncertainty of the flux value more than 8% if the time interval between samples is shorter than the appropriate integral timescale [Lenschow et al., 1994].

In order to evaluate the statistical uncertainty of the fluxes processed by DEC, we recalculated the olefin flux and sensible heat for the entire campaign from the 10 Hz raw data using sample intervals of 0.6, 1.2, 2.4 and 3.6 s. The DEC fluxes were compared with the fluxes calculated by EC and we found good agreement for sensible heat flux with a correlation coefficient of 0.99 and slope of 1.00 for all sampling intervals; however, for olefins, a clear difference was found when the sampling interval was higher than 1.2 s (see Figure 3.A.3). It seems that the origin, mixing and reactivity of the anthropogenic VOC in the atmosphere affects the integral timescale in DEC. Assuming similar behaviour between the olefin flux and the fluxes of the four species analyzed by the PTR-MS, whose time interval between samples was not constant, the potential error due to the DEC statistical uncertainties ranges from 9% to 40%, with a median of 30%. This error can be reduced by making the time step between samples shorter or using a longer averaging time.

The raw data to calculate the disjunct fluxes is post-processed following the same steps for EC.

3.A.6. Footprint analysis

By definition the footprint is the contribution, per unit surface flux, of each unit element of the upwind surface area to the measured vertical flux. The footprint term is also known as effective fetch. Both Eulerian analytical models [Horst and Weil, 1994; Kormann and Meixner, 2001] and Lagrangian stochastic dispersion models [Leclerc and Thurtell, 1990; Hsieh et al., 1997] have been used to investigate the footprint. To evaluate the effective fetch we used a hybrid model based on similarity theory and Lagrangian stochastic simulations [Hsieh et al., 2000]. The main advantage of this model is its ability to analytically relate atmospheric stability,

measurement height and surface roughness length to flux and footprint with relative simplicity. The performance is comparable to complex Eulerian and Lagrangian models [Schmid, 2002]. We applied this model to the complete set of 30 min periods measured during the campaign to determine the fraction of the flux measured as function of the upwind distance and stability condition.

The effective fetch can be evaluated through the fraction of the flux measured (F/S_0) at the tower height versus the upwind distance (x). F is the measured flux and S_0 the source strength. Following the chosen footprint model, this ratio is calculated as:

$$\frac{F}{S_0} = \exp\left(\frac{-1}{k^2 x} D z_u^P |L|^{1-P}\right) \tag{4}$$

where k is the Von Karman constant, L the Monin-Obuhkov length, D and P are similarity constants depending on the atmospheric stability:

$D = 0.28$; $P = 0.59$	for unstable conditions ($\xi = z_m / L < 0$)
$D = 0.97$; $P = 1$	for near neutral and neutral conditions ($\lvert \xi \rvert < 0.02$)
$D = 2.44$; $P = 1.33$	for stable conditions ($\xi > 0$)

z_u is a third characteristic length defined as:

$$z_u = z_m \left(\ln\left(\frac{z_m}{z_0}\right) - 1 + \frac{z_0}{z_m}\right) \tag{5}$$

where z_0 represents the surface roughness parameter (1 m), and z_m the measurement height ($z_m = z_{tower} - d$), considering a zero displacement plane of 8.4 m, approximately equal to 70% of the urban canopy ($d = 0.7(z_{city})$).

It is worthwhile to identify the effective fetch as function of the wind direction and hour of the day; Figure 3.A.4 shows the average footprint during the entire study for selected F/S_0 ratios and for different intervals of time. At night during stable and neutral conditions the footprint extends to longer distances than during unstable conditions during daytime. The effective fetch is also distributed over larger distances during stable conditions; 80% of its accumulation occurs in a radius between 1.5 and 4 km. Unstable conditions prevail during the morning and early afternoon, and produce shorter footprints with a small range and a predominant direction between south and southeast, encompassing a major roadway and intersection. During the middle of the day, the prevailing winds shifted somewhat more to the south and the footprint contracted so that emissions were measured from a smaller area with fewer mobile sources. During late afternoon, unstable conditions also prevail, but with less frequency and strength, to produce footprints longer than in previous hours and smaller than during the night.

3.A.7. Validity for the eddy covariance system

The quality of flux measurements is difficult to assess, because there are various sources of errors that range from failure to satisfy any of a number of theoretical assumptions to failure of the technical setup. We investigated three criteria: the statistical characteristics of the raw instantaneous measurements, the frequency resolution of the eddy covariance system through the spectra and cospectra of the measured variables, and the stationarity of the measurement process.

The largest number of rejected periods that did not fulfill at least one of the three criteria occurred at night during stable conditions; approximately 65% of the nighttime sample periods were excluded. However, during the day, the number of rejected periods decreased drastically. Around noon, more than 90% of periods fulfilled all criteria.

3.A.7.1. Statistical characteristics of the raw instantaneous measurements

The quality control of raw instantaneous data is applied during the postprocessing of the fluxes, where hard and soft spikes were identified and removed. Hard spikes can be caused by

random electronic spikes or sonic transducer blockage (e.g. during precipitation). They are identified by absolute limits for each variable. We found between 1 and 5 hard spikes for each period of 18,000 readings. Soft spikes are large short-lived departures from the period means. We followed an algorithm used in previous flux studies [Schmid et al., 2000] to identify and remove soft spikes; these occurred at a rate of approximately 37 soft spikes per period. In addition to spike removal, plausibility tests were applied to reject averages that fell outside statically defined constraints (e.g. wind speed not to exceed 25 m s^{-1}).

3.A.7.2. Spectral and cospectral analyses

All eddy covariance systems attenuate the true turbulent signals at sufficiently high and low frequencies. This loss of information results from limitations imposed by the physical size of the instruments, their separation distances, the inherent time response, and any signal processing associated with detrending or mean removal. In our system the FOS and PTR-MS were located in a shelter at the base of the tower. Sample air was pumped through 45 m of Teflon tubing.

Figure 3.A.5 shows that there is a positive correlation between mixing ratios of olefins and methanol with vertical wind speed at the measurement height. Methanol was selected as representative specie of the measured species by the PTR-MS. Although the sample interval for methanol is slower than for olefins, the same pattern exists for both species. Downdrafts (periods with negative vertical wind speed) are related to relatively low mixing ratios, and while updrafts are related to VOC rich air (e.g. in Figure 3.A.5 from 6 to 10 s).

Spectra and cospectra were calculated for sonic temperature (T), vertical wind speed (w), water vapor, CO_2 and olefins with a standard fast Fourier transform routine. For the first 4 parameters, we observed the expected frequency distributions in an unstable surface layer, showing the characteristic -5/3 and -7/3 slopes for spectra and cospectra, respectively, in the inertial subrange (range where the net energy coming from the energy-containing eddies is in equilibrium with the net energy cascading to smaller where it is dissipated). Figure 3.A.6 shows the spectra and cospectra between w and olefin concentration for 6 periods of 30 minutes at

different hours of the day, showing the expected -5/3 and -7/3 slopes in the inertial subrange up to a frequency of 0.7 Hz. This frequency attenuation is due to a number of error sources associated with the inevitable compromises with an eddy covariance system. In our experiment this attenuation is mainly associated with the long tube used to pump the sample air down the tower and the analyzer response. This lack of high frequency contribution to the fluxes can be corrected using a low-pass filtering method [Massman and Lee, 2002].

The simplest flux correction factor based on the low-pass filter method is the ratio of the measured sonic temperature flux ($\overline{w'T_s'}$) to the temperature flux calculated with the filtered temperature ($\overline{w'T_{sr}'}$) designed to match the overall response (including sample line effects of the FOS instrument), the corrected flux is estimated by equation (6). The resulting correction term was between 0.95 and 1.2.

$$F_\chi = \left(\overline{w' c_\chi'}\right)_{corrected} = \left(\overline{w' c_\chi'}\right)\left(\frac{\overline{w'T_s'}}{\overline{w'T_{sr}'}}\right) \tag{6}$$

The same spectral correction factor was applied to the VOC fluxes measured by the PTR-MS. The PTR-MS sampling interval was not constant during the experiment; masses were added and dwell times adjusted to improve signal to noise. Sampling intervals thus varied between 0.6 and 3.6 s so spectral analyses were not conducted. However, the loss of flux at high frequencies is assumed to be similar in both the FOS and PTR-MS.

3.A.7.3. Stationarity test

One of the basic assumptions of the eddy covariance technique is the stationarity of the measuring process based upon the separation between the time scales of the rapid turbulent fluctuations and the slow synoptic variations of atmospheric variables. There are several techniques to detect periods where the turbulent variables are nonstationary [Dutaur et al., 1999]. We applied a stationarity test based on the basic equation of the eddy covariance technique to

determine fluxes (equation 2) [Aubinet et al., 2000]. The measured time series of 30 min duration is divided into n/m = 6 intervals of 5 min. The covariance of a measured signal ξ and η of the interval l with m = 3000 (3000 measuring values in 5 min for 10 Hz scanning, i.e. n = 18000 in 30 min) measuring value is:

$$\overline{\xi'\eta'} = \frac{1}{m-1}\left[\sum_{k=1}^{m}\xi_{kl}\eta_{kl} - \frac{1}{m}\left(\sum_{k=1}^{m}\xi_{kl}\right)\left(\sum_{k=1}^{m}\eta_{kl}\right)\right] \tag{7}$$

for the test, the mean covariance of the n/m single interval is used:

$$\overline{\xi'\eta'} = \frac{1}{n/m}\left[\sum_{l=1}^{n/m}\overline{\xi_l'\eta_l'}\right] \tag{8}$$

For practical use, if the difference between the covariances determined by equations (2) and (8) is < 30%, the data is considered of high quality and if the difference is between 30% and 60%, the data have an acceptable quality [Aubinet et al., 2000]. We applied this test to the olefin fluxes for each measured period during the entire study; Figure 3.A.7 compares the average flux differences between 6 subperiods of 5 min and the 30 min averages versus their respective atmospheric stability conditions through the Monin-Obukhov length. In this case, 82% of the periods showed a difference lower than 60%, and 70% of the periods had flux differences lower than 30% and, thus, met the stationarity criteria. In general, conditions of non-stationarity were related to Monin-Obukhov lengths near zero which correspond to very unstable or stable (depending on the sign) conditions. Periods that did not meet the stationarity criteria were not used in the subsequent analyses.

3.A.8. Evaluation of random and systematic errors in the measured daily mean olefin flux

Although error propagation cannot be quantified accurately for flux measurements, a sensitivity analysis on the effects of errors can help to determine flux uncertainties [Montcrieff et al., 1996]. Thus, we evaluated the random and systematic errors on the mean daily flux. When

errors are random, errors in computed means diminish with increasing size of data set according to $N^{-1/2}$, where N is the number of points. Thus, random errors can be estimated by examining the convergence of calculations of the net flux. In contrast, systematic errors are not affected by increasing data set size, because they simply add in a linear fashion.

Figure 3.A.8a shows results of applying diverse values of percentage random error (p_r) to each half hour olefin flux of the entire data set. The horizontal line represents the mean daily flux, 0.36 μg m^{-2} s^{-1}. The symmetrical set of lines above and below this line represents the overall random error as a function of the magnitude of p_r and the given number of days. If we assume a random error of 20% on each 30 minute mean flux for the 23 days studied, the total random error on the net flux is 0.17 μg m^{-2} s^{-1} (47% of the net flux). If we also assume a systematic error (p_s) of 10%, we see from Figure 3.A.8b that the total systematic error on the net flux is 0.035 μg m^{-2} s^{-1}. Adding these two errors gives the total uncertainty of the net flux: 0.20 μg m^{-2} s^{-1} (57% of the total flux). This error analysis allows us to determine how many days of measurements are required to obtain the real flux at a site. For example, considering a random error of 20% and a systematic error of 10%, 100 days of measurements would resolve a net flux of 0.47 μg m^{-2} s^{-1}, 34% higher than the mean daily flux, while a year of measurements would resolve a net flux of 0.43 μg m^{-2} s^{-1}, at a level 22% greater than the base case. However, flux measurements can be continued only for a finite time before seasonal trends become important. The annual climate in Mexico City has three climatic seasons, dry warm season from March to May, raining season from June to October and dry cold season from November to February. Thus a seasonal evaluation of olefins fluxes in Mexico City using a 3 month period will yield fluxes resolved to within 11% of the mean daily fluxes assuming an optimistic point of view (random and systematic errors of 5%) and resolved to within 35% assuming large errors (random errors of 20% and systematic errors of 10%).

3.A.9. Diurnal profile of olefin concentration

Figure 3.A.9 shows the diurnal profile of average olefinic VOC concentrations detected by the FOS. This pattern is similar to what would be expected for typical pollutants emitted by mobile sources, such as NO and CO [INE, 2000]. The highest olefin concentrations were measured at 7 am and ranged from 30 to 87 ppbv, with 58 ppbv as average. This morning peak is attributed to the rapid increase of anthropogenic emissions into a shallow mixed layer followed by a rapid dilution by an expanding mixed layer as the sun warms the surface. Low olefin concentrations were observed during the afternoon, with an average of 6.6 ppbv, when dilution through the deep mixed layer was large and emissions were reduced compared to morning periods. The diurnal pattern was relatively constant during the entire study. There was a small difference of 6 ppbv in the early morning peak between Holy Week (national holyday period, characterized by reduction in traffic) and the other two measurement weeks.

3.A.10. Similarity between fluxes of VOC and CO_2, and their relationship with vehicular traffic

During the MCMA-2003 field campaign, traffic counts were performed at two intersections, one between avenues labelled 1 and 2 ($I_{1\text{-}2}$) in Figure 3.3 from the main text, and the other between avenues 2 and 3 ($I_{2\text{-}3}$). Figure 3.A.10 presents the diurnal olefin flux pattern along with the vehicular count distributions, where the vehicular fleet was classified into four different groups: passenger cars, taxi cabs, light trucks/buses, and heavy trucks/buses. Although both intersections share avenue 2, $I_{2\text{-}3}$ has a higher traffic density than $I_{1\text{-}2}$, since avenue 3 encircles the entire city, making it one of the busiest avenues, and one of the largest pollutant emission sources. Several routes of "colectivos" (small buses with a capacity for 20 passengers) start from $I_{1\text{-}2}$, which can be observed in the higher number of light buses and trucks compared to $I_{2\text{-}3}$.

The typical morning and afternoon urban traffic peaks do not occur at either intersection, instead a single peak is observed during the day. This peak begins at 6 am, and extends until late afternoon for $I_{1\text{-}2}$, and into the night for $I_{2\text{-}3}$. Assuming that the spike in the olefin flux profile

during the morning is due, in part, to the early morning release of olefins stored in the near surface layer during the night, we can affirm that the olefin flux profile matches the vehicular traffic density diurnal profile. Both remain constant during most of the daytime and then decline at night. Figure 3.A.11a shows the ratio formed by the normalized fluxes of olefins and CO_2 during the entire diurnal cycle. This ratio is close to one during the afternoon and part of the night which suggests that both pollutants have the same emission sources. Additionally, linear regressions between the olefin fluxes and traffic counts for both intersections confirm a degree of correlation between the measured flux and the traffic density with correlation coefficients of 0.69 for $I_{1\text{-}2}$ and 0.62 for $I_{2\text{-}3}$.

Figure 3.A.11 also shows the ratios formed by the normalized fluxes of the four species analyzed by the PTR-MS and CO_2. For these four VOC, we did not find a very close relationship to CO_2 fluxes, as for olefins. Table 3.A.2 shows the average ratios of the normalized fluxes between each VOC and CO_2 for different periods of the diurnal cycle. The two oxygenated species, methanol and acetone, and the two aromatic species, toluene and C_2-benzenes showed ratios above 0.89 during the morning; this suggests that they are emitted by similar sources emitting also CO_2. In the afternoon, their ratios were not higher than 0.61, and during the night, not higher than 0.41 which indicates stronger contributions from emission sources different than those emitting CO_2. In general, acetone showed the lowest similarity to CO_2 fluxes with a diurnal average ratio of 0.47.

3.A.11. Comparison between the measured VOC fluxes and VOC emissions used for air quality models in Mexico City

In order to compare the measured VOC fluxes with the emissions reported in the emissions inventory, we used the corresponding VOC emissions for the grid cell where our flux system was located, from the input data used for the most recent gas-phase modelling for Mexico City [West et al., 2004]. These emissions were based on the annual emissions reported in the official emissions inventory for 1998 [CAM, 2001]. This inventory was created by local government

authorities using bottom-up methods and emissions factors which were either measured locally or taken from elsewhere; for mobile sources, the MOBILE5 emissions model was adapted to account for local vehicle characteristics. The annual emissions were distributed spatially and temporally (hourly) for each of 21 species categories in the SAPRC-99 chemical mechanism according to data from a variety of sources. For mobile source emissions, it was used information compiled by the Metropolitan Environmental Commission of Mexico City (CAM), who estimated the spatial and temporal distributions separately for each pollutant on the basis of traffic count data. For emissions from vegetation, it was used the spatial distribution modeled by Velasco [2003], and temporal distributions estimated by Guenther et al. [2000]. Emissions from area sources were distributed spatially for each category separately, using population, commercial, or other distributions, as appropriate. For emissions from point sources, it was used a database compiled by the CAM including 6230 industries. The database contains the location, emissions, work hours, and other data that were used for estimating spatial and temporal distributions. The VOC speciation was based on the SAPRC-99 chemical mechanism for VOC reactivity assessment [Carter, 2000] and a standard mixture of hydrocarbons in urban atmospheres in the United States [Jeffries et al., 1989]. The speciation was determined for each source category using emissions profiles measured in Mexico City [Mugica et al., 1998, 2002; Vega et al., 2000]. These profiles were adjusted to include species and source categories not measured in Mexico City using emissions profiles from the SPECIATE database [Environmental Protection Agency (EPA), 1993].

Emissions of species belonging to the groups OLE1 and OLE2 in the SAPRC-99 mechanism were weighted by their apportionment to the standard mixture of hydrocarbons to these two groups and added to the emissions of isoprene and ethene to compare the olefin fluxes. Emissions from the emissions inventory were weighted also by their sensitive response to the FOS (see Table 3.A.1), for C4 and C5 olefins (C4 terminal alkenes, 3-methyl-1-butene, isobutene, 2-methyl-1-butene, trans-2-butene, cis-2-butene, and 2-methyl-2-butene) we used the same response factor for 1-butene. For species whose sensitive factors were unknown we

assumed null factors (1-pentene, 1-hexene, C5, C6, C7, C8, C9, C10 and C11 alkenes, cyclohexene, C4, C5, C6, C7, C8, C9, C10 and C11 internal alkenes, and cyclic or di-olefins).

For toluene, its apportionment to the standard mixture of hydrocarbons was weighted with the total apportionment of species lumped in the group ARO1 of the SAPRC-99 mechanism. For C_2-benzenes, apportionments of o,m,p-xylenes were weighted to the total emissions of hydrocarbons lumped in the group ARO2 and added to the reported emissions of ethyl benzene. Acetone emissions were directly compared to the measured fluxes of acetone, since the SAPRC-99 model considers a specific group for it. For methanol, no comparison was possible because methanol emissions were not considered in the model.

Figure 3.A.11 shows the diurnal profiles of the measured fluxes and emissions of toluene, C_2-benzene and acetone. Emissions from a landfill reported for the grid where the flux tower was located were excluded from the emissions profile of the emissions inventory, since the landfill was outside of the analyzed footprint.

For the studied grid, the major contributor to the olefins and C_2-benzenes budget according to the emissions inventory are mobile sources, mainly gasoline vehicles, with a contribution close to 60%. Other important sources for both hydrocarbons are painting buildings and cleaning surfaces. For olefin emissions, leakages of LPG account for only 5%. For C_2-benzenes another important source is solvent consumption, which represents 8% of total emissions. For emissions of toluene and acetone, the sum of emissions from area sources is higher than emissions from mobile sources. However, emissions from gasoline vehicles account for 39% of all toluene emissions, while for acetone mobile sources account for only 8%. Again, painting buildings and cleaning surface represent the major area sources for these two compounds.

3.A.12. References

Arriaga-Colina, J.L., J. J. West, G. Sosa, S. S. Escalona, R. M. Orduñez, and A. D. M. Cervantes (2004), Measurements of VOCs in Mexico City (1992-2001) and evaluation of VOCs and CO in the emissions inventory, *Atmos. Environ., 38*, 2523-2533.

Aubinet, M., et al. (2000), Estimates of the annual net carbon and water exchange of forests: the EUROFLUX methodology, *Adv. Ecol. Res., 30*, 113-175.

Auble, D.L., and T. P. Meyers (1992), An open path, fast response infrared absorption gas analyzer for H_2O and CO_2, *Bound.-Layer Meteor., 59*, 243-256.

CAM (2001), Inventario de emisiones a la atmósfera, Zona Metropolitana del Valle de México, 1998, Comisión Ambiental Metropolitana, México, D.F.

Carter, W. P. L. (2000), Documentation of the SAPRC-99 Chemical Mechanism for VOC reactivity assessment, final report to California Air Resources Board, contracts 92-329 and 95-308, Calif. Air Res. Board, Sacramento, Calif. (available at www.cert.ucr.edu/~carter)

de Gouw, J. A., P. D. Goldan, C. Warneke, W. C. Kuster, J. M. Roberts, M. Marchewka, S. B. Bertman, A. A. P. Pszenny, and W. C. Keene (2003), Validation of proton transfer reaction-mass spectrometry (PTR-MS) measurements of gas-phase organic compounds in the atmosphere during the New England Air Quality Study (NEAQS) in 2002, *J. Geophys. Res., 108*, 4682-4199.

Dorsey, J. R., E. Nemitz, M. W. Gallagher, D. Fowler, P. I. Williams, K. N. Bower, and K. M. Beswick (2002), Direct measurements and parameterisation of aerosol flux, concentration and emission velocity above a city, *Atmos. Environ., 36*, 791-800.

Dutaur, L., S. Cieslik, A. Carrara, and A. Lopez (1999), The detection of nonstationarity in the determination of deposition fluxes, in Proceedings of EUROTRAC Symposium ’98 Vol. 2, edited by P. M. Borrell and P. Borrell, pp. 171-176, WIT Press, Southampton.

Environmental Protection Agency (1993), SPECIATE, VOC/PM speciation data system, version 1.50, Environ. Prot. Agency and Radian Corp., Research Triangle Park, N. C.

Goldan, P.D., M. Trainer, W. C. Kuster, D. D. Parrish, J. Carpenter, J. M. Roberts, J. E. Yee, and F. C. Fehsenfeld (1995), Measurements of hydrocarbons, oxygenated hydrocarbons, carbon monoxide, and nitrogen oxides in an urban basin in Colorado: implications for emission inventories, *J. Geophys. Res., 100*, 22771-22783.

Grimmond, C. S. B., J. A. Salmond, T. R. Oke, B. Offerle, and A. Lemonsu (2004), Flux and turbulence measurements at a densely built-up site in Marseille: heat, mass (water and carbon dioxide), and momentum, *J. Geophys. Res., 109*, 24101-24120.

Guenther, A., et al. (1996), Isoprene fluxes measured by enclosure, relaxed eddy accumulation, surface layer gradient, mixed layer gradient, and mixed layer mass balance techniques, *J. Geophys. Res., 101*, 18555-18567.

Guenther, A., and A. Hills (1998), Eddy covariance measurement of isoprene fluxes, *J. Geophys. Res., 103*, 13145-13152.

Guenther, A., C. Geron, T. Pierce, B. Lamb, P. Harley, and R. Fall (2000), Natural emissions of non-methane volatile organic compounds, carbon monoxide, and oxides of nitrogen from North America, *Atmos. Environ., 34*, 2205– 2230.

Horst, T. W., and J. C. Weil (1994), How far is far enough? The fetch requirements for micrometeorological measurement of surface fluxes, *J. of Atmos. and Oceanic Technol*., *11*, 1018-1025.

Hsieh, C. I., G. G. Katul, J. Schieldge, J. T. Sigmon, and K. K. Knoerr (1997), The Lagrangian stochastic model for fetch and latent heat flux estimation above uniform and nonuniform terrain, *Water Resour. Res., 33*, 427-438.

Hsieh, C. I., G. Katul, and T. Chi (2000), An approximate analytical model for footprint estimation of scalar fluxes in thermally stratified atmospheric flows, *Adv. Water Resour., 23*, 765-772.

INE (2000), Almanaque de datos y tendencias de la calidad del aire en ciudades mexicanas, INE-SEMARNAT, México, D.F.

INEGI (2000), Estados Unidos Mexicanos Resultados Prelimanares XII Censo General de Población y Vivienda, INEGI, México, D.F.

Jeffries, H. E., K. G. Sexton, J. R. Arnold, and T. L. Kale (1989), Validation testing of new mechanisms with outdoor chamber data, Volume 2: analysis of VOC data for the CBA and CAL photochemical mechanisms, final report EPA-600/3-89-010b, EPA, Research Triangle Park, NC.

Kaimal, J. C., and J. J. Finnigan (1994), Atmospheric boundary layer flows: Their structure and measurement, 289 pp., Oxford Univ. Press, New York.

Karl, T. G., C. Spirig, J. Rinne, C. Stroud, P. Prevost, J. Greenberg, R. Fall, and A. Guenther (2002), Virtual disjunct eddy covariance measurements of organic compound fluxes from a subalpine forest using proton transfer reaction mass spectroscopy, *Atmos. Chem. Phys., 2*, 279-291.

Kormann, R., and F. X. Meixner (2001), An analytical footprint model for neutral stratification, *Bound.-Layer Meteor., 99*, 207-224.

Leclerc, M. Y., and G. W. Thurtell (1990), Footprint prediction of scalar fluxes using a Markovian analysis, *Bound.-Layer Meteor., 52*, 247-258.

Lenschow, D. H., J. Mann, and L. Kristensen (1994), How long is long enough when measuring fluxes and other turbulence statistics?, *J. Atmos. Oceanic Technol., 11*, 661-673.

Lindinger, W., A. Hansel, and A. Jordan (1998), On-line monitoring of volatile organic compounds at pptv levels by means of proton-transfer-reaction mass spectroscopy (PTR-MS):

Medical applications, food control and environmental research, *Int. J. Mass Spectrom., 173*, 191-241.

Massman, W. J. and X. Lee (2002), Eddy covariance flux corrections and uncertainties in long-term studies of carbon and energy exchanges, *Agric. For. Meteor., 113*, 121-144.

McMillen, R (1998), An eddy correlation technique with extended applicability to non-simple terrain, *Bound.-Layer Meteor., 43*, 231-245.

Montcrieff, J. B., Y. Malhi, and R. Leuning (1996), The propagation of errors in long-term measurements of land-atmosphere fluxes of carbon and water, *Global Change Biol., 2*, 231-240.

Moriwaki, R., and M. Kanda (2004), Seasonal and diurnal fluxes of radiation, heat, water vapor, and carbon dioxide over a suburban area, *J. Appl. Meteor., 43*, 1700-1710.

Mugica, V., E. Vega, J. L. Arriaga, and M. E. Ruiz (1998), Determination of motor vehicle profiles for non-methane organic compounds in the Mexico City metropolitan area, *J. Air Waste Manage. Assoc., 48*, 1060–1068.

Mugica, V., J. Watson, E. Vega, E. Reyes, M. E. Ruiz, and J. Chow (2002), Receptor model source apportionment of nonmethane hydrocarbons in Mexico City, *Sci. World J., 2*, 844– 860.

Nemitz, E., K. J. Hargreaves, A. G. Mcdonald, J. R. Dorsey, and D. Fowler (2002), Micrometeorological measurements of the urban heat budget and CO_2 emissions on a city scale, *Environ. Sci. Technol., 36(14),* 3139-3146.

Oke, T. R., R. A. Spronken-Smith, E. Jáuregui, and C. S. B. Grimmond (1999), The energy balance of central Mexico City during the dry season, *Atmos. Environ., 33*, 3919-3930.

Rinne, H. J. I., A. Guenther, C. Warneke, J. A. de Gouw, and S. L. Luxembourg (2001), Disjunct eddy covariance technique for trace gas flux measurements, *Geophys. Res. Lett., 28*, 3139-3142.

Sawyer, R. F., R. A. Harley, S. H. Cadle, J. M. Norbeck, R. Slott, and H. A. Bravo (2000), Mobile sources critical review : 1998 NARSTO assessment, *Atmos. Environ., 34*, 2161-2181.

Schmid, H. P., C. S. B. Grimmond, F. Cropley, B. Offerle, and H. B. Su (2000), Measurements of CO_2 and energy fluxes over a mixed hardwood forest in the mid-western United States, *Agric. For. Meteor., 103*, 357-374.

Schmid, H. P. (2002), Footprint modeling for vegetation atmosphere exchange studies: a review and perspective, *Agric. For. Meteor., 113*, 159-183.

Shaw, W. J., C. W. Spicer, and D. V. Kenny (1998), Eddy correlation fluxes of trace gases using a tandem mass spectrometer, *Atmos. Environ., 32*, 2887-2898.

Sillman, S. (1999), The relation between ozone, NO_x, and hydrocarbons in urban and polluted rural environments, *Atmos. Environ., 33*, 1821-1845.

Soegaard, H., and L. Møller-Jensen (2003), Towards a spatial CO_2 budget of a metropolitan region based on textural image classification and flux measurements, *Remote Sens. Environ., 87*, 283-294.

Trainer, M., D. D. Parrish, P. D. Goldan, J. Roberts, and F. C. Fehsenfeld (2000), Review of observation-based analysis of the regional factors influencing ozone concentrations, *Atmos. Environ., 34*, 2045–2061.

Vega, E., V. Mugica, R. Carmona, and E. Valencia (2000), Hydrocarbon source apportionment in Mexico City using the chemical mass balance receptor model, *Atmos. Environ., 34*, 4121–4129.

Velasco, E. (2003), Estimates for biogenic non-methane hydrocarbons and nitric oxide emissions in the Valley of Mexico, *Atmos. Environ., 37*, 625-637.

Watson, J. G., J. C. Chow, and E. Fujita (2001), Review of volatile organic compound source apportionment by chemical mass balance, *Atmos. Environ., 35*, 1567-1584.

Webb, E. K., G. I. Pearman, and R. Leuning (1980), Correction of flux measurements for density effects due to heat and water vapour transfer, *Q. J. R. Meteorol. Soc. 106(447),* 85-100.

West, J. J., M. A. Zavala, L. T. Molina, M. J. Molina, F. San Martini, G. J. McRae, G. Sosa, and J. L. Arriaga-Colina (2004), Modeling ozone photochemistry and evaluation of hydrocarbon emissions in the Mexico City Metropolitan Area, *J. Geophys. Res., 109*, 19312, doi: 10.1029/2004JD004614.

Westberg, H., B. Lamb, R. Hafer, A. Hills, P. Shepson, and C. Vogel (2001), Measurement of isoprene fluxes at the PROPHET site, *J. Geophys. Res*., *106*, 24347-24358.

Table 3.A.1. Sensitivities, average concentrations measured during selected days throughout the campaign between 6 and 10 am from the sampling line of the eddy covariance system by a canister sampling system, FOS responses to those average concentrations, and relative sensitivities to propylene for the 6 evaluated species

Compound	**Sensitivity (photons ppb^{-1} s^{-1})**	**Average conc., 6–10 am (ppb)**	**Average FOS response (photons s^{-1}) [c]**	**Relative sensitivity to propylene [d]**
Propylene	25.4	7.50	191	1.00
Isoprene	74.7	0.304	23	2.94
Ethylene	17.7	20.7	366	0.70
1-3 butadiene	49.8	0.791	39	1.96
1-Butene	7.9	3.90 [a]	31	0.31
NO	~0.0	61.2 [b]	0	~0.0

[a] As i-butene

[b] From continuous monitoring during the entire campaign.

[c] Average response = (sensitivity)(average conc.) + (zero value), in this table is considered a zero value equals to zero.

[d] Relative sensitivity = (compound sensitivity) / (propylene sensitivity)

Table 3.A.2. Average ratios of the normalized fluxes of each analyzed VOC and CO_2 for different periods of the diurnal cycle. A high ratio indicates that the VOC specie and CO_2 are emitted by the same sources, while a low ratio indicates that the VOC and CO_2 species are emitted by different sources

	Olefins	**Methanol**	**Acetone**	**Toluene**	**C_2-benzenes**
Morning (6:30-12:00)	0.70	0.89	0.96	0.92	0.95
Afternoon (12:30-19:00)	0.84	0.57	0.55	0.61	0.59
Night (19:30-6:00)	0.82	0.36	0.18	0.41	0.38
Day (6:30-19:00)	0.87	0.72	0.74	0.76	0.76
Diurnal average	0.85	0.55	0.47	0.59	0.59

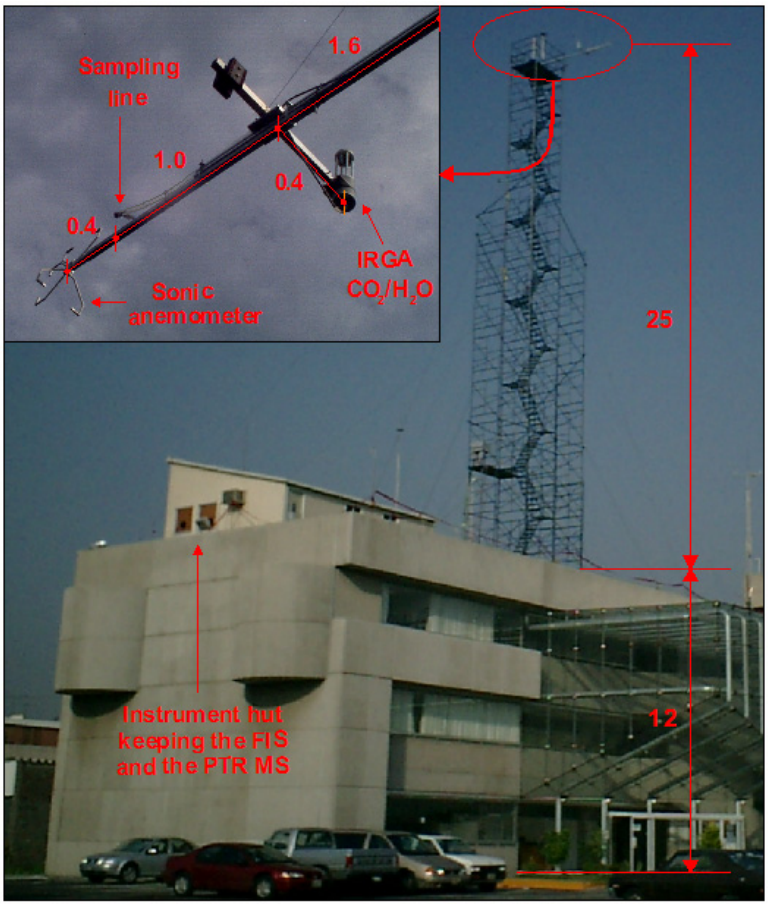

Figure 3.A.1. Schematic diagram of the instrumented flux tower. The azimuth orientation of the sonic anemometer is 16º from north. Dimensions are in meters.

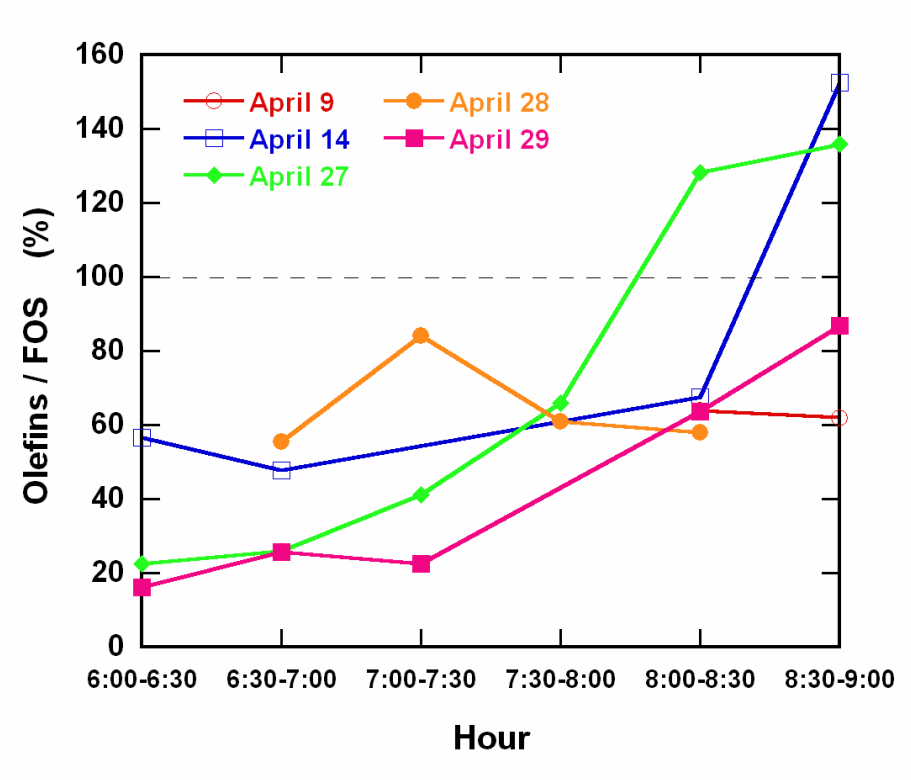

Figure 3.A.2. Comparison of identified olefins weighted by their corresponding FOS sensitivities from GC-FID measurements versus FOS measurements for 21 sample periods during selected days throughout the campaign between 6 and 10 am.

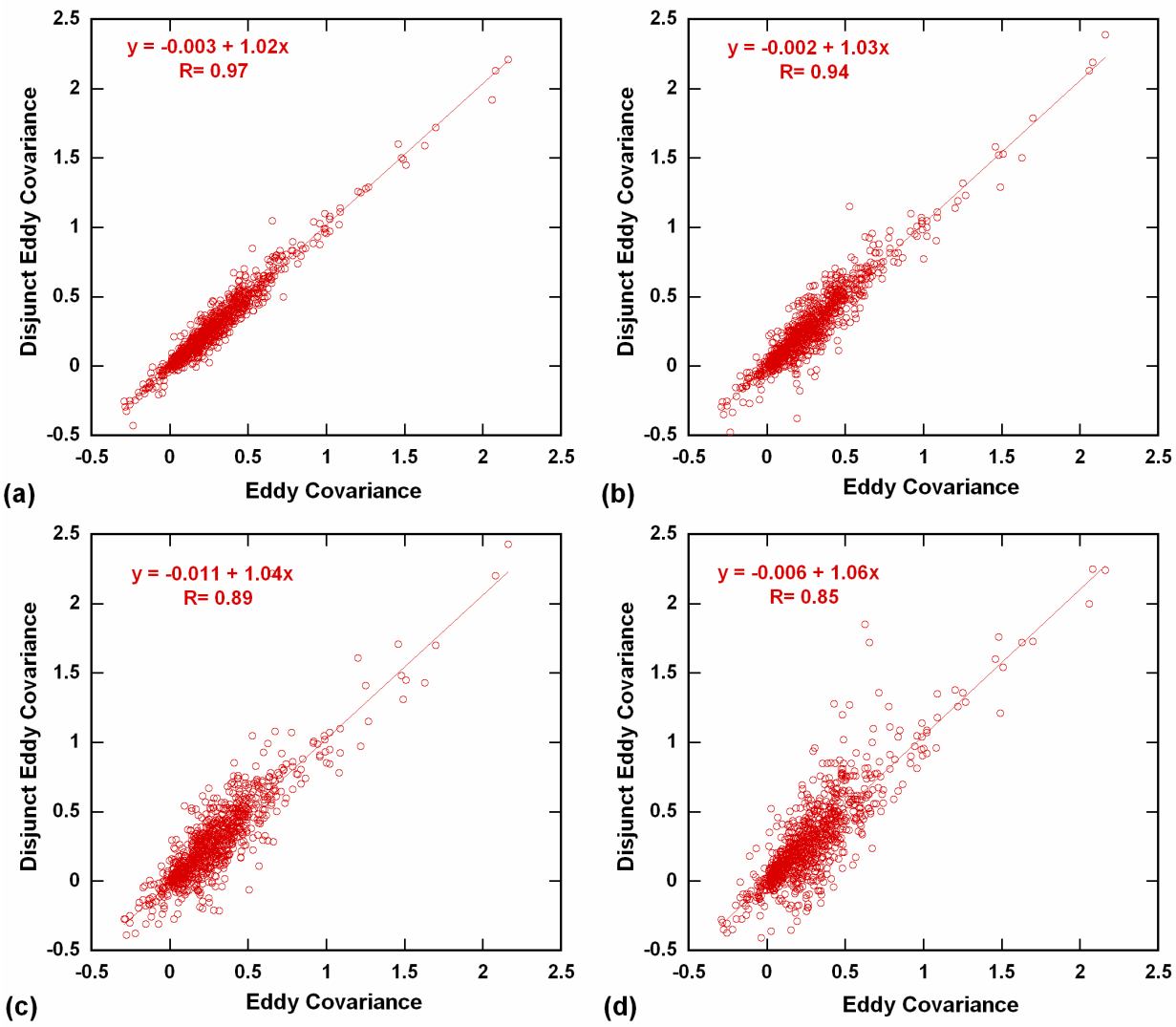

Figure 3.A.3. Comparison between olefin fluxes (μg m^{-2} s^{-1}) calculated using the techniques of eddy covariance and disjunct eddy covariance with different sampling intervals (a) 0.6 s, (b) 1.2 s, (c) 2.4 s and (d) 3.6 s.

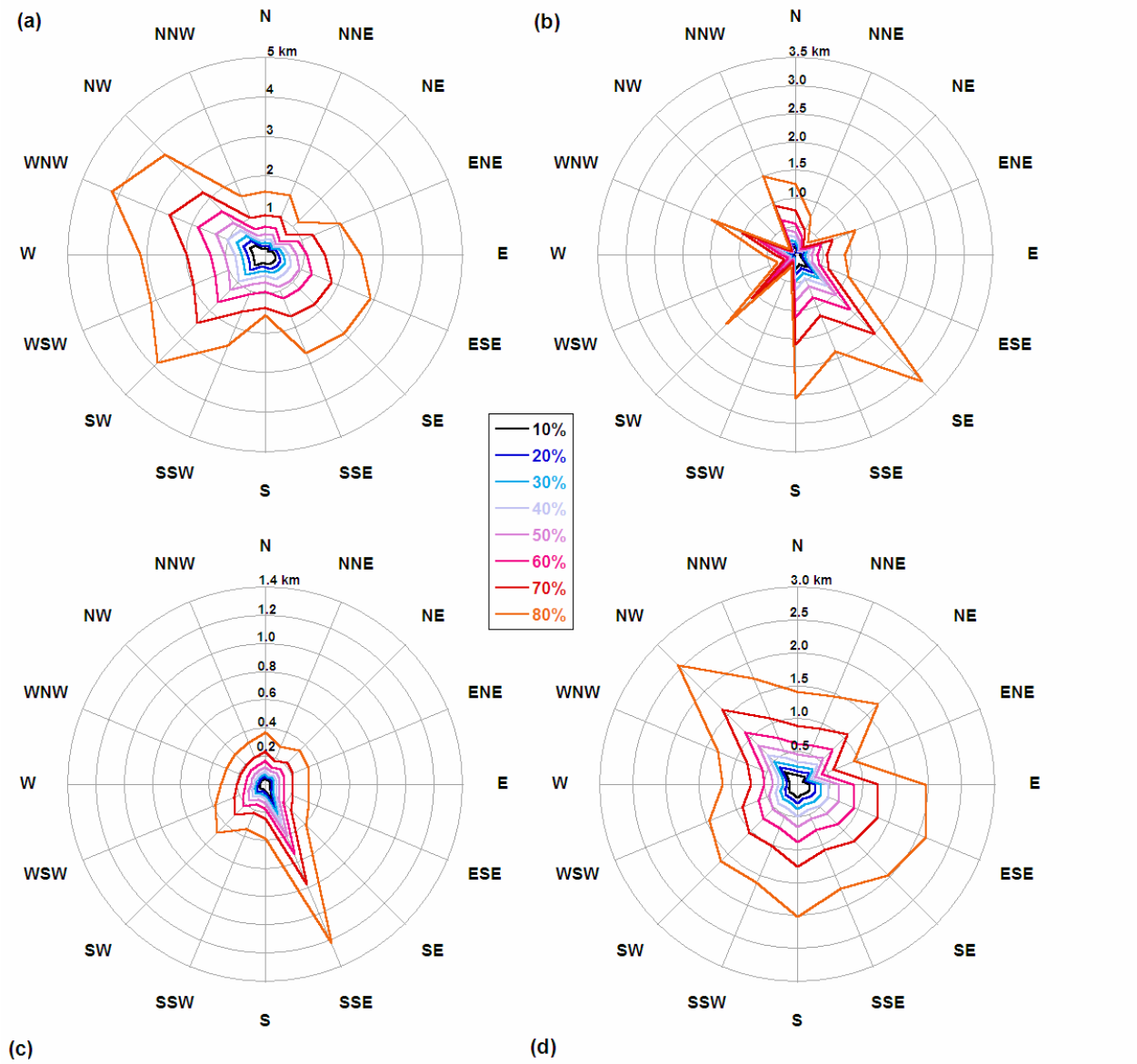

Figure 3.A.4. Different fractions of the measured flux (F/S_0) during the entire campaign as function of the wind direction for different intervals of time, (a) from 0:00 to 6:00 h, (b) from 6:00 to 9:00 h, (c) from 9:00 to 15:00 h and (d) from 14:00 to 21:00 h.

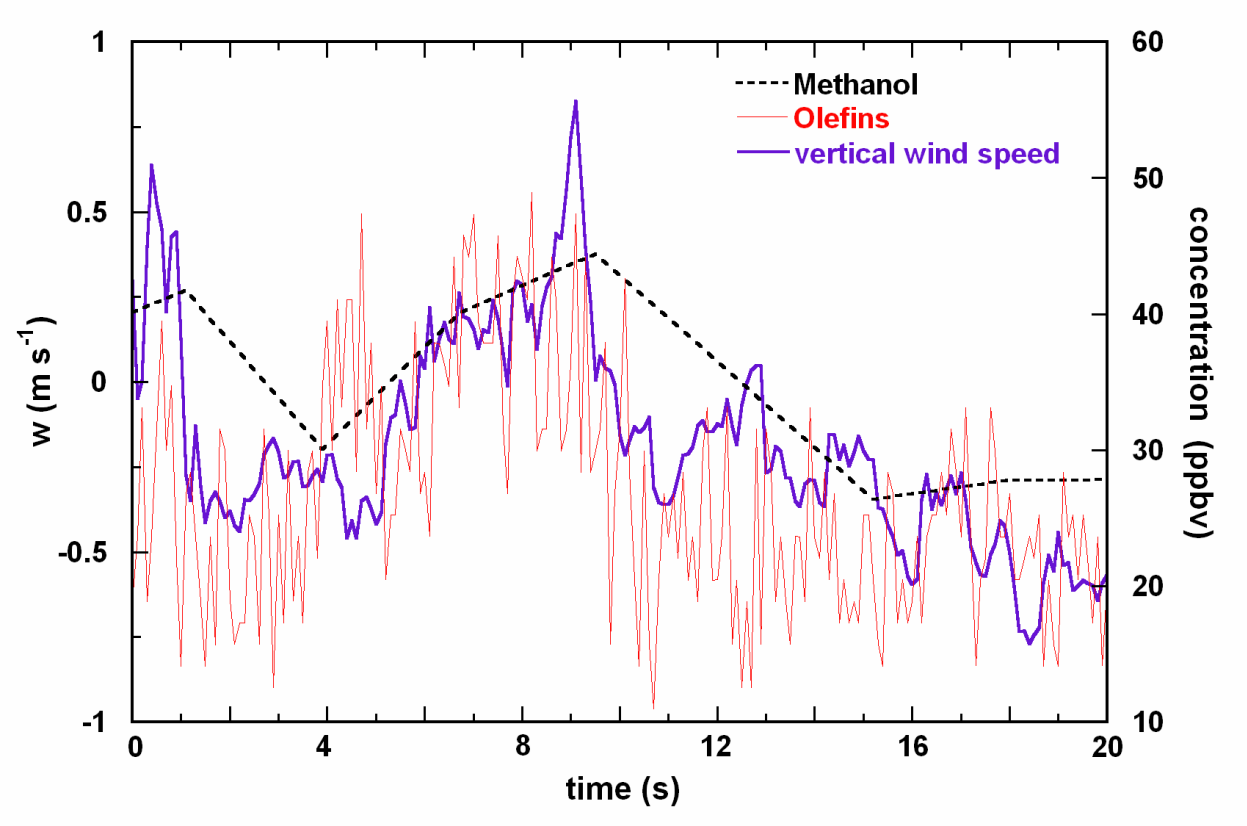

Figure 3.A.5. A 20-s trace of methanol and olefins mixing ratios plotted together with vertical wind speed beginning at 9:40 h local time on April 11, 2003.

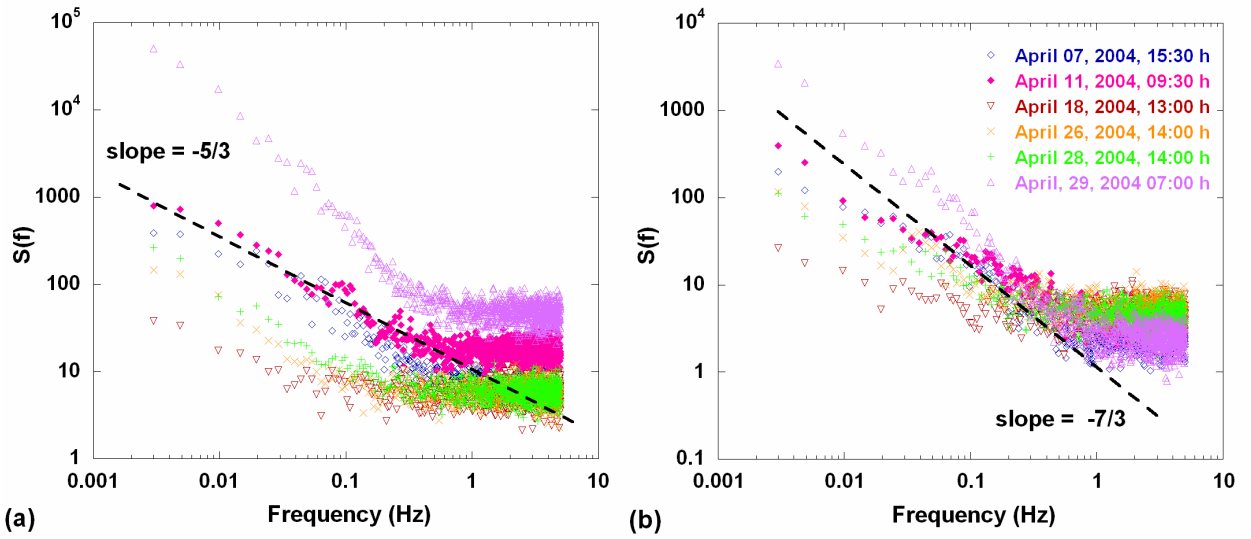

Figure 3.A.6. Spectra for olefins mixing ratio (a) and cospectra for olefins mixing ratio and vertical wind speed (b) for 6 different periods of 30 minutes before the low-pass filter correction. The -5/3 and -7/3 slopes indicate the theoretical slopes of the inertial subrange.

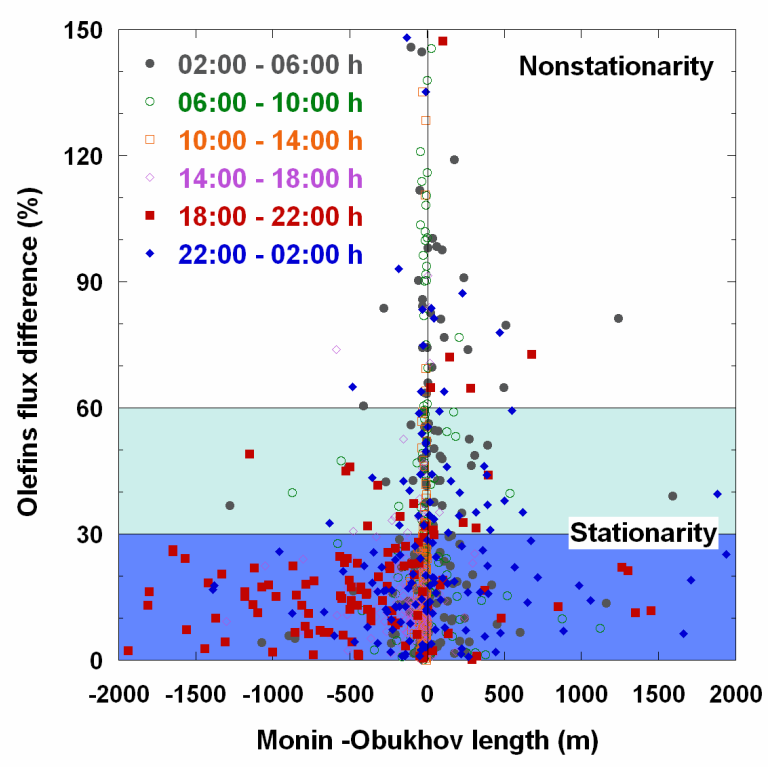

Figure 3.A.7. Stationarity test for olefin flux: a measured period is stationary if the average flux from 6 continuous subperiods of 5 min is within 60% of the flux obtained from a 30 min average. In our study 82% of the periods fulfilled this criterion.

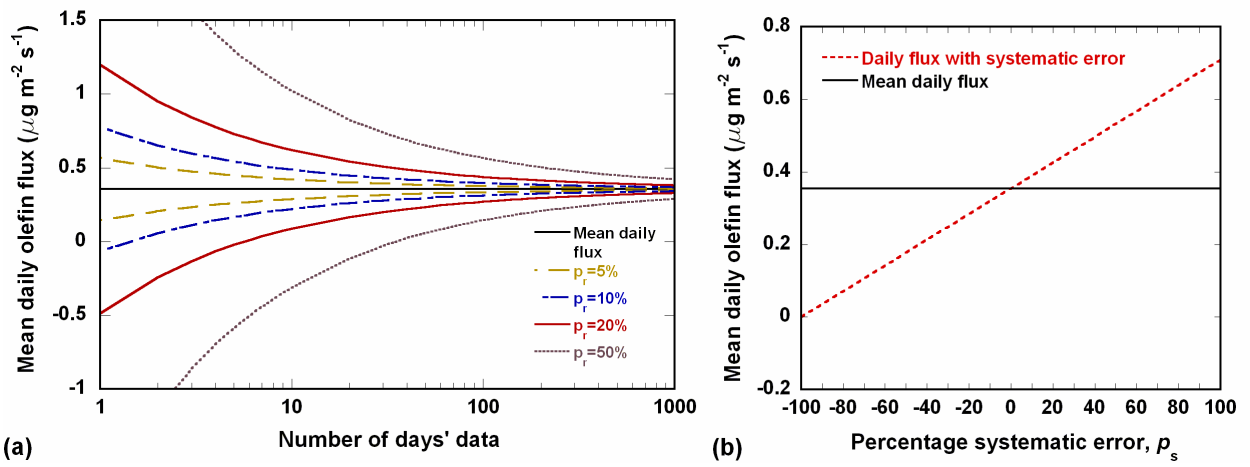

Figure 3.A.8. Effects of random and systematic errors for the mean daily olefin flux. (a) Effects due to random errors for various percentages of error. (b) Effects due to systematic errors as a function of the error percentage. In both figures the horizontal line represents the mean daily flux, 0.355 μg m^{-2} s^{-1}.

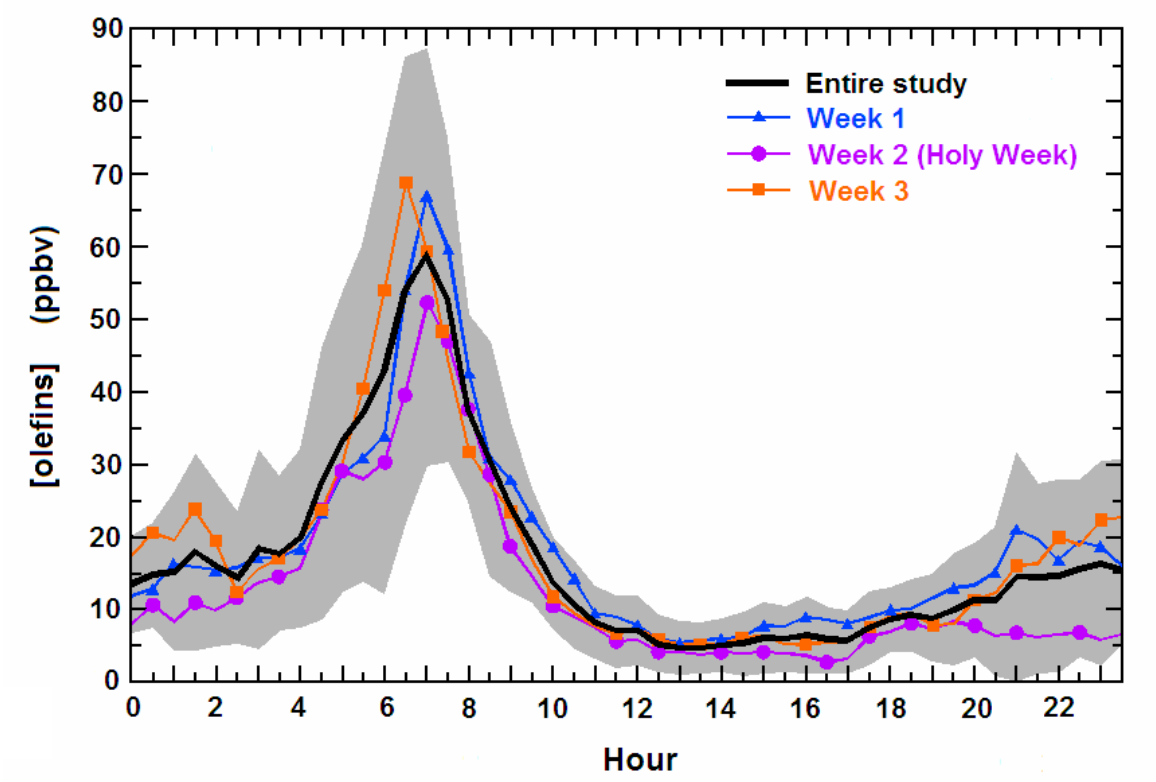

Figure 3.A.9. Average diurnal pattern of olefinic concentration detected by the FOS for the entire study (black line) and for individual weeks. The gray shadow represents ±1 standard deviation from the total average, and gives an indication of the day-to-day variability in each phase of the daily cycle.

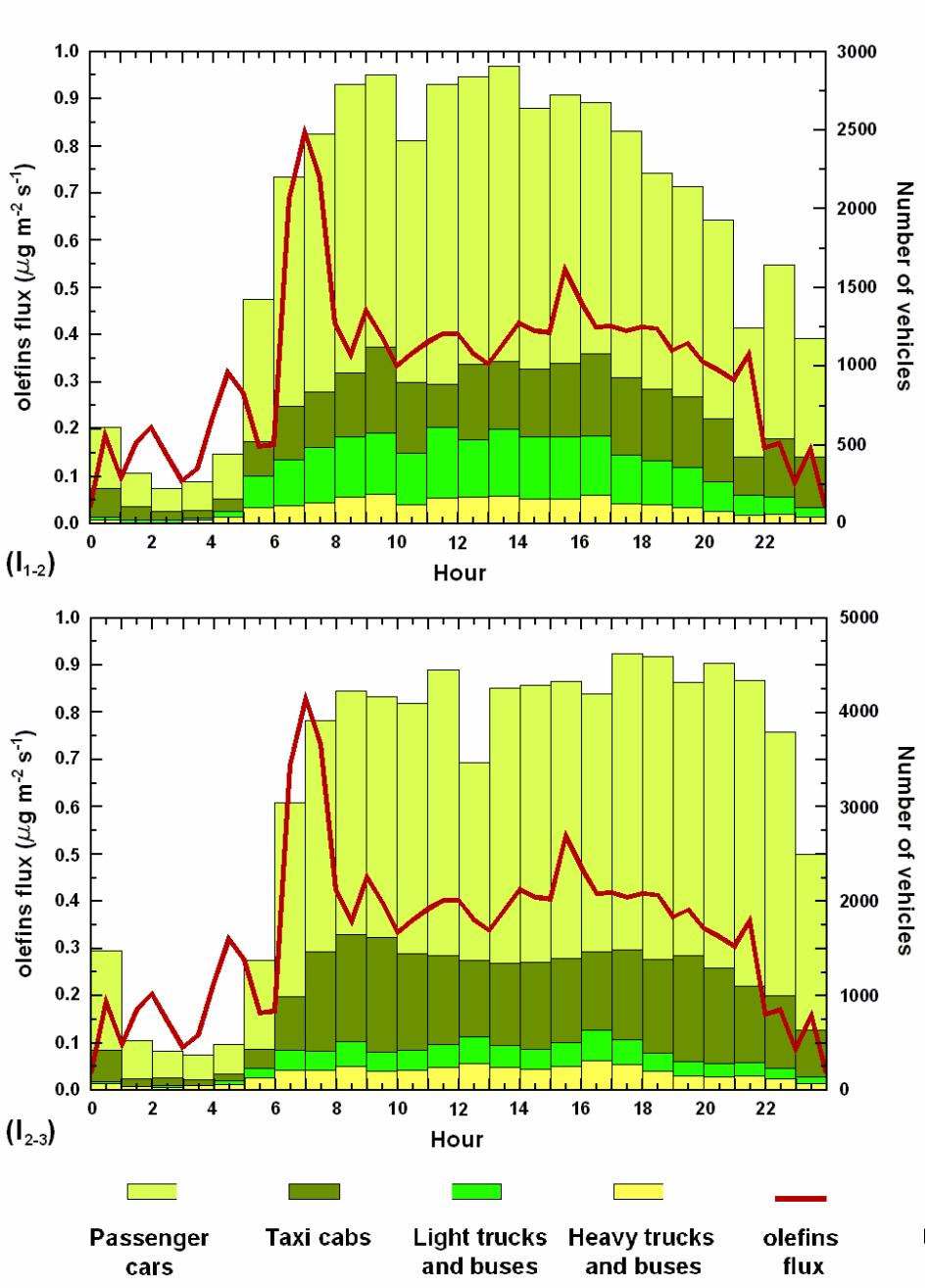

Figure 3.A.10. Diurnal profile of olefin fluxes and traffic counts for two intersections within the tower footprint (intersection between Av. Ermita Iztapalapa and Av. Rojo Gomez $I_{1\text{-}2}$, and the intersection between Av. Ermita Iztapalapa and Av. Anillo Periferico $I_{2\text{-}3}$).

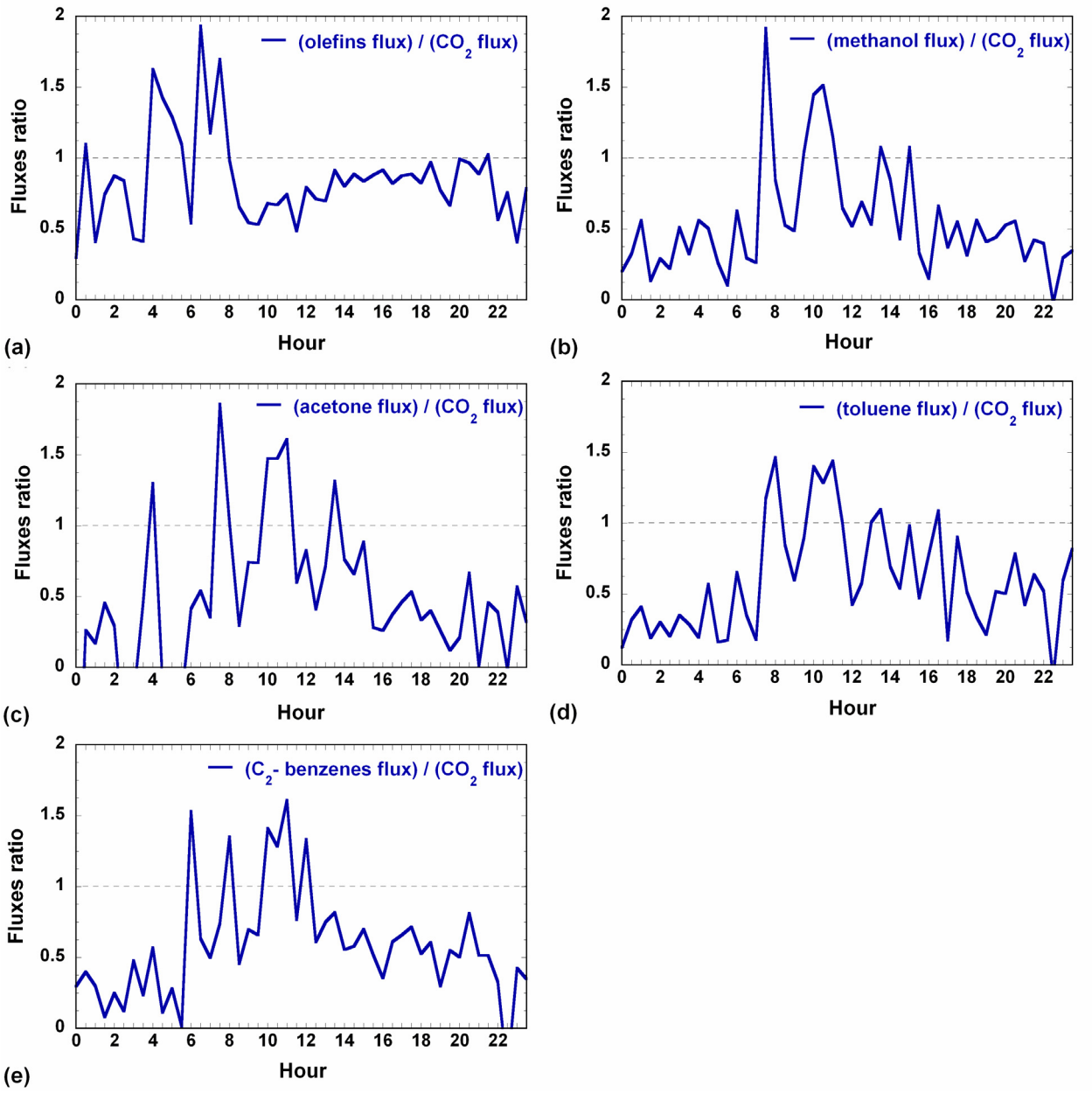

Figure 3.A.11. Ratios between the normalized fluxes of VOC and CO_2. (a) for olefins, (b) methanol, (c) acetone, (d) toluene, and (e) C_2-benzenes.

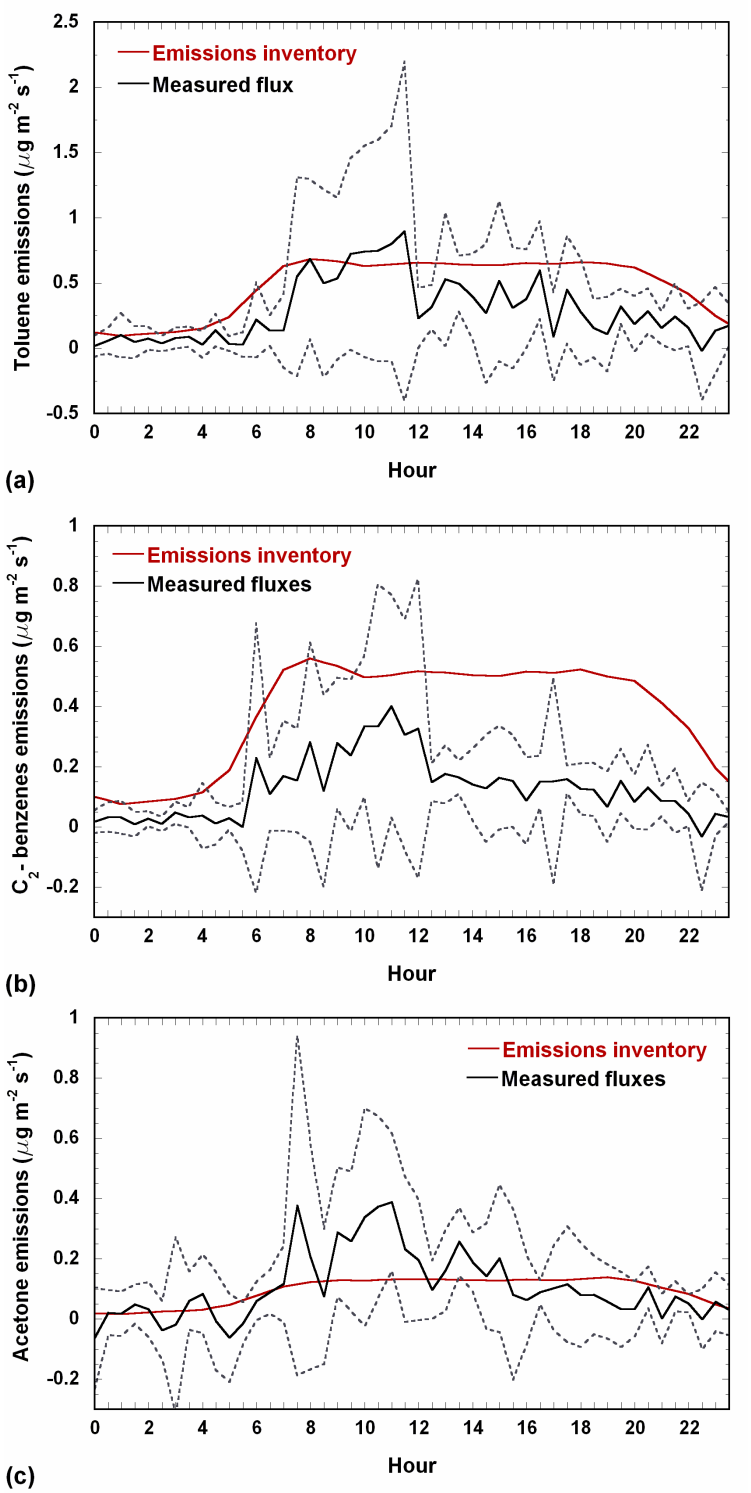

Figure 3.A.12. Comparison of the diurnal profiles of fluxes of toluene (a), C_2-benzenes (b), and acetone (c) with the diurnal profiles of emissions used in the CIT three-dimensional photochemical model for Mexico City. The dashed lines indicate ±1 standard deviation of the measured fluxes.

CHAPTER 4

MEASUREMENTS OF CO_2 FLUXES FROM THE MEXICO CITY URBAN LANDSCAPE*

4.1. Abstract

In a densely populated section of Mexico City, an eddy covariance flux system was deployed on a tall urban tower to obtain direct measurements of CO_2 emissions from an urban neighborhood located in a subtropical megacity. The measured fluxes and boundary layer conditions satisfy eddy covariance assumptions of stationarity, and co-spectral analyses of the turbulence measurements exhibit the required boundary layer patterns for acceptable flux measurements. Results from a field experiment conducted during April, 2003 show that the urban surface is a net source of CO_2. The CO_2 flux measurements showed a clear diurnal pattern, with the highest emissions during the morning (up to 1.60 mg m^{-2} s^{-1}), and lowest emissions during nighttime. The measured fluxes were closely correlated to traffic patterns in the area. The mean daily flux was 0.41 mg m^{-2} s^{-1}, which is similar to that observed in European and U.S. cities.

4.2. Introduction

Urban landscapes are suspected to be major sources of anthropogenic CO_2, however, there are few direct measurements of CO_2 emissions in urban areas. Micrometeorological techniques have only recently been applied to urban landscapes, while they have been widely used to measure fluxes of CO_2, water vapor, volatile organic compounds (VOCs) and other trace gases above vegetation (Baldocchi, et al., 2001; Schmid et al., 2000; Westberg, et al., 2001). Recent urban studies have focused on cities from developed countries in mid-latitudes, such as

* Velasco E, Pressley S, Allwine E, Westberg H, Lamb B, 2005. Measurements of CO_2 fluxes from the Mexico City urban landscape. *Atmospheric Environment* 39(38), 7433-7446.

Edinburgh (Nemitz et al., 2002), Chicago (Grimmond et al., 2002), Copenhagen (Soegaard and Møller-Jensen, 2003), Basel (Vogt et al., 2003), Tokyo (Moriwaki and Kanda, 2004), Vancouver (Walsh et al., 2004), and Marseille (Grimmond et al., 2004). Despite the fact that three-quarters of the world's 3 billion urban residents live in developing countries, there have been few, if any, flux measurements in urban areas in developing countries. Mexico City is a good example of an urban area in a less developed country. It is the second largest city in the world, and it is characterized by rapid population growth with a wide range of both direct and indirect CO_2 sources, such as mobile emissions and land use changes due to urbanization.

CO_2 levels in urban environments have typically been quantified through emission inventories from estimates of fossil fuel consumption, evaluations of the amount of carbon sequestered in urban vegetation, and short-term studies of ambient CO_2 concentrations (see Grimmond et al., 2002). For Mexico City, results of only two studies have been reported; the first was a study during 1981 and 1982, in which CO_2 was sampled at different locations in the city and analyzed by gas chromatography (Baez et al., 1988). In the second study, CO_2 concentrations were measured by a Fourier Transform Infrared (FTIR) spectrometer at the southwest of the city during the fall of 2001 (Grutter, 2003).

As part of a large air quality field campaign conducted in Mexico City (MCMA-2003), we deployed an eddy covariance (EC) flux system on a tall urban tower within a densely populated section of the city to obtain direct measurements of CO_2 emissions in a typical Mexican neighborhood. In this paper, we demonstrate the applicability of the EC technique to a heterogeneous urban landscape where the spatial variability of surface cover and roughness is high. The results are analyzed in terms of the magnitude of the CO_2 fluxes in relation to the source footprint as a function of wind direction and in relation to vehicular activity.

4.3. Methods

4.3.1. Measurement site and study period

Mexico City is characterized by an enormous social difference, where approximately 10% of the population lives in affluent neighborhoods, 20% in medium class neighborhoods and 70% in poor neighborhoods. Overall, poor neighborhoods are formed by residential areas built with scarce planning around original buildings, industries or services located throughout the city. The flux measurements were performed in Iztapalapa, a poor neighborhood located in southeast Mexico City (19º 21' 29'' N, 99º 04' 24'' W). Iztapalapa is the suburb with the highest population in Mexico City (1.8 million inhabitants) and the highest density (12,000 inhabitants km^{-2}) (INEGI, 2000). Mexico City is located at 2240 m above sea level in a subtropical region surrounded by mountains; the city experiences mild weather, temperatures of over 20ºC, and intense solar radiation all year.

CO_2 fluxes were measured for 23 days during the warm dry season in April 2003 (April 7 - 29). April is the second warmest month of the year with an average monthly precipitation rate less than 25 mm of rain. The study period included the Holy Week (April 14 – 20), when traffic is significantly reduced because many city residents leave for the holiday period. By taking measurements before, during and after this period, we expected to obtain a better understanding of the influence of the vehicular emissions upon CO_2 fluxes.

The EC flux system was deployed at the CENICA super site. Surrounding topography around this site is flat. At 2.4 km in the southeast direction, there is a small hill with a height of 160 m. This hill embraces the national park "Cerro de la Estrella" (see Figure 8). Including the vegetation of this park, the total vegetation cover in Iztapalapa represents 16% of the total area; however only 27% of that vegetation cover corresponds to woodland, the remaining 73% corresponds to grasslands and shrubs (SMA-GDF, 2004). This means that the biomass of the region is scarce and the potential for CO_2 uptake from vegetation is small. In contrast, the number of CO_2 sources is large, and composed of a mix of commercial, industrial, residential and mobile sources. The predominant land use in the 30^{o}-280º sector is residential and

commercial, with buildings of 3 and 4 stories of height, and roadways of 1 and 2 lanes with a density of ~16 km km^{-2}. In general during the daytime, this sector is the predominate upwind direction. At night, winds from all directions were observed, but winds blowing from the north and northwest sectors were predominant. This sector is mainly occupied by light industries, storage buildings and the Autonomous Metropolitan University. In this section, the number of roadways is lower with an average density of 7 km km^{-2}. Overall, the average building height (z_{city}) in all sectors is 12 m. Most buildings are built of concrete with flat roofs of concrete or sheet metal.

4.3.2. Instrumentation

The EC flux system was mounted on a 25 m tower on the rooftop of a building, with a total height of 37 m, more than 3 times the height of the surrounding buildings, and of sufficient height to be in the constant flux layer. To instrument the flux tower (Figure 1), a three-dimensional (3-D) sonic anemometer (Applied Technologies, Inc., model SATI-3K), and a NOAA open-path infrared gas analyzer (IRGA) were mounted at the top of the tower at the end of a 3 m boom. The length of the boom was enough to minimize the effects of flow distortion from the tower, and the sensors were arranged to be as aerodynamic as feasible. Signal/power cables were run from the sensors to a shelter on the roof where the pc data acquisition system was operated through LabVIEW (National Instruments) software specifically designed for this experiment. In operation, the flux system collected data at 10 Hz, and the turbulence data were used to calculate 30 min average fluxes.

The NOAA IRGA is an instrument designed for fast response measurements of H_2O and CO_2 fluctuations and developed by the Atmospheric Turbulence and Diffusion Division (ATDD) of the National Oceanic and Atmospheric Administration (NOAA). Noise levels for H_2O and CO_2 are less than 0.1 g m^{-3} and 0.3 mg m^{-3}, respectively. These levels are much lower than the observed variations in the atmosphere of Mexico City; the standard deviation of H_2O and CO_2 mixing ratios on a 30 min basis were more than 2.4 g m^{-3} and 70 mg m^{-3}, respectively. Auble

and Meyers (1992) have given a detailed description of this instrument. Although open path instruments do not require frequent calibrations, we performed CO_2 calibrations twice per week since in a polluted urban atmosphere the mirrors and windows become dirty quickly. The CO_2 calibration used two standard gas mixtures (Scott-Marrin Inc. 327 and 402 ppm ± 1%, National Institute of Standards and Technology (NIST)). We compared the water vapor response to a humidity sensor (Vaisala, model HMP45A) on the tower as a basis for calibration of the instrument for water vapor.

4.3.3. Postprocessing for eddy covariance flux calculations

The flux of a trace gas (F_χ) is calculated according to the EC technique as the covariance between the instantaneous deviation of the vertical wind velocity (w') and the instantaneous deviation of the trace gas concentration (c_χ') from their 30 minute means. The equation is given below, where the over bar denotes a time-averaged quantity.

$$F_\chi = \overline{w' c_\chi'} = \frac{1}{N} \sum_{i=1}^{N} w'(t_i) c'(t_i) \qquad (1)$$

Fundamental aspects of EC have been widely discussed elsewhere (e.g. McMillen, 1988; Aubinet et al., 2000). Briefly the post-processing includes the following steps:

1) Convert raw data signals to scientific units, apply IRGA calibration coefficients, remove hard spikes and identify data gaps. Hard spikes can be caused by random electronic spikes or sonic transducer blockage (e.g. during precipitation). Data gaps may occur as a result of system breaks for routine maintenance or calibration, inadequacy of the meteorological conditions or complete system failures. We found between 1 and 5 hard spikes for each period of 18,000 readings. A period is rejected if it does not successfully fulfill 83% of the readings.

2) Identify and remove soft spikes which are large short-lived departures from the period means. We followed the algorithm proposed by Schmid et al. (2000). These spikes occurred at a rate of approximately 37 per period.

3) Perform coordinate rotation on three-dimensional velocity components. The aim is to eliminate errors due to sensor tilt relative to the terrain surface or aerodynamic shadow due to the sensor or tower structure (Aubinet et al., 2000).

4) Calculate the mean and standard deviation for each variable.

5) Remove means from each signal to obtain fluctuations (prime quantities).

6) Apply a low pass filter to all the processed variables to eliminate the presence of a possible trend in the 30 min time series. We used a recursive digital filter (Kaimal and Finnigan, 1994).

7) Calculate 30 minute average vertical fluxes for momentum, sensible heat, latent heat, and CO_2.

8) Account for the effects of density fluctuations upon the fluxes, applying the Webb corrections (Webb et al., 1980) to water vapor and CO_2.

9) Apply a second phase of quality control. All measured or derived variables (30 min averages) are submitted to a plausibility test and are rejected if they fall outside statically defined constraints for each variable (e.g. wind speed not to exceed 25 m s^{-1}).

The quality of flux measurements is difficult to assess, because there are various sources of errors, ranging from failure to satisfy a number of theoretical assumptions to failure of the technical setup. Conflicts with the assumptions of the eddy covariance technique to estimate fluxes arise under certain meteorological conditions and site properties. As these effects cannot be quantified solely from eddy covariance data, a classical error analysis and error propagation will remain incomplete. Instead, Aubinet et al. (2000) suggest an empirical approach to determine whether the fluxes meet certain plausibility criteria. Besides the statistical characteristics of the raw instantaneous measurements, we investigated the frequency resolution

of the eddy covariance system through the spectra and cospectra of the measured variables, and through the stationarity of the eddy flux process.

4.3.4. Spectral and cospectral analysis

An EC system attenuates the true turbulent signal at sufficiently high and low frequencies due to limitations imposed by the physical size of the instruments, their separation distances, their inherent time response, and any signal processing associated with detrending or mean removal (Massman and Lee, 2002). Inspection of the spectra and cospectra of the measured variables helps to determine the influence of these attenuations. Power density spectra of CO_2 concentration and ambient temperature (T) are shown in Figure 4.2.a, while cospectra of vertical velocity with CO_2 concentration and T are shown in Figure 4.2.b. These spectra and cospectra were computed via the Fast Fourier Transform (FFT) method. Each spectrum and cospectrum was normalized by the corresponding average scalar or covariance to facilitate the comparison between CO_2 and T, and they were plotted against the normalized frequency, $f\,(z_m / u)$, where z_m is the measurement height and u is the mean wind velocity. The height z_m is calculated as the difference between the tower height and the zero displacement plane, which is based on rule-of-thumb estimates (where $z_d = 0.7 z_{city}$, Grimmond and Oke, 1999) as 8.4 m. We use logarithmic scales in both axes to emphasize power-law relationships.

Both spectra and cospectra of CO_2 and T show similar patterns at high frequencies, $f\,(z_m / u) > 2$. At that same frequency range, the spectra show the expected -5/3 slope in the inertial subrange, which is the range where the net energy coming from the energy-containing eddies is in equilibrium with the net energy cascading to smaller scales where it is dissipated. The cospectrum provides an additional mean to identify frequency-dependent behavior in an EC system that can lead to systematic errors in flux measurements. This is because the cospectrum reflects the phase relationship between two variables and their respective amplitudes as a function of frequency. CO_2 concentration and T were measured by independent instruments;

therefore, the correspondence between their cospectra with vertical wind velocity indicates that there is no systematic phase shift and no cospectral distortion.

The spectra and cospectra results clearly show that our flux system is fully capable of measuring turbulence fluxes of CO_2 via the EC mode in an urban environment. However, sampling periods that did not fulfill the stationarity requirements (described below) generally did not meet the spectral and cospectral analysis criteria. Those sampling periods were not omitted from further analysis based on the spectral and cospectral analysis, but they were discarded based on the stationarity test which is easier to apply in an objective manner.

4.3.5. Stationarity test

The applicability of an urban flux tower is confined to stationarity conditions, such that the measurement height exceeds the blending height at which the small scale heterogeneity merge into a net exchange flux above the city. One criterion for stationarity is to see if the difference between the flux obtained from a 30 min average and the average of fluxes from 6 continuous subperiods of 5 min from that same period of 30 min is less than 60% (Aubinet et al., 2000). When the turbulent variables are not stationary, the fluxes could be suspicious, and therefore they should not be considered for subsequent analyses. In our study, the stationarity condition was fulfilled in 74% of the half hour periods. Figure 3 compares the average flux differences between 6 subperiods of 5 min and the 30 min averages versus their respective atmospheric stability conditions through the stability index (ξ) during the entire campaign. If $\xi < 0$ atmospheric conditions are unstable and if $\xi \geq 0$ conditions are stable where $\xi = z_m / L$ and L is the Monin-Obukhov length.

The stationarity test can also eliminate sampling periods affected by short term horizontal advection from local sources. Short term advection is produced by plumes emitted during short periods of time, or plumes transported during changing wind conditions. Advection periods longer than 30 minutes with constant upwind blowing directly from a large emission source cannot be removed by the stationary test. To investigate this latter effect, we plotted the one

minute average CO_2 concentrations measured during the entire study against the mean wind velocity and wind direction trying to identify build-ups of elevated concentrations related to specific upwind characteristics. We found that only four periods from nine possible periods with advection were not removed by the stationarity test. The high CO_2 concentrations observed in these four periods were not because of daily activities, and although they present fluxes above the average at that time of the day, they do not represent spikes and their influence in the diurnal course is not significant. Therefore, we consider these periods as part of the variability in our results.

4.3.6. Footprint analysis

In a homogeneous surface, the footprint is not an issue because the fluxes from all parts of the surface are by definition equal. However, in an inhomogeneous surface such as a city, the measured signal depends on which part of the surface has the strongest influence on the sensor and, therefore, the location and size of the footprint. To evaluate the footprint in our experiment, we used the model developed by Hsieh et al. (2000) with the previously estimated zero plane displacement and an assumed roughness height of 1 m. We applied this model to the complete set of 30-minute periods measured during the campaign to determine the fraction of the flux measured (F/S_0) as a function of the upwind distance (x) and the atmospheric stability condition. F represents the flux and S_0 the source strength. If the footprint is defined to encompass 80% of the total flux, we observe in Figure 4 that the longest footprints (~ 5 km) correspond to stable conditions, which prevail at nighttime; while the smaller footprints (500 m) correspond to unstable conditions, characteristic of morning and early afternoon. The average footprint, considering all stability conditions, was 1.3 km, which represents a distance large enough to characterize the CO_2 fluxes of a typical neighborhood in Mexico City. Figure 5 shows different footprint fractions for selected time periods of the day. At night, the footprint is distributed over larger distances; 80% of its accumulation occurs in a radius between 1.5 and 4 km. The unstable conditions during morning and early afternoon produce shorter footprints, and from a

predominant direction between south and southeast. During late afternoon, unstable conditions also prevail, but with less frequency and strength, to produce footprints longer than in previous hours and smaller than during the night.

4.4. Results

4.4.1. Concentrations

The CO_2 concentrations showed a clear diurnal pattern similar to other pollutants emitted by mobile sources, such as NO_X and CO (INE, 2000). As indicated in Figure 6, the highest concentrations occurred between 6:30 and 8:00 h (all times are reported in LST) with a range from 398 to 444 ppm and an average of 421 ppm. This morning peak is attributed to anthropogenic emissions (mainly vehicles), nocturnal respiration, and the shallow early morning mixed layer. The growth of the boundary layer depth for Mexico City has been identified to occur between 10:00 and 12:30 h (Whiteman et al., 2000), passing from mixing heights lower than 500 m to heights above 2000 m at noon. The lowest CO_2 concentrations were observed during the afternoon, with an average of 375 ppm. In the afternoon, the growth of the boundary layer slows significantly, and begins to decay around 18:00 h, when the CO_2 concentration starts rising again. This CO_2 concentration diurnal profile is consistent with observations at other urban sites, such as Chicago (Grimmond et al., 2002). The diurnal pattern was relatively constant during the entire study. However, an average difference of 20 ppm was observed during the morning rush hour between the Holy Week (week 2) and the first week of the campaign. This difference represents the vehicular traffic reduction due to the national holiday period during week 2. The average difference between week 1 and week 3, in which almost all schools were still on holiday was 6 ppm. The mean diurnal concentration of 388 ppb with a standard deviation of 14 ppm observed in this study was similar to those reported for other cities (Grimmond et al., 2002; Nemitz et al., 2002; Reid and Steyn, 1997) and also to measurements collected in Mexico City in 2001 (Grutter, 2003). However, Grutter identified a later and longer morning rush hour peak in CO_2 concentrations, probably due to a more dense network of roads

near his site, and a second peak at night that we did not observe. The nighttime peak in Grutter's measurements was probably because his measurements were made next to a large forest reserve.

4.4.2. Fluxes

The CO_2 flux measurements showed a clear diurnal pattern, with the highest emissions during the morning, and lower emissions during nighttime (see Figure 7). Fluxes ranged from -0.22 to 1.60 mg m^{-2} s^{-1}, with an average of 0.41 mg m^{-2} s^{-1}. Although negative fluxes were observed occasionally during unstable conditions, fluxes were predominately positive during our study. This indicates that the urban surface is a net source of CO_2, and that the uptake by urban vegetation during the day is not strong enough to offset the flux from anthropogenic sources.

Fluxes exhibited a relatively constant diurnal pattern during the three study weeks. The highest fluxes were observed in the first week, and the lowest during the second week. Figure 7 shows the average diurnal patterns for weekdays and weekends. Lower fluxes occurred on weekends between 5:00 and 9:00 h compared to fluxes at these times on weekdays. This effect is directly related to vehicular traffic, since on weekends the traffic is usually lower during morning hours. During the remainder of the day, fluxes are similar between weekends and weekdays.

Diurnal patterns of concentrations and fluxes are different. Concentrations not only reflect the variability in the emissions, but also the evolution of the atmospheric boundary layer. During the early morning, concentrations increase until 7:00 h, while fluxes remain constant until 6:00 h, when they start to increase, reaching their maximum at 9:00 h. At this hour, concentrations have already started to decline, continuing until noon, while fluxes remain high during the entire morning. This shows the dilution of CO_2 from the actual emissions and from the pool stored in the residual layer, as a function of the atmospheric boundary layer growth. Both concentrations and fluxes remain constant during the afternoon. After 19:00 h, fluxes start to decrease, but concentrations increase again, indicating that a new nocturnal boundary layer has started to form.

The CO_2 flux diurnal pattern in Figure 7 shows three consistent peaks during the morning, 7:00, 9:00 and 11:30 h. The earliest peak was observed only during weekdays, while the other two peaks were observed on both weekdays and weekends. The peak at 7:00 h was observed in 20% of the days, the peak at 9:00 h 40% and the peak at 11:30 h in 35% of the cases. These peaks are not related to the upwind direction or any other measured parameter and they do not appear to be caused by horizontal advection as discussed previously. Overall our results show that the CO_2 fluxes are higher during the morning than during the afternoon, and that the morning peaks illustrate the variability of the morning CO_2 emissions in the study area. With a longer campaign, the features involved with those peaks might be resolved, or they could be absorbed in a broad morning peak.

Overall, the magnitude and diurnal pattern of the CO_2 fluxes in Mexico City are between those observed in winter and summer in mid-latitude cities. In mid-latitude cities, the CO_2 fluxes depend on the season. During summer CO_2 emissions tend to be lower, the benign weather reduces the fuel consumption for heating and trees are in full leaf increasing the CO_2 uptake by photosynthesis. During winter the opposite occurs, CO_2 emissions are accentuated by heating necessities and CO_2 uptake by vegetation is reduced. For example, reported CO_2 fluxes in Tokyo during July vary between 0.2 and 0.5 mg m^{-2} s^{-1}, while during December measured fluxes in Tokyo are between 0.2 and 1.1 mg m^{-2} s^{-1} (Moriwaki and Kanda, 2004). Our CO_2 fluxes match both the magnitude and diurnal pattern of fluxes reported by Walsh et al. (2004) for a residential area of Vancouver for April and June.

In addition to the CO_2 fluxes, sensible and latent heat fluxes were also measured with the same flux system. Sensible heat flux was always directed upward with peak values around 270 W m^{-2} at noon, while latent heat fluxes were small with peak values below 90 W m^{-2} also at midday. From heat fluxes reported previously for other urbanized sections of Mexico City during the cold season (Oke et al., 1999; Tejeda and Jauregui, 2005), we found that differences in the energy balance between the coldest and warmest months are not significant, and if we add

that the scarce vegetation cover in Mexico City is relatively constant throughout the year, we can infer that CO_2 fluxes should be also relatively constant throughout the annual cycle.

4.4.2.1. Fluxes as a function of the upwind direction

In an urban area, where the emission sources are not homogeneous, it is necessary to determine the magnitude of the fluxes as a function of the upwind direction to identify the strongest sources. Figure 8 shows the CO_2 flux distribution as a function of the wind direction superimposed on a map of the study area. Fluxes were lower from areas with fewer streets, for example from the north and northwest directions. The largest emissions came from the east and southeast directions, where the avenue (Anillo Periferico) with the highest vehicular traffic near the measurement site is located. The vegetation cover in the National park "Cerro de la Estrella", located southwest from the tower, should be a sink for CO_2 emitted in the region, but it does not appear to be strong enough to offset local emissions.

4.4.2.2. Fluxes as a function of the vehicular activity

During the MCMA field campaign, traffic counts were performed at two intersections, one between the avenues labeled 1 and 2 (I_{1-2}) in Figure 8, and the other between avenues 2 and 3 (I_{2-3}). Figure 9 presents the diurnal flux pattern for the 45º upwind sectors corresponding to each intersection along with the vehicular count distributions, where the vehicular fleet was classified into four different groups: passenger cars, taxi cabs, light trucks/buses, and heavy trucks/buses. Although both intersections share avenue 2, I_{2-3} has a higher traffic density than I_{1-2}, since avenue 3 encircles the entire city, making it one of the busiest avenues, and one of the largest emission sources. Several routes of "colectivos" (small buses with a 20 passenger capacity) start from I_{1-2}, which can be observed in the higher number of light buses and trucks compared to I_{2-3}. The high CO_2 fluxes emitted from the southwest shown in Figure 8 may be due to these colectivos, which remain stopped and idling at a short distance from this intersection, while waiting for passengers.

The typical morning and afternoon traffic peaks are not identified at either intersection, instead a single peak is observed during the entire day. This peak begins at 6:00 h, and extends until late afternoon for $I_{1\text{-}2}$, and into the night for $I_{2\text{-}3}$. The morning and noon gaps in the CO_2 flux courses for the upwind sectors corresponding to $I_{1\text{-}2}$ and $I_{2\text{-}3}$ are because of the lack of sampling periods with winds from those directions. Although two large peaks are observed in the CO_2 fluxes (16:30 h at $I_{1\text{-}22}$ and 9:30 h at $I_{2\text{-}3}$), we conclude that CO_2 fluxes follow the vehicular traffic diurnal profile. Both remain constant during most of the day and then decline at night. Figure 10 confirms the high correlation between vehicular traffic and CO_2 emissions, where the correlation coefficients from linear regressions are 0.85 and 0.58 for $I_{1\text{-}2}$ and $I_{2\text{-}3}$, respectively. The higher correlation coefficient for $I_{1\text{-}2}$ is because that intersection was closer to the flux tower (1580 m) than the intersection $I_{2\text{-}3}$ (2100 m). The statistical offset indicates the presence of other sources, such as cooking, water heating, and combustion processes from factories and stores, among others. According to the greenhouse gas emission inventory for Mexico City, the transportation sector contributes with 60% to the CO_2 emissions burden (33.6 Mton $year^{-1}$ for the year 1996), followed by the industrial and residential sectors, with contributions of 20% and 16%, respectively (Sheinbaum et al., 2000).

Using the Mexican vehicular fleet distribution (SMA-GDF, 2002), the emission factors developed by Zavala (2004) using the stoichiometric combustion equation, and the characteristics of Mexican fuels, we roughly determined the fraction of CO_2 emitted by each vehicle class for the two intersections discussed above. We found that the emission contributions are similar for both intersections, where the group of passenger cars has the largest vehicular source (60%). Colectivos and taxis contribute 17% each, while heavy trucks and buses represent 6% of the mobile CO_2 emissions.

4.4.2.3. Evaluation of random and systematic errors in the measured daily mean CO_2 flux

Although error propagation cannot be quantified precisely for flux measurements, a sensitivity analysis on the effects of errors on an average day basis can help to quantify the flux

uncertainties. We applied the approach proposed by Moncrieff et al. (1996) to evaluate the random and systematic errors on the mean daily flux. When errors are random, errors in computed means diminish with increasing size of data set according to $N^{-1/2}$, where N is the number of measurements. Thus random errors can be estimated by examining the convergence of calculations of the net flux. In contrast, systematic errors are not affected by increasing data set size, because they simply add in a linear fashion. In general, systematic errors are difficult to detect.

Figure 11a shows the results of applying diverse values of a percentage random error (p_r) to each half hour CO_2 flux in the entire data set. The horizontal line represents the mean daily flux, 0.41 mg m^{-2} s^{-1}. The symmetrical set of lines above and below this line represent the overall random error as a function of the magnitude of p_r and the given number of days. If we assume a random error of +20% for each 30-minute mean flux for the 23 days studied, the total random error on the net flux is 0.202 mg m^{-2} s^{-1} (50% of the net flux). If we also assume a systematic error (p_s) of +10%, we see from Figure 11b that the total systematic error on the net flux is 0.041 mg m^{-2} s^{-1}. Adding these two errors, the total uncertainty of the net flux is 0.243 mg m^{-2} s^{-1} (60% of the total flux). This technique allows us to determine the required number of days to obtain the best possible flux estimate. For example, considering a random error of 20% and a systematic error of 10%, 100 days of measurements would resolve a net flux of 0.508 mg m^{-2} s^{-1}, 25% higher than our observed mean daily flux. One year of measurements would resolve a net flux of 0.460 mg m^{-2} s^{-1} and reduce the offset to 13%. However, flux measurements can only be compiled for a certain length of time before possible seasonal trends become important. Although the weather in Mexico City throughout the annual cycle is relatively constant in comparison to the weather in mid-latitude cities, three climatic seasons can be differentiated, a dry, warm season from March to May, a rainy season from June to October, and a dry, cold season from November to February. Thus, a seasonal evaluation of CO_2 fluxes in Mexico City will require measurement periods of 3 months for each season; for this duration the estimated error would be 36% based on a random error of 20% and a systematic error of 10%.

4.5. Conclusions

Results of this study have demonstrated the capacity of the eddy covariance technique to measure CO_2 fluxes in an urban area, where the inhomogeneous surface, high roughness, and wide distribution of emission sources complicate the measurements. Micrometeorological techniques are capable of quantifying CO_2 emissions from sources that are not usually accounted with other methods, such as factories hidden in residential areas or street food cooking.

Our CO_2 measurements show clear diurnal patterns for both concentrations and fluxes, which are strongly correlated to vehicular traffic during the day. The consistently positive CO_2 fluxes measured in Mexico City are in agreement with other urban studies, which have shown that the urban surface is a net source of CO_2 (Grimmond et al., 2002; Nemitz et al. 2002; Walsh et al., 2004 ; Moriwaki and Kanda et al., 2004; Grimmond et al., 2004). The effects of CO_2 uptake by urban vegetation during the daytime do not appear to be significant for this site.

Even though the weather and vegetation cover in Mexico City is relatively constant, some differences in the CO_2 fluxes can be expected during the different climatic seasons of the year. But if we assume that these differences are small, and that fluxes measured during the studied period could be representative of the entire year, we could infer from the average flux an annual CO_2 emission of 12.8 kg m^{-2}. Annual emissions obtained from other cities using similar flux techniques agree quite well with our measurements. Moriwaki and Kanda (2004) reported an annual CO_2 emission 4% lower than Mexico City for a residential area of Tokyo, while Soegaard and Møller-Jensen (2003) determined essentially the same annual emission for the urban area of Copenhagen. This finding is somewhat surprising, since we expected to observe higher emissions in Mexico City compared to more developed cities, because of the higher population, scarce green areas, dense traffic with a relatively old vehicle fleet, and the extensive presence of aged technologies for daily commercial and residential activities. In Mexico City, CO_2 emissions from combustion sources are accentuated by the high elevation of the city, which makes the combustion process less efficient.

The ability to make CO_2 flux measurements over an urban landscape is an important step in improving our understanding of the role megacities play in global climate change. Because emission inventories for CO_2 are typically based on fuel inventories or by other indirect means and since this kind of information may not be available or reliable in less developed areas, it is important to evaluate available emission estimates with direct measurements. In the future, long term measurements similar to those described in this paper would be a valuable contribution to quantification of CO_2 emissions from megacities. Fluxes reported here are for a short period of time; clearly more measurements are needed to confirm the representativeness of the CO_2 fluxes measured in Iztapalapa for a poor neighborhood of Mexico City and their temporal variability throughout the year. In a separate paper (Velasco et al., 2005), we have also demonstrated that these flux methods can also be applied to measure VOCs that are important for urban and regional atmospheric chemistry.

4.6. Acknowledgements

This study was supported by the Integrated Program on Urban, Regional and Global Air Pollution from the Massachusetts Institute of Technology (MIT) in collaboration with the Metropolitan Commission of Environment (CAM) of Mexico City. The authors would like to acknowledge the support and assistance of Mario and Luisa Molina as the directors of the MCMA-2003 field campaign, as well as the National Center for Environmental Research and Training (CENICA) of the Mexican National Institute of Ecology (INE) as hosts of this study. Authors also wish to thank the two anonymous reviewers, who provided very helpful comments for the final manuscript.

4.7. References

Aubinet, M., Grelle, A., Ibrom, A., Rannik, Ü., Moncrieff, J., Foken, T., Kowalsky, A.S., Martin, P.H., Berbigier, P., Bernhofer, Ch., Clement, R., Elbers, J., Granier, A., Grünwald, T., Morgenstern, K., Pilegaard, K., Rebmann, C., Snijders, W., Valentini, R., Vesela, T., 2000. Estimates of the annual net carbon and water exchange of forests: the EUROFLUX methodology. Advances on Ecological Research 30, 113-175.

Auble, D.L., Meyers, T.P., 1992. An open path, fast response infrared absorption gas analyzer for H_2O and CO_2. Boundary Layer Meteorology 59, 243-256.

Baez, A., Reyes, M., Rosas, I., Mosiño, P., 1988. CO_2 concentrations in the highly polluted atmosphere of Mexico City. Atmósfera 1, 87-98.

Baldocchi, D., Falge, E., Gu, L., Olson, R., Hollinger, D., Running, S., Anthoni, P., et al., 2001. FLUXNET: a new tool to study the temporal and spatial variability of ecosystem scale carbon dioxide, water vapor and energy flux densities. Bulletin of the American Meteorological Society 82, 2414-2434.

Grimmond, C.S.B., Salmond, J.A., Oke, T.R., Offerle, B., Lemonsu, A., 2004. Flux and turbulence measurements at a densely built-up site in Marseille: heat, mass (water and carbon dioxide), and momentum. Journal of Geophysical Research 109, 24101-24120.

Grimmond, C.S.B., King, T.S., Cropley, F.D., Nowak, D.J., Souch, C., 2002. Local-Scale fluxes of carbon dioxide in urban environments: Methodological challenges and results from Chicago. Environmental Pollution 116, 243–254.

Grimmond, C.S.B., Oke, T.R., 1999. Aerodynamic properties of urban areas derived from analysis of surface form. Journal of Applied Meteorology 38, 1262-1292.

Grutter, M., 2003. Multi-gas analysis of ambient air using FTIR spectroscopy over Mexico City. Atmósfera 16, 1-13.

Hsieh, C.I., Katul, G. & Chi, T., 2000. An approximate analytical model for footprint estimation of scalar fluxes in thermally stratified atmospheric flows. Advances in Water Resources 23, 765-772.

INE, 2000. Almanaque de datos y tendencias de la calidad del aire en ciudades mexicanas. Instituto Nacional de Ecología, SEMARNAT. México D.F.

INEGI, 2000. Estados Unidos Mexicanos Resultados Prelimanares XII Censo General de Población y Vivienda. INEGI, México D.F.

Kaimal, J.C., Finnigan, J.J., 1994. Atmospheric boundary layer flows. Their structure and measurement. Oxford University Press, US.

Massman, W.J., Lee, X., 2002. Eddy covariance flux corrections and uncertainties in long-term studies of carbon and energy exchanges. Agricultural and Forest Meteorology 113, 121-144.

McMillen, R., 1988. An eddy correlation technique with extended applicability to non-simple terrain. Boundary Layer Meteorology 43, 231-245.

Moncrieff, J.B., Malhi, Y., Leuning, R., 1996. The propagation of errors in long-term measurements of land-atmosphere fluxes of carbon and water. Global Change Biology 2, 231-240.

Moriwaki, R., Kanda, M., 2004. Seasonal and diurnal fluxes of radiation, heat, water vapor, and carbon dioxide over a suburban area. Journal of Applied Meteorology 43, 1700-1710.

Nemitz, E., Hargreaves, K.J., Mcdonald, A.G., Dorsey, J.R., Fowler, D., 2002. Micrometeorological measurements of the urban heat budget and CO_2 emissions on a city scale. Environmental Science and Technology 36(14), 3139-3146.

Oke, T.R., Spronken-Smith, R.A., Jauregui, E., Grimmond, C.S.B., 1999. The energy balance of central Mexico City during the dry season. Atmospheric Environment 33, 3919-3930.

Reid, K.H., Steyn, D.G., 1997. Diurnal variations of boundary-layer carbon dioxide in a coastal city–observations and comparison with model results. Atmospheric Environment 31, 3101-3114.

Sheinbaum, C., Ozawa, L.V., Vasquez, O., Robles, G., 2000. Inventario de emisiones de gases de efecto invernadero asociados a la producción y uso de energía en la Zona Metropolitana del Valle de México. Reporte Final del Grupo de Energía y Ambiente. Universidad Nacional Autónoma de México, México D.F.

Schmid, H.P., Grimmond, C.S.B., Cropley, F., Offerle, B., Su, H.B., 2000. Measurements of CO_2 and energy fluxes over a mixed hardwood forest in the mid-western United States. Agricultural and Forest Meteorology 103, 357-374.

Soegaard, H., Møller-Jensen, L., 2003. Towards a spatial CO_2 budget of a metropolitan region based on textural image classification and flux measurements. Remote Sensing of Environment 87, 283-294.

SMA-GDF, 2004. Inventario de Áreas Verdes en el Distrito Federal. Gobierno del Distrito Federal, México D.F. Available in the website: http://www.sma.df.gob.mx. Visited on May 2005.

SMA-GDF, 2002. Inventario de emisiones Zona Metropolitana del Valle de México 1998. Gobierno del Distrito Federal, México D.F.

Tejeda, A., Jáuregui, E., 2005. Surface energy balance measurements in the Mexico City region: a review. Atmósfera 18, 1-23.

Velasco, E., Lamb, B., Pressley, S., Allwine, E., Westberg, H., Jobson, T., Alexander, M., Prazeller, P., Molina, L., Molina, M., 2005. Measurements of urban VOC fluxes. Geophysical Research Letters 32, doi: 10.1029/2005GL023356.

Vogt, R., Christen, A., Rotach, M.W., Satyanarayana, A.N.V., 2003. Fluxes and profiles of CO_2 in the urban roughness sublayer. Fifth International Conference on Urban Climate. September 1-5, 2003, Lodz, Poland.

Walsh, C.J., Oke, T.R., Grimmond, C.S.B., Salmond, J.A., 2004. Fluxes of atmospheric carbon dioxide over a suburban area of Vancouver. Fifth Symposium on the Urban Environment 23 - 27 August, 2004. Vancouver, Canada.

Webb, E.K., Pearman, G.I., Leuning, R., 1980. Correction of flux measurements for density effects due to heat and water vapour transfer. Quarterly Journal of the Royal Meteorological Society 106, 85-100.

Westberg, H., Lamb, B., Hafer, R., Hills, A., Shepson, P., Vogel, C., 2001. Measurement of isoprene fluxes at the PROPHET site. Journal of Geophysical Research 106(D20), 24,347-24,358.

Whiteman, C.D., Zhong, S., Bian, X., Fast, J.D., Doran, J.C., 2000. Boundary layer evolution and regional-scale diurnal circulations over the Mexico Basin and Mexican plateau. Journal of Geophysical Research 106(D8), 10,081-10,102.

Zavala, M., 2004. Personal communication. Massachusetts Institute of Technology, Boston, MA.

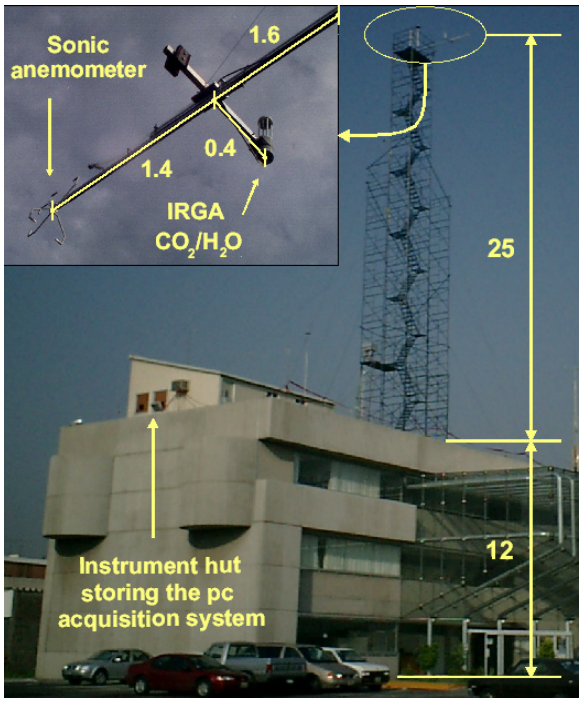

Figure 4.1. Schematic diagram of the instrumented flux tower. The azimuth orientation of the sonic anemometer is 16º from north. Dimensions are in meters.

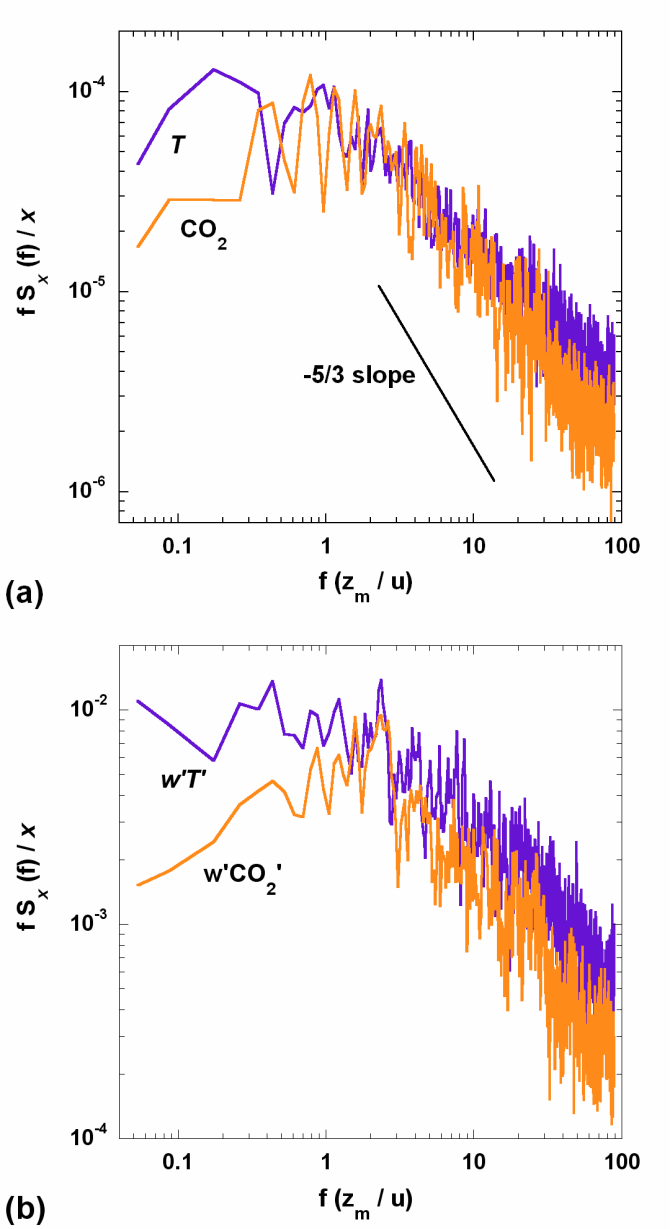

Figure 4.2. (a) Power density spectra for CO_2 concentration and ambient temperature, normalized for comparison. The -5/3 slope indicates the theoretical slope in the inertial subrange. (b) Cospectra of vertical velocity with ambient temperature and CO_2 concentration, normalized for comparison. *X* represents the average CO_2 concentration and ambient temperature for the spectra, and the covariances of those scalars with the vertical wind speed for the cospectra. Overall, the shape and details of the CO_2 and ambient temperature spectra and cospectra correspond closely over the entire range of frequencies measured. The data correspond to the 30 minute sampling period on April 7 at 15:30 h.

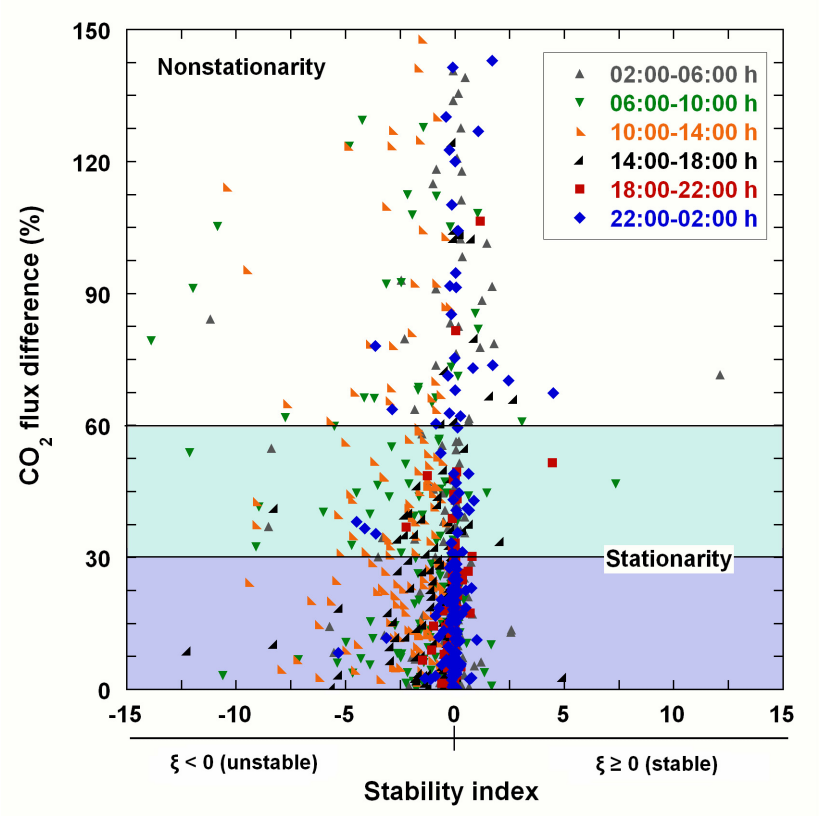

Figure 4.3. Stationarity test for CO_2 flux: in 56% of the periods, the flux difference was less than 30%, which indicates periods that meet and exceed the stationarity criteria. In 18% of the periods, the flux difference was between 30 and 60%, which means that these periods have an acceptable quality.

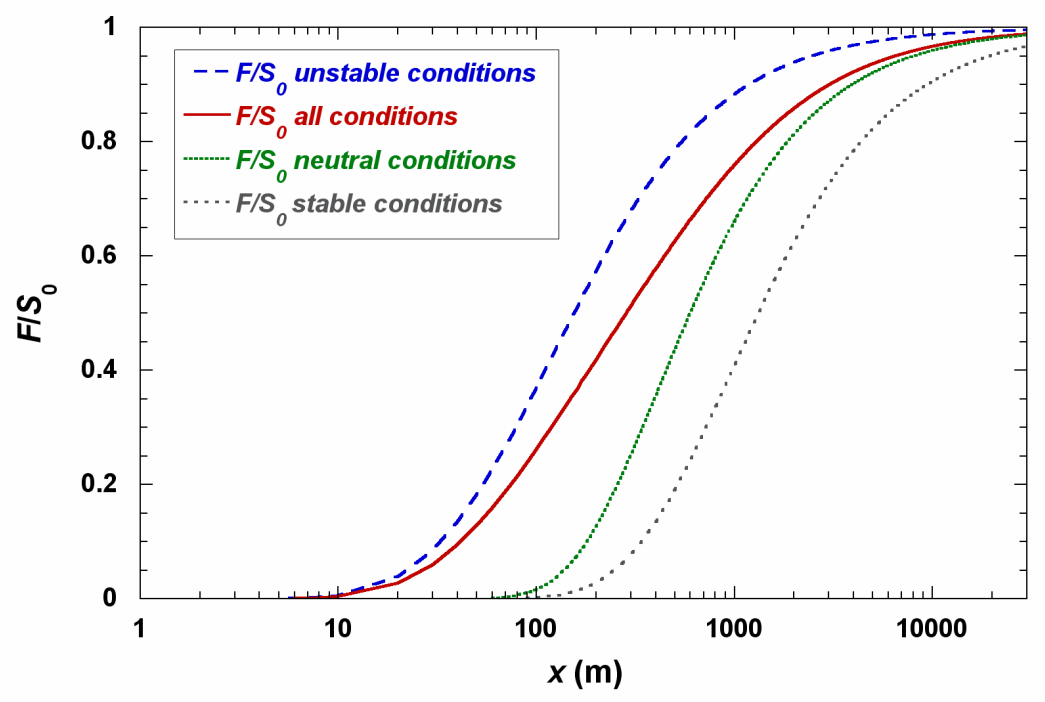

Figure 4.4. Fraction of the flux measured (F/S_0) versus the upwind distance or effective fetch (x).

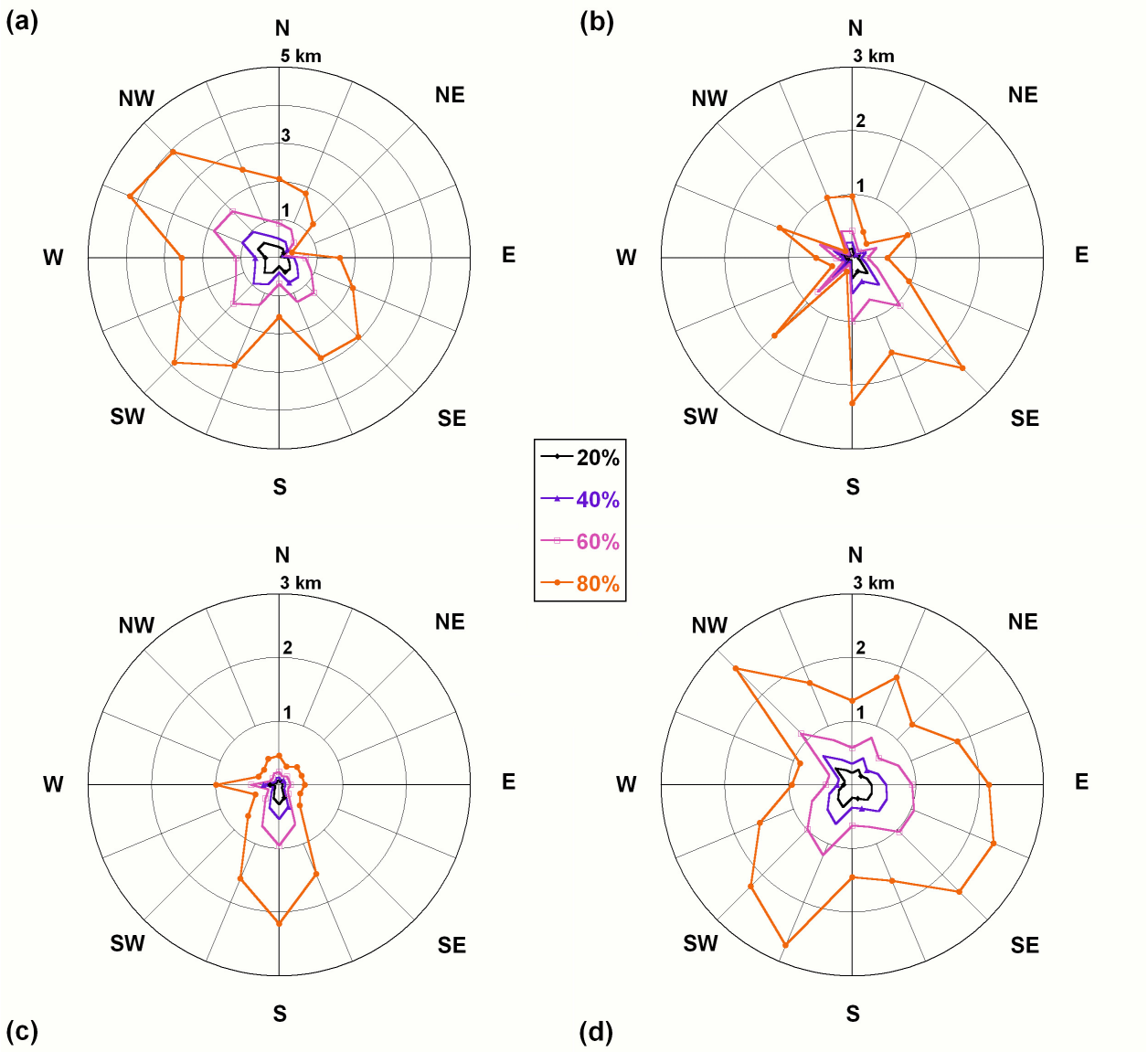

Figure 4.5. Different fractions of the measured flux (F/S_0) during the entire campaign as function of the wind direction for different intervals of time, (a) from 0:00 to 3:00 h, (b) from 6:00 to 9:00 h, (c) from 12:00 to 15:00 and (d) from 18:00 to 21:00 h.

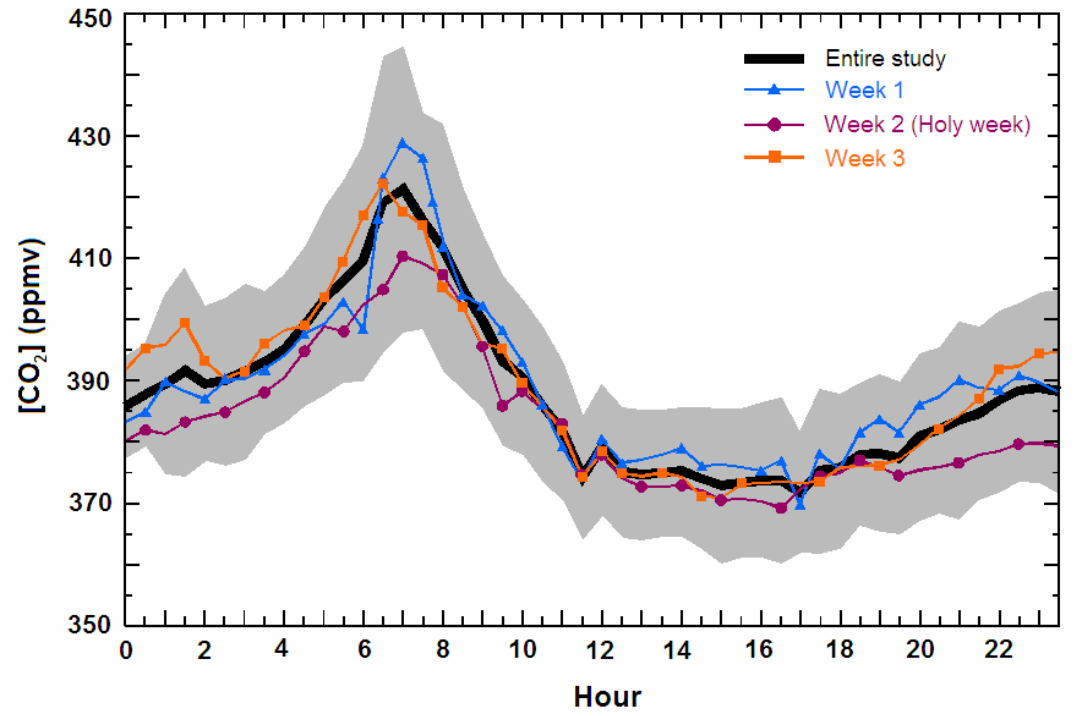

Figure 4.6. Average diurnal pattern of CO_2 concentrations for the entire study and for separate weeks. The gray shadow represents ±1 standard deviation from the total average.

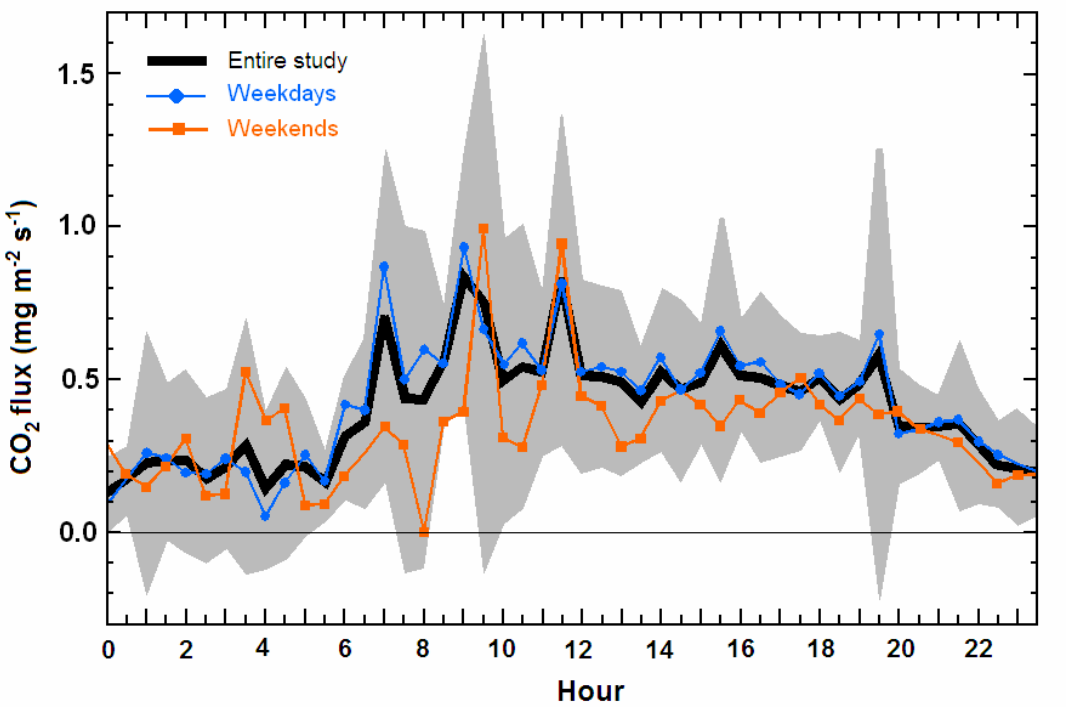

Figure 4.7. Average diurnal pattern of CO_2 fluxes for the entire study and for weekdays and weekends. The gray shadow represents ±1 standard deviation from the total average.

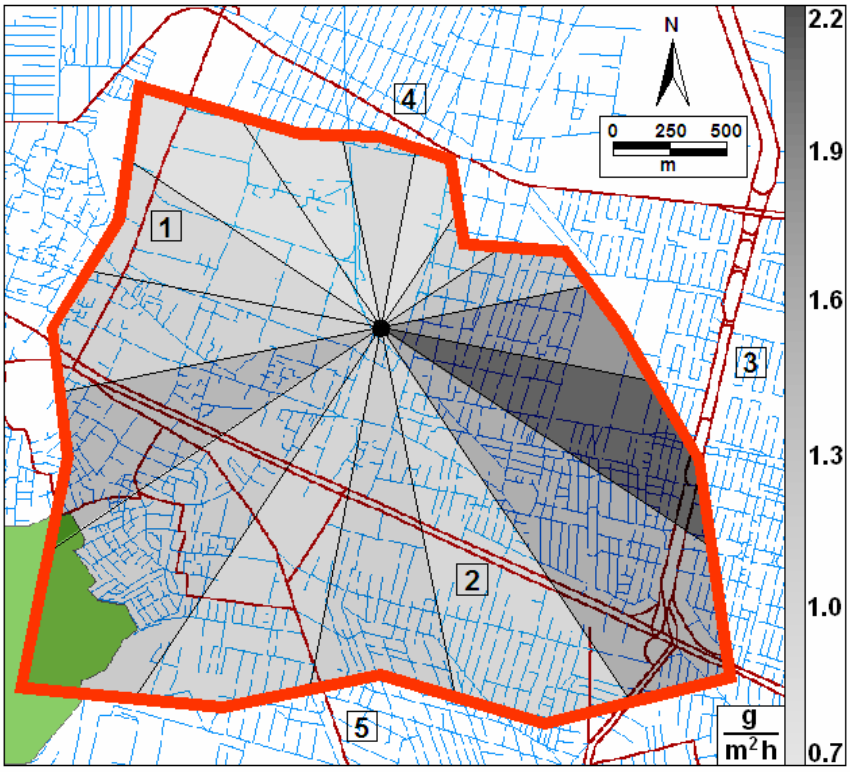

Figure 4.8. CO_2 flux distribution as a function of the upwind direction during the entire study. The contour shape indicates the fraction of the flux measured equal to 80% and the shading indicates the magnitude of the CO_2 fluxes. The black spot indicates the position of the flux tower; and the solid area in the left bottom corner represents part of the National park "Cerro de la Estrella". The four primary roads surrounding the measurement site are: (1) Av. Rojo Gomez, (2) Av. Ermita Iztapalapa, (3) Anillo Periferico, (4) Av. Jalisco, and (5) Calz. San Lorenzo.

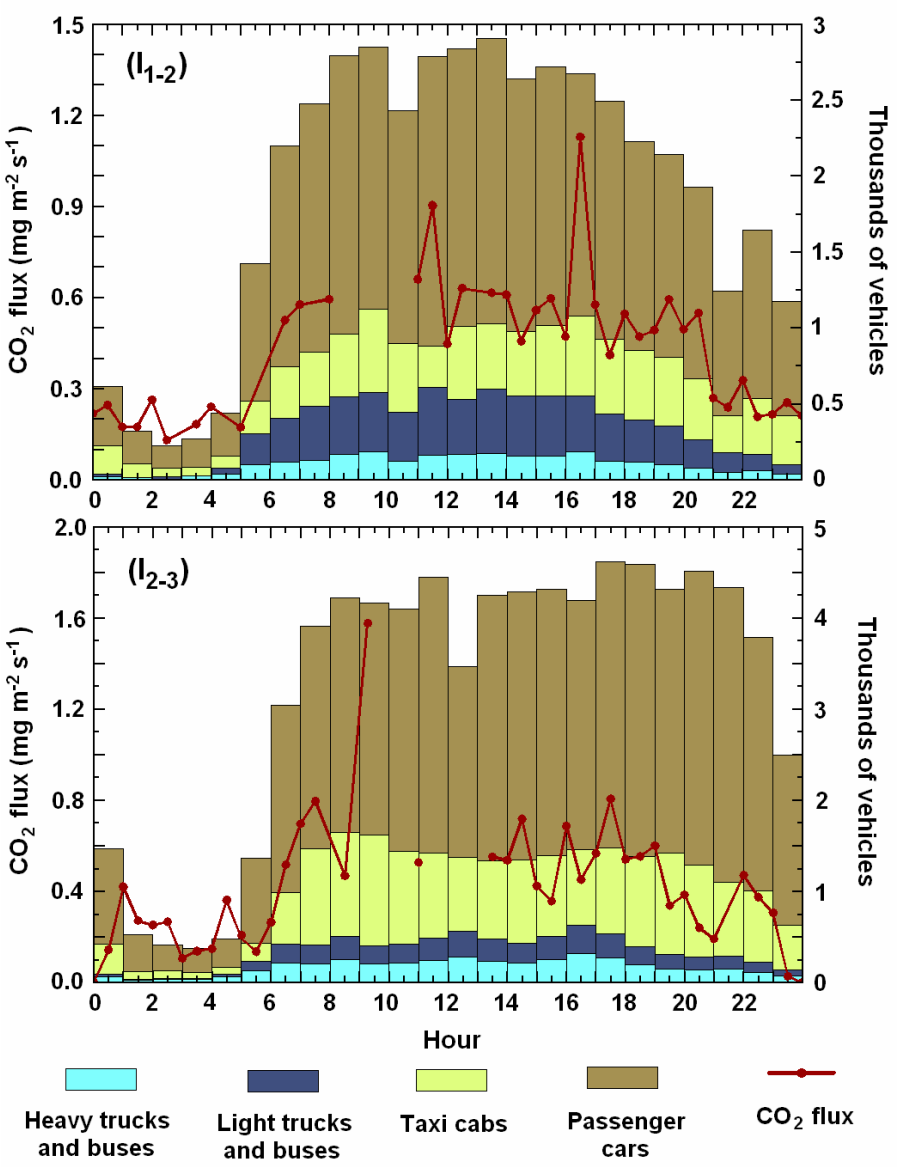

Figure 4.9. Diurnal profile of CO_2 fluxes superimposed over plots of traffic counts for two intersections within the footprint: intersection $I_{1\text{-}2}$ between Av. Ermita Iztapalapa and Av. Rojo Gomez, and intersection $I_{2\text{-}3}$ between Av. Ermita Iztapalapa and Anillo Periferico. Fluxes correspond to the upwind sectors where both intersections are located, for $I_{1\text{-}2}$ the sector between 240 and 285º and for $I_{2\text{-}3}$ the sector between 115 and 160º.

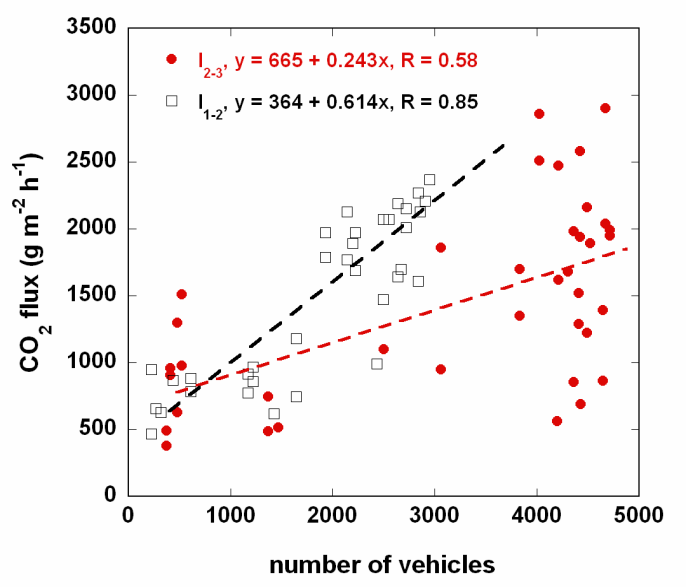

Figure 4.10. Correlation between CO_2 fluxes and vehicular traffic for two intersections, $I_{1\text{-}2}$ and $I_{2\text{-}3}$. Fluxes correspond to the 45º upwind sectors where both intersections are located, respectively.

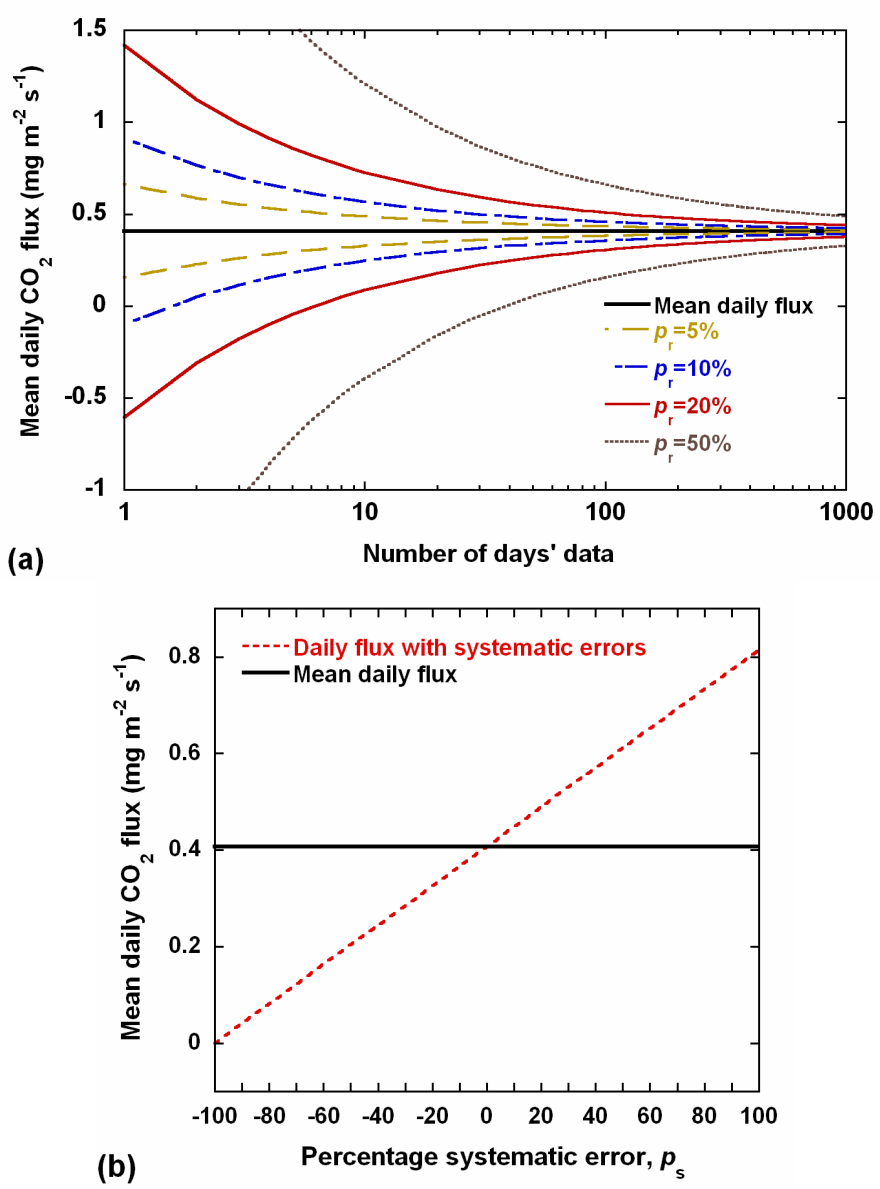

Figure 4.11. Effects of random and systematic errors for the mean daily CO_2 flux. (a) Effects due to random errors for various percentages of error. (b) Effects due to systematic errors as a function of the error percentage (p_s). In both figures the horizontal line represents the mean daily CO_2 flux, 0.41 mg m^{-2} s^{-1}.

CHAPTER 5

SUMMARY AND CONCLUSIONS

5.1. Summary

The work presented in this dissertation investigated the ambient concentrations and fluxes of volatile organic compounds (VOCs) and CO_2 in the atmosphere of Mexico City. There are many individual reactive VOCs in the troposphere that contribute to the creation of photochemical smog and tropospheric ozone. In addition, some individual VOCs are toxics, e.g., the carcinogenic benzene and 1-3-butadiene. CO_2 is the dominant greenhouse gas of anthropogenic origin.

The overall goal of this research was to quantify the emissions of these trace gases in a megacity. Better emissions should lead to better strategies for reducing air pollution. To pursue this goal, we participated in the Mexico City Metropolitan Area (MCMA) field campaigns in 2002 and 2003. Our participation involved two main activities. First we investigated the ambient concentrations of VOCs in terms of their distribution, diurnal pattern, origin and reactivity at different locations of the Valley of Mexico. This task was completed in collaboration with other participants in the MCMA field campaigns, who provided us with VOC data. Our second activity involved the deployment of micrometeorological flux instruments on a tall tower in a typical Mexican neighborhood to directly measure fluxes of selected VOCs and CO_2 from the urban landscape. Fluxes of olefinic VOCs were measured using a Fast Olefin Sensor (FOS) and processed by the eddy covariance technique (EC). Fluxes of acetone, methanol, C_2-benzenes and toluene were measured using a Proton Reaction Mass Spectrometer (PTR-MS) and computed by the disjunct eddy covariance technique (DEC). Fluxes of CO_2 were measured by an open path infrared sensor and processed by EC.

The use of different techniques to measure ambient VOC concentrations provided confidence in the data, as well as a basis for comparison with grid model simulations of selected VOCs. During the MCMA-2002 field campaign only canister samples were collected and

analyzed by gas chromatography/flame ionization detection (GC-FID) with the aim to determine the VOC signature at different sites within and near Mexico City. Those monitoring sites included locations in the urban core, a heavily industrial area and boundary sites in rural environments. For the MCMA-2003 field campaign the VOC measurements were extended in both, monitoring sites and instrumentation. Besides of GC-FID, VOC concentrations were measured by two PTR-MS, one FOS and, two UV Differential Optical Absorption Spectrometers (DOAS) located in different sites of the city. The following points summarize the main findings of the ambient VOC measurements:

- During the morning the entire Valley of Mexico presents a homogeneous distribution of VOCs: 60% alkanes, 15% aromatics, 5% olefins and a remaining 20% of oxygenated, alkynes, esters and other unidentified VOCs (percentages are based on concentrations in pbbC). In the afternoon, the VOC mix changes according to the characteristics of each site. If reactivity with OH and atmospheric abundance are used to measure photochemical reactivity, olefins are the most important hydrocarbons in the atmosphere of Mexico City. The top three contributors are ethylene, propylene and propane. Even though propane and butane are not overly reactive with OH, their elevated concentrations in Mexico City are sufficient to rank these two alkanes in the top 5 reactive VOCs.
- Elevated levels of toxic hydrocarbons, such as 1,3-butadiene, vinyl chloride and the BTEX hydrocarbons were observed. These hydrocarbons are of significant public health concern since there is evidence that they increase the risk of cancer, leukemia, congenital malformations and many other adverse health effects.
- In general, VOC mixing ratios observed in this study were slightly lower than those reported in earlier studies in Mexico City. This observation is consistent with previous reports indicating that ambient VOC concentrations have reach a stabilization level and possibly have decreased. This is a good indicator that policies and actions enacted to decrease VOC emissions have been successful, despite the growth in the vehicular fleet and other activities.

- VOC diurnal patterns show a strong correlation with the daily vehicular traffic pattern. At some urban sites, one single peak concentration is observed coinciding with the morning rush hour and the major vehicular activity of the day. In contrast, other sites show two peaks corresponding to the morning and afternoon rush hours, when increments in the vehicular activity are also registered. Diurnal patterns at boundary sites are not influenced by vehicular traffic or biogenic emissions; instead they depend more on wind patterns and rural sources such as burnings of agriculture debris and trash.
- Comparisons of ambient VOC concentrations with concentrations of acetylene and VOCs with similar lifetime demonstrated that many olefin and aromatic species, such as xylenes, toluene, ethylbenzene, t-2-pentene, c-2-pentene, etc. are mainly emitted in vehicle exhausts,. Also, MTBE and some alkanes such as 2-methylpentane and 3-methylpentane showed excellent correlations with acetylene, indicating that their main source is also vehicle exhaust. Furthermore, comparisons of light alkanes with acetylene showed that certain species related with the use of residential LPG are emitted also by mobile sources, particularly propane and n-butane.
- Examination of the VOC data in terms of lumped modeling VOC classes and comparison to the local emissions inventory suggests that some, but not all, classes are underestimated in the inventory by factors between 1 and 3. Overall, the emissions inventory underestimates the contribution of some alkanes and overestimates the contributions of some olefins and aromatics.

The flux measurements presented in this dissertation represented the first experiment in which micrometeorological techniques are applied to measure fluxes of VOCs in an urban environment. Micrometeorological techniques have not previously been used in urban areas to measure VOC fluxes because of the lack of fast-response VOC sensors and the uncertainties associated with flux measurements in a city, where the spatial variability of surface cover, emission sources and roughness is high. However, in this study, we have demonstrated the use of EC and DEC techniques to perform VOC flux measurements in an urban area using state of

the art VOC sensors. The CO_2 EC measurements represented the first CO_2 fluxes quantified in an urban area of a developing country. The most significant findings from our flux measurements are listed below.

- Fluxes of olefins and CO_2 exhibited a clear diurnal pattern with a strong relationship to vehicular traffic. In addition, examination of these fluxes as a function of the upwind direction indicated that the highest fluxes were observed in sectors with a high density of streets and avenues with heavy traffic.
- Olefin fluxes were lower on the weekends than on weekdays, and on weekends the morning rush hour peak was not observed. On average, the daily flux on weekdays was 21% higher than during weekends. This effect is directly related to changes in vehicular traffic and to industrial and commercial activities.
- Fluxes of methanol, acetone, toluene and C_2-benzenes showed similar diurnal patterns, with the highest fluxes during the morning and lowest during night. In general, fluxes for these species were always positive. Fluxes of acetone were negative in early morning, which suggests that deposition of acetone may occur before sunrise.
- The CO_2 flux measurements showed that the urban landscape is a net source for CO_2 with similar diurnal patterns and magnitudes to those observed in US or European cities. The effects of CO_2 uptake by urban vegetation do not appear to be significant, at least for the analyzed footprint in this study.
- The diurnal profile of olefins, acetone, toluene and C_2-benzenes fluxes was compared with the emission profiles reported in the local gridded emissions inventory. There was general agreement between measured fluxes and reported emissions, with the exception of C_2-benzenes, whose emissions in the inventory were more than two times higher than the measured fluxes.

5.2. Conclusions

In this dissertation indirect and direct methods to evaluate emissions inventories were applied to the actual emissions inventory of VOCs for Mexico City. Detailed measurements of individual VOCs and CO_2 concentrations were also conducted with the aim to better understand their distribution, magnitudes, diurnal patterns, and principal emission sources. Therefore, from all our evaluations and analysis we derive the following conclusions:

- In this work, we have demonstrated the use of EC and DEC techniques to perform VOC flux measurements in an urban area using state of the art VOC sensors. The ability to evaluate emissions inventories using micrometeorological techniques is a valuable and new tool for improving air quality management.
- Comparisons of the measured fluxes versus the emissions of olefin, toluene and acetone reported in the most recent emissions inventory for air quality modeling indicate that fluxes and emissions agree for the grid where the flux tower was located and do not support recent modeling results suggesting that VOC emissions are underestimated by a factor of 3. If this is true for other VOC classes and in other sections of the city, it implies that factors other than an underestimation of VOC emissions may be causing poor agreement between modelled and measured ozone levels. At the same time, it is important to note that the species we measured do not account for a majority of the VOC emissions which tend to be dominated by alkane species. For this reason, it is important to extend these direct VOC flux measurements to include other compounds and to also make measurements in other parts of the city. The comparison between the ambient VOC concentrations in terms of lumped modeling classes versus the emissions inventory neither support the statement that VOC emissions are underestimated by a factor of 3.
- We found that the developing megacity of Mexico City emits essentially the same annual amount of CO_2 per unit of area as that released in developed cities such as Tokyo and Copenhagen. This is in spite of the higher population, scarce green areas, dense traffic with a relatively old vehicle fleet, and the extensive presence of aged technologies for daily commercial

and residential activities in Mexico City. The higher fuel consumption in developed cities could explain this similitude.

- Through the different analysis performed in this work, vehicle exhaust was identified as the main source of VOCs and CO_2 in the atmosphere of Mexico City. This result suggests that control strategies need to be focused on improving fuel quality and vehicle emission technology. However, these kinds of control strategies alone are not going to solve the air pollution problem of a developing megacity, where not all of the population have access to cleaner transportation technologies and less polluting methods for cooking and water heating. First, the economic necessities of the major population need to be solved, and the actual style of life needs to be modified. It is not sustainable to have private cars being the main transport mode. New kinds of high-quality mass public transport need to be implemented to reduce the use of private cars. Also, new policies promoting environmental education, the use of the bicycle and a greater support to environmental research are needed to reduce the harmful VOC and CO_2 levels reported here, and overall, the air pollution problem in Mexico City.

5.3. Advantages and disadvantages of a flux system in an urban area

As an additional conclusion based on the experience gained through this study, we present a list of the advantages and disadvantages of a flux system in an urban area to evaluate fluxes of trace gases.

Advantages:

- Direct flux measurements during the entire diurnal cycle.
- Experimental validation of gridded emission inventories.
- Footprint of 0.5 to 5 km (significant fraction of one model grid).
- Simultaneous measurements of energy fluxes and turbulence data for evaluation of urban boundary layer models.

- Micrometeorological techniques are capable of quantifying emissions from sources that can not be identified, such as factories hidden in residential areas or street food cooking.

Disadvantages:

- One fixed site.
- Uncertainties about sensor sensitivity and source strengths.
- Effects of chemical loss on measured fluxes.
- Uncertainty about footprint in urban area.
- The cost of the required fast response sensors may be high.

5.4. Future work

In order to reduce the disadvantages listed above and to solve the uncertainties marked in this dissertation about flux systems in urban environments, it is clear that more research is needed. In this context we plan to go back to Mexico City and collect VOC flux measurements at a new site as part of a large field campaign named "Megacity Initiative: Local and Global Research Observations" (MILAGRO) scheduled for March 2006. In this second flux study we expect to answer the question whether the results from our MCMA-2003 campaign would hold for other locations in the city and for other VOC compounds. Answers to these questions will be important for modeling analyses and for future air quality management within Mexico City and other megacities.

We will identify a suitable location for flux measurements where the emissions are relatively high and where a tower can be safely erected and instrumented. We have already located the building hosting the offices of the local atmospheric monitoring network (RAMA) situated near central Mexico City where traffic densities are high and there is a range of residential and commercial facilities. Again we will measure olefin and CO_2 fluxes using a FOS and IRGA sensor, respectively, and the number of aromatic and oxygenated VOCs measured by PTR-MS

will be expanded. Also, we plan to expand the list of all VOC compounds measured by using a disjunct eddy accumulation (DEA) method coupled with individual VOC GC-FID analyses.

In the DEA method, updrafts and downdrafts are detected with the sonic anemometer and air is sampled during the up (down) draft into an up (down) sample volume at a volume proportional to the strength of the up (down) draft. The flux is calculated from measured velocities and concentrations using:

$$F = w^{+}C^{+} + w^{-}C^{-} - WC \quad (1)$$

where w^{+} and w^{-} are the mean updraft and downdraft velocities, C^{+} and C^{-} are the corresponding mean concentrations, and W and C are the overall means during the sampling period. With this system, the up/down samples are collected during a 30 min period and then require analyses using a gas chromatography system. With this batch approach, the frequency of sampling is limited to approximately 2 hours. Thus, we plan to collect 30 min flux samples on a 2 hour basis during each sample day. For some days, the frequency can be increased, for example every hour during the morning rush hour, to obtain more detailed data during selected periods. This system will give us information on compounds not measured otherwise and also provide data for some species for intercomparison to the other flux methods.

In addition, we plan to measure fluxes of CO. Emissions of VOCs and CO_2 from combustion sources are strongly correlated to emissions of CO. CO fluxes will valuable to identify better the emission sources of VOCs and CO_2.

Prior to the MILAGRO campaign we plan to reduce the uncertainty of the 52% of olefins detected by the FOS that remain unknown through response tests. And after the campaign, through comparison of FOS data with the individual VOC analyses from the DEA flux system.

Beyond the MILAGRO campaign, we suggest to continue the flux measurements for a longer period (e.g. one year) to confirm the representativeness of the fluxes throughout the different climatic seasons of the year. This would be a valuable contribution for quantifying trace gas

emissions that could have regional and global impacts and to reduce the uncertainties due to the own variability of the emissions. To characterize the three different climatic seasons of Mexico City, we suggest seasonal measurements of three-months. An analysis of random and systematic errors using the flux data reported here indicates that a three-months period will yield fluxes resolved within 11 and 35% of the mean daily flux.

Finally, we recommend that ambient concentrations of individual VOCs need to be measured in a periodic basis throughout the entire year at different locations of the city with the aim to determine the seasonal variability and evaluate the effectiveness of the control strategies. Local authorities should consider the addition to the actual monitoring network of instruments to measure continuously key hydrocarbons in terms of their reactivity and toxicity, such as toluene or benzene.